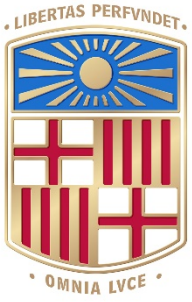

UNIVERSITAT DE BARCELONA

Final Degree Project

Biomedical Engineering Degree

"Development of a microphysiological system with integrated electrodes for cardiac cell culture, stimulation and sensing"

Barcelona, 7th June, 2023

Author: Berta Lloveras Borràs

Director/s: Romen Rodríguez Trujillo

Abstract

This project focuses on the development and experimentation of a microfluidic device with integrated electrodes, specifically designed to support the growth and maturation of a 3D cardiac cell matrix. The goal is to create a functional system that not only enables the cells to thrive and pump, but also facilitates the propagation of electrical stimuli, mimicking the behavior of natural cardiovascular tissue.

The motivation behind this research stems from the limited regenerative capacity of adult heart tissue, particularly when it comes to cardiomyocytes. Traditional healing methods are often inadequate, necessitating heart transplants as the only definitive treatment option. To address this challenge, scientists are exploring the potential of biomaterial scaffolds to regenerate cardiovascular tissue by replacing damaged or necrotic tissue.

The microfluidic device developed in this project holds great promise for researchers in the pharmaceutical field, offering a valuable tool for drug testing and disease modeling. Despite facing challenges in incorporating gold electrodes into the device, the team has successfully characterized it using an EIS machine. The design of the microelectrodes and microchannels, along with the overall functionality of the microchip, have been accomplished. While the current focus has been on a 2D layer of cells, the future objectives involve achieving a fully functional 3D matrix to fulfill the original research goals.

Overall, this project aims to represent a significant step towards the advancement of regenerative medicine and the potential for innovative solutions in treating cardiovascular diseases.

Keywords: Cardiomyocyte, Organ-on-chip, Microelectrode, Microchannel, Electrical Impedance.

Acknowledgements

I would like to express that the elaboration of this Final Degree Project would not have been possible without the help that the research team from where this project belongs has given me. I am so thankful to Eduardo Yanac Huertas and Matilde Roquette for their support. I also want to thank my thesis director Romen Rodríguez for his support during all the process and for teaching me all I've had to know to carry out this challenging project. Moreover, for being patient with me and supporting me during the process, I want to thank my parents, Georgina Borràs and Joan Lloveras, and my twin sister Laura Lloveras. Lastly, I also want to express a special gratitude to my partner Marc Palomer, for encouraging me to always go ahead with everything I set my mind to.

List of figures

List of tables

Glossary of abreviations

CHDs: Coronary Heart Disease

MPS : Microphysiological Systems

GM: Genetically Modified

DDT: Dichlorodiphenyltrichloroethane

LAA: Laboratory Animal Allergy

WAGs: Waste Anesthetic Gases

LAI: Laboratory Acquired Infections

IBEC: Institut de Bioenginyeria de Catalunya

EIS: Electrochemical Impedance Spectroscopy

CMs: Cardiomyocytes

ECs: Endothelial Cells

RyRs: Ryanodine Receptors

RMP: Resting Membrane Potential

MeTro: Methacrylated Tropoelastin

GelMA: Gelatin Methacryloyl

ECM: Extracellular Matrix

MTF: Muscular Thin Film

PDMS: Polydimethylsiloxane

PBS: Phosphate-buffered Saline

HMD: Heart-on-a-chip Microdevice

MEMS: Micro Electro-Mechanical System

OoCs: Organs-on-chips

UB: University of Barcelona

CVD: Cardiovascular Disease

BBB: Blood-Brain Barrier

DLW: Direct Laser Writing

HUVECs: Human Umbilical Vein Endothelial Cells

SACNTs: Super-Aligned Carbon Nanotube Sheets

FBS: Fetal Bovine Serum

PLA: Polylactic acid

WBS: Work Breakdown Structure

Table of contents

1. Introduction

1.1. Project introduction and definition

Coronary heart disease (CHDs) refers to a range of conditions that impact the structure and functioning of the heart. These conditions arise due to insufficient delivery of oxygen-rich blood to the heart tissue, particularly the myocardium, leading to hypoxia and subsequent tissue necrosis. The surrounding tissue experiences hypoxia as well, resulting in the formation of an irreversible necrotic wall covered by fibrotic tissue. Consequently, the heart's pumping strength is compromised, and its overall function is permanently altered.

Moreover, there exists a wide range of dysfunctions that impact cardiac tissue, leading to disturbances in the normal operation of the heart and posing a significant risk of cardiac failure, which can significantly diminish the quality of life. Among these dysfunctions, cardiomyopathies are particularly noteworthy. Cardiomyopathies encompass a diverse group of diseases that affect the muscle of the heart, presenting considerable heterogeneity in their characteristics and manifestations.

Cardiovascular tissue encompasses the fully specialized and mechanically supportive components of the heart, including the myocardium, heart valves, and vasculature. Unlike certain regenerative tissues, such as the skin or liver, the adult heart tissue has limited regenerative capacity, specifically in relation to cardiomyocytes (CMs). Consequently, the natural healing ability of the heart is inadequate, and the only definitive treatment option in such cases is a transplant.

As an encouraging alternative, numerous research teams are investigating the potential to regenerate cardiovascular tissue by replacing abnormal or necrotic tissue with biomaterial scaffolds that mimic natural tissue. This endeavor is highly demanding due to the intricate and complex structure of healthy heart tissue, necessitating careful considerations in its design. Some of the crucial factors that need to be considered include:

- The element of cardiac tissue (selecting suitable cells and biomaterials).
- Arrangement (aligned muscle fibers and the ability to support blood flow): Mechanical characteristics.
- Biologically significant capabilities (electro-mechanical connection and coordinated contraction).

The specific arrangement and cellular makeup, along with consistent exposure to various dynamic influences, are vital for sustaining the normal functioning of the heart. Therefore, achieving successful construction of engineered heart tissues requires careful consideration of several factors. These include selecting the right combination of cells and 3D processed hydrogels (such as different cell types, biomaterials, and biochemical signals), as well as considering the topological and structural features, along with mechanical and electrical cues.

This project, therefore, aims to work on and experiment with the design and fabrication of a microfluidic device with integrated electrodes that is capable to maintain inside it a 3D cardiac cells matrix for cells to be able to grow and mature there and still be able to pump, to properly propagate

the electrical stimuli. This device, then, is aimed to be useful for researchers in the pharmaceutic field in terms of drug testing and disease modeling [1].

1.2. Project justification

1.2.1. Clinical impact

Microphysiological Systems (MPS) technologies may provide a way to better understand and address the main failures of clinical programs: lack of efficacy or unacceptable side effects that are not predicted in animals or simpler cell systems during early preclinical stages. The key advantage that MPS offer is the creation of more physiologically relevant human organ–like models that can potentially yield data on drug action that will better translate to humans than that from *in vivo* animal models or conventional cell systems. Whereas research data from animals do not always translate to humans because of differences in the physiology of the different species, traditional human *in vitro* models lack three-dimensionality, tissue-tissue interfaces, and mechanical cues, which leads to dedifferentiation of cultured cells and, consequently, reduced human relevance. Despite the mostly exploratory nature of current MPS, there is an appetite for the uptake of the technology by pharmaceutical and biotechnology industries to improve on human predictivity, with the long-term goal of eventually replacing animal models wherever possible. Simultaneously, both academic groups and multiple biotech companies are developing increasingly refined MPS models to meet the needs and quality standards required for drug development such as scalability and robustness [2].

1.2.2. Environmental impact

The extensive use of animals in research and toxicity testing across various industries entails an obvious environmental impact. Global estimates suggest that millions of non-human vertebrate animals are used annually, with the United States leading in animal usage. The actual number of animals used may be higher due to unreported species such as cold-blooded animals, farmed animals, rats, mice, and birds. The development of genetically modified (GM) mice has led to increased animal usage and significant waste, as many bred mice do not meet research requirements and are disposed of. The disposal of surplus animals and the associated waste pose environmental challenges [3].

There is emphasis in the need for environmental analysis regarding animal use in biomedical, cosmetic, and product industries. Evidence suggests that the use and disposal of animals, along with the use of chemicals and supplies, contribute to pollution, biodiversity loss, and health risks. Every year, millions of animal bodies used in research and testing are discarded, often contaminated with toxic chemicals, viruses, or infectious diseases. This results in significant amounts of laboratory waste, including animal excrement, bedding, excess feed, caging, needles, syringes, and gavages, being disposed of as well. Animal research facilities also generate large quantities of hazardous wastes, emitting harmful substances like ignitable, corrosive, reactive, and toxic wastes, as well as air pollutants such as nitrogen dioxide, sulfur dioxide, particulate matter, and carbon monoxide. Among the hazardous chemical substances handled by these facilities are known carcinogens like benzene, arsenic, and formaldehyde, as well as possible carcinogens like

lead, DDT, and chloroform. Disposal methods for animal carcasses and tissues, which may contain a combination of chemical, radioactive, and/or biological hazards, include rendering, landfill disposal, and incineration. Incineration is commonly used, especially for radioactive animal carcasses and tissue, but the disposal of chemically and biologically hazardous waste poses challenges since few waste facilities are equipped to handle them.

Moreover, the environmental hazards associated with animal research have direct implications for human health, particularly for personnel working with laboratory animals. The tight confinement of animals in indoor facilities with modern air filtration systems can lead to exposure to laboratory animal allergens, resulting in allergic reactions and asthma. Laboratory animal allergy (LAA) has been recognized as an occupational hazard, and exposure to laboratory animals is a common cause of occupational asthma. LAA encompasses symptoms such as allergic conjunctivitis, rhinitis, asthma, and dermatological reactions, caused by allergens found in animal hair, dander, urine, saliva, and serum. Inhalation of airborne allergen particles is the primary route of exposure, although direct contact with the skin and eyes can also contribute. Workers in direct contact with animals are at the highest risk of developing LAA, but indirect exposure can occur through the transfer of allergens from the animal facility to the home or general public. Children of parents exposed to animals in laboratories have shown increased sensitization to animals.

Furthermore, waste anesthetic gases (WAGs) are gases and vapors that can escape into the surrounding environment and the breathing space of laboratory staff during medical procedures. Breathing in these gases has been linked to both immediate and long-term health effects.

Also, the transmission of zoonotic diseases in an animal research facility poses a risk to the safety and health of laboratory animal handlers. Laboratory acquired infections (LAI) can be acquired directly from the animals or indirectly through contact with contaminated tissue, equipment, and supplies. The main method of transmission is through the air, as infectious material becomes aerosolized. There are additional risks of exposure from animal bites, scratches, contact with contaminated equipment, and accidental ingestion of contaminated material.

Finally, there are other environmental impacts such as biodiversity impacts, which englobes capture from the wild and genetically modified animals.

1.2.3. Justification of our commitment

The environmental impacts, the environmental hazards and the associated occupational safety concerns could be eliminated by replacing animal research and testing with *in vitro* alternatives. For all the just mentioned reasons, this project pretends to avoid all these possible problems and to work with the most human-like and environmentally safety possible systems.

1.3. Objectives

The main objective of this project is to develop a microphysiological system with integrated electrodes for cardiac cell culture, stimulation, and sensing. It will consist of developing an affordable in vitro model of the myocardium that possesses personalized attributes and accurately mimics human characteristics. This model aims to serve as a significant tool in cardiac tissue

research, studies, and medical applications, with the goal of decreasing or even eliminating the need for animal models.

To achieve this goal, in this final degree project, the following specific objectives must be reached [1]:

Specific Objective 1: Designing and developing a microphysiological platform that can integrate microelectrodes for stimulation purposes.

Specific Objective 2: Validating the process. It involves testing the device in different conditions. The highest objective to reach is to test the myocardium-on-a-chip device, which replicates healthy tissue, to evaluate its cellular accuracy, sensing capabilities, adaptability, and physiological significance.

1.4. Structure and methodology

This final degree project has consisted of different phases. First of all, it has been necessary to carry out a study on the morphology and electrical properties of cardiac cells in order to understand their function and to know how to replicate it so that it is the same once these cells are introduced into the microfluidics device. In addition, the objectives to be achieved had to be determined.

The second phase of the project has consisted of conducting a study on the technologies that already exist in order to be able to start from a specific, not non-existent, point. The development of the microfluidic device has started from an existing model, created by the same research group that has supported this final degree thesis, to make the final design of the device that occupies this project.

The third phase has consisted of designing a model of the device wanted. This has been done using a design program. Tutorials have been useful for the author to learn how to use this program, including the drawing and the importation of the designs, as well as the operation of the program itself.

Once designed, in the fourth phase the device has been fabricated. The fabrication has taken place in a specific facilities with certain regulations. There has been a previous selection of materials and fabrication techniques to carry out this manufacturing process. Moreover, a cardiac cell culture has been maintained along the time in order to be used at the moment the device has been fabricated. To do so, cell trypsinization, cell counting, and culture medium generation knowledge have had to be achieved.

The fifth phase has consisted of coupling all the fabricated to obtain the final microchip and of using the cardiac cell culture mentioned before to introduce its cells inside the microfluidic device.

Finally, in the sixth phase the sensing and testing of the microdevice have taken place. It has been characterized one chip with fibers and one chip without fibers in different conditions: without any

medium (open system), with PBS (Phosphate-buffered Saline), and finally with medium. This characterization has been done using an EIS (Electrochemical Impedance Spectroscopy) machine.

1.5. Scope of the project

1.5.1. Scope

The scope of this project is to design and fabricate a microfluidic device which has integrated electrodes in order to characterize it and see if it has optimal conditions to host cardiac cells stimulating and sensing them. Considering this main requirement, the scope of the project includes:

- Definition of the tasks carried out throughout the project and establishment of the times each one of them will mean.

- Study of the background that exists towards technology, techniques and studies that have to do with what is to do in this project.

- Study of the current market situation to define the sectors to which the product result of this project is directed. In this way, product opportunities and risks can be defined, as well as to investigate and determine what weaknesses and strengths are in order to be able to study their viability and be able to ensure the success of the project.

- Study of the technical and economic feasibility of the project in order to achieve the main initial objectives and predict a possible future of the product.

- Application of project management methods in order to be able to achieve the objectives within the available time limit established. The application of these methods consists of:

    - Carrying out a SWOT matrix that aims to place the product in the market as optimally as possible.
    - Carrying out a Work Breakdown Structure (WBS) and its respective dictionary. These two documents are useful for defining the costs and times of all activities and tasks to be performed that make up the project.
    - Realization of a PERT-RM graph to define the timetable for the realization of the project and study its critical points that jeopardize the achievement of the main objective and delivery deadlines.
    - Carrying out a GANTT diagram for optimal control and monitoring of all project activities and tasks.

- Concrete and establish what type of channels and electrodes are to be designed, specify which type of cells are to be introduced and choose the materials of which the device is made.

- Design of different types of electrode conformations, including material, shape and sizes. Design of different types of microchannels, which include, among other components, a central chamber where the cardiac cells are inserted. These designs are detailed in the detailed engineering part of this project.

- Fabrication of the microchannels and the electrodes using specific fabrication techniques, which are detailed in the detailed engineering part of this project.

- Characterization of the different parts that have been fabricated to determine if the fabrication result has been as expected and if it is optimal.

- Assembly of the device once all parts have been designed and fabricated.

- Validation of the final product obtained. Different tests are performed to characterize the device. This validation is carried out using an EIS machine to measure the impedance of the system. The validated chips

1.5.2. Limitations

The project's scope aligns with achieving its objectives, but there are various limitations due to its nature as a final degree project. These limitations primarily stem from time and financial constraints, which must be taken into account.

This final degree project excludes:

- The introduction of a 3D hydrogel matrix composed of cardiac cells.

- The design and fabrication of electrodes that correspond to one of the two different designs of microchannels. The difference between one and the other is the width size of the central chamber. The electrodes have been only designed in reference to the small-sized chamber.

- The fabrication of all the models of electrodes designed.

- The cell seeding of all the microchips fabricated.

- The validation of the microchips seeded with cells.

- The validation of two microchips non-seeded with cells. Only one chip with fibers and one chip without fibers have been characterized in different conditions.

1.5.3. Localization

This final degree project was proposed by the Nanobioengineering and Biomaterials research group of the Faculty of Physics, University of Barcelona and has been released at this faculty and at the IBEC (Institut de Bioenginyeria de Catalunya).

The Nanobioengineering and Biomaterials group is dedicated to using nanotechnology and biomaterials to advance the development of innovative systems, protocols, and biomedical devices. Their objective is to create novel diagnostic platforms, models, biological microenvironments, and regenerative therapies. The group's primary research focuses on biochemical engineering, soft lithography, microfabrication techniques, the integration of biomaterials with microfluidic systems, and the construction of three-dimensional scaffolds using biodegradable and bioactive biomaterials [4].

2. Background

2.1. General concepts

2.1.1. Physiology and electrical properties of cardiac cells

Cardiac muscle cells, also known as cardiomyocytes (CMs) (Figure 1), possess unique characteristics and structures that enable their role in the involuntary contraction of the heart. These cells are striated and branched, housing numerous mitochondria for energy production. Unlike skeletal muscle, they are not under voluntary control. Each cardiomyocyte contains a centrally located nucleus and is surrounded by a specialized cell membrane called the sarcolemma. The sarcolemma of cardiac muscle cells possesses voltage-gated calcium channels, which are absent in skeletal muscle cells.

Cardiac muscle cells are interconnected through intercalated discs, which contain gap junctions (Figure 2) and desmosomes. These interconnections allow for synchronized contractions of the cardiomyocytes, facilitating the coordinated pumping action of the heart. Gap junctions enable the propagation of electrical signals, known as action potentials, between adjacent cells. Desmosomes play a crucial role in maintaining the structural integrity of the heart by anchoring the muscle fibers together.

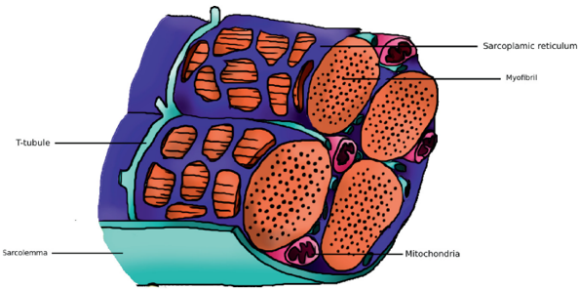

Figure 1: Cardiomyocyte structure [5]

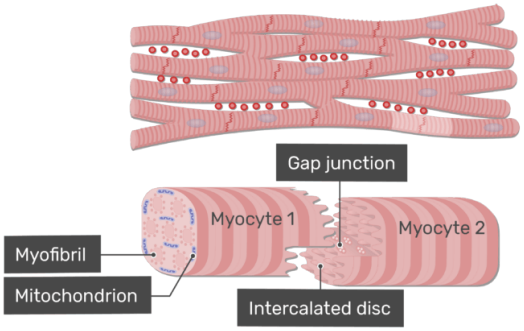

Figure 2: Cardiomyocyte gap junctions [6]

Cardiac tissue contractile function is mediated through the CMs that are organized in parallel arrays of myofibril bundles. The contractility of CMs is mediated through chemical, mechanical, and electrical stimuli. In addition to CMs, cardiac tissue is composed of fibroblasts and microvessels, which consist of endothelial cells (ECs) and vascular smooth muscle cells.

The contraction of cardiomyocytes occurs at the level of the sarcomere, which is the functional unit of contraction. The sarcomere consists of thick (myosin) and thin (actin) filaments, and their interactions follow the sliding filament theory, causing muscle contraction.

The sarcolemma of cardiomyocytes also contains transverse tubules (t-tubules), which are highly branched invaginations. T-tubules are involved in several important functions, including excitation-contraction coupling, initiation and regulation of action potentials, maintenance of the resting membrane potential, and signal transduction. They concentrate voltage-gated L-type calcium channels and position them close to ryanodine receptors (RyRs) located on the sarcoplasmic

reticulum. This arrangement allows for the efficient release of calcium ions, which is crucial for the contraction of cardiac muscle.

Overall, the unique characteristics and structures of cardiac muscle cells contribute to their synchronized contraction, enabling the heart to effectively pump blood throughout the body.

The cardiac action potential (Figure 3) normally lasts 200ms and can be divided into five phases: resting membrane potential (RMP: -90mV), upstroke, early repolarization, plateau, and final repolarization. During phase 4, the RMP is maintained by the activity of the Na/K ATPase pump. In phase 0, depolarization occurs due to the influx of sodium ions through fast sodium channels. Phase 1 involves partial repolarization caused by the closure of fast sodium channels and the efflux of potassium and chloride ions. Phase 2 is the plateau phase, sustained by the influx of calcium ions and some potassium efflux. Phase 3 is the final repolarization phase, where potassium efflux and the closure of sodium and calcium channels bring the membrane potential back to resting.

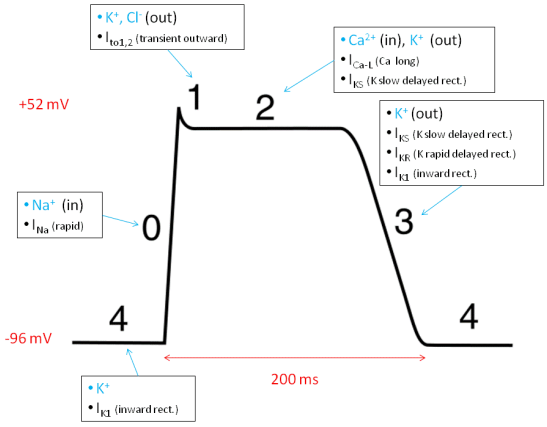

Figure 3: Cardiac action potential [7]

The generation of a cardiac action potential is an involuntary process called excitation-contraction coupling (ECC). Action potentials propagate along the sarcolemma and t-tubules, leading to membrane depolarization. During the plateau phase, calcium influx occurs through L-type calcium channels, facilitated by voltage-sensitive dihydropyridine (DHP) receptors on t-tubules. This increased intracellular calcium concentration triggers the release of more calcium from the sarcoplasmic reticulum through the ryanodine receptor, known as calcium-induced calcium release.

The released calcium attaches to troponin C, causing tropomyosin to detach from the myosin-binding sites on actin, allowing actin and myosin to form cross-bridges and initiate contraction. The duration of cross bridges is dependent on the presence of calcium attached to troponin. The relaxation of the myocardium after ECC is known as lusitropy, which is mediated by the SERCA pump, responsible for sequestering calcium into the sarcoplasmic reticulum, leading to calcium removal from troponin-C and returning the myocardium to its relaxed state.

In contrast to cardiac muscle cells, pacemaker cells, which include the sinoatrial (SA) and atrioventricular (AV) nodes, have a different action potential with three phases instead of five. Phases 1 and 2 are absent in pacemaker cells. Pacemaker cells exhibit autorhythmicity and spontaneously generate electrical activity without external stimulation. This is due to the presence of "funny current" channels that allow sodium ions to leak into the cell during phase 4, gradually increasing the membrane potential until a threshold is reached, causing depolarization (phase 0). Subsequently, calcium channels open, leading to calcium influx and further membrane potential

increase. After a positive membrane potential is reached, potassium channels open during phase 3, resulting in outward ion flow and the restoration of the resting potential [8].

2.1.2. Principles of microfluidic device fabrication

Microfluidics is a multidisciplinary field combining principles from physics, chemistry, biology, fluid dynamics, microelectronics, and material science. Microfluidic devices are miniaturized chips that contain channels and chambers in the microscale range. The fabrication of these devices involves various methods that allow for customization in terms of size, shape, and geometry. Microfluidic chips have a wide range of applications, including nanoparticle preparation, drug encapsulation, delivery, and targeting, cell analysis, diagnosis, and cell culture. Depending on their application and functional particularities, microfluidic devices can also be found in the literature as microreactors, lab-on-a-chip, or organ-on-a-chip.

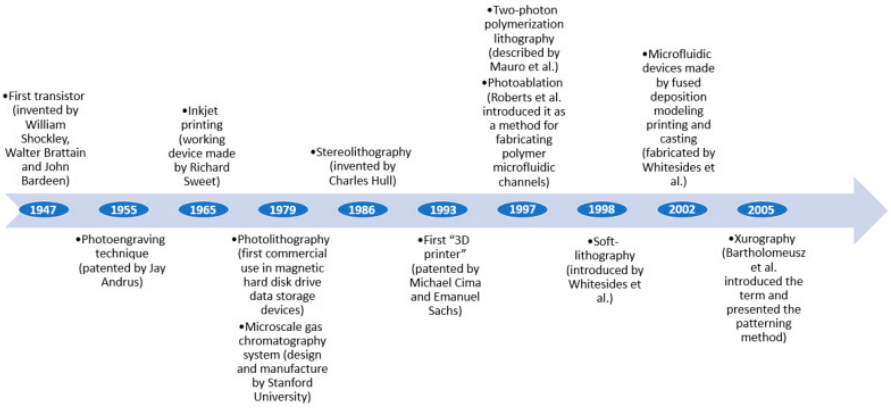

Figure 4: Breakthroughs in development of microfluidics [9]

Microfluidics has made significant progress within a relatively brief period, thanks to advancements in technology originating from different fields. These advancements have captured the attention of researchers and have been adapted to produce microfluidic chips. Figure 4 illustrates some of the key breakthroughs that have played a crucial role in the development of microfluidics.

A variety of materials are available for fabricating microfluidic devices, and each material possesses unique properties that influence its behavior during processing. Consequently, fabrication methods need to be tailored to the specific characteristics of the chosen material and the desired product specifications. Cost is another crucial consideration when selecting a fabrication technique. This is particularly important for microfluidic platforms as they are often used as disposable devices that are challenging to clean. Therefore, the chosen method should be economically viable for one-time use chips. Additionally, for widespread adoption, it is important to manufacture chips in a manner that is accessible and scalable. Waldbaur et al. presented a classification (Table 1) system for microfluidic fabrication methods based on how the microfluidic structure is created. The first classification distinguishes between methods that involve removing material (removing techniques) and methods that involve depositing material (depositing techniques). Additionally, another classification categorizes fabrication methods based on the nature of the processes employed, including chemical, mechanical, laser-based, and other processes [10].

Table 1: Classification of microfluidic fabrication techniques

	Material Removing Techniques	Material Depositing Techniques
Chemical processes	Electrochemical discharge machining Wet etching Dry etching	Silicon surface micromachining Lithography Inkjet 3D printing Powder 3D printing Direct writing Two-dimensional virtual hydrophilic channels
Mechanical processes	Micro-milling Micro-grinding Micro-abrasive air-jet machining Micro-abrasive water jet machining Ultrasonic machining Xurography	Injection molding Hot embossing
Laser-based processes	Photothermal process Ultra-short pulse process Absorbent material process Photochemical modification process Laser direct machining	Selective laser sintering Stereolithography Two-photon polymerization
Other processes	Focused ion beam	Forming process Soft lithography Layer-to-layer manufacturing Layer-on-layer manufacturing Fused deposition modeling 2.5-Dimensional printing

2.2. State of the art

2.2.1. Microfluidic and organ-on-a-chip systems for cardiac tissue and cell applications

Due to the need of mimicking human *in vivo* conditions, better and more predictive human-based *in vitro* models have been developed to assess the safety and efficacy of potential new drugs [11].

Numerous studies have successfully engineered biologically relevant models of heart and vasculature tissues *in vitro*. These three-dimensional (3D) microtissues hold promise for various applications, including *in vitro* drug testing, disease modeling, and biological mechanistic studies. These models possess myocardium-like and blood vessels-like physiological characteristics, thanks to tissue-like properties such as cell interactions (paracrine and cell-to-cell signaling), cell-extracellular matrix interactions, and mechanical stimulation. Recently, innovative microfluidic platforms have been developed, enabling the creation of biomimetic cardiovascular tissues *in vitro*. These microfluidic organs-on-a-chip (OoCs) models replicate important organ-level functions, multicellular microarchitecture, and dynamic environmental conditions. Consequently, they provide a technological platform that can expedite cardiovascular drug development. Therefore, these engineered heart and vasculature models-on-a-chip hold potential for the establishment of high-

throughput platforms for drug development and disease modeling, targeting major cardiovascular diseases such as myocardial infarction, hypertension, heart failure, and atherosclerosis.

During the pasts years organ-on-a-chip studies and developments have been done in order to mimic the cardiac tissue. Following there are some of them:

In a recent study by Annabi et al. [12], a method was developed to address the challenge of the limitation of attachment and spreading of cells by coating microfluidic channels with hydrogels (Figure 5), creating a favorable environment for cardiac cell culture on the chip. Specifically, methacrylated tropoelastin (MeTro) and gelatin methacryloyl (GelMA) were used to promote cellular adhesion within the microfluidic channels, an adhesion that were reported also in other cell types. The introduction of MeTro hydrogels resulted in enhanced attachment, proliferation, and beating rate of the seeded CMs compared to GelMA. Hence, this system holds the potential for investigating the impact of biomimetic signals on cardiac function. The findings from this research indicate that hydrogels based on tropoelastin could provide a favorable microenvironment for the effective functioning of cardiomyocytes in laboratory settings. Key characteristics of tropoelastin, such as its adjustable elasticity and compatibility with biological systems, contribute to this suitability. Furthermore, this microfluidic platform could be employed to assess the safety and effectiveness of drugs under conditions that resemble physiological environments. However, it should be noted that this simplified extracellular matrix (ECM) approach may not fully replicate the intricacies of cardiac ECM composition.

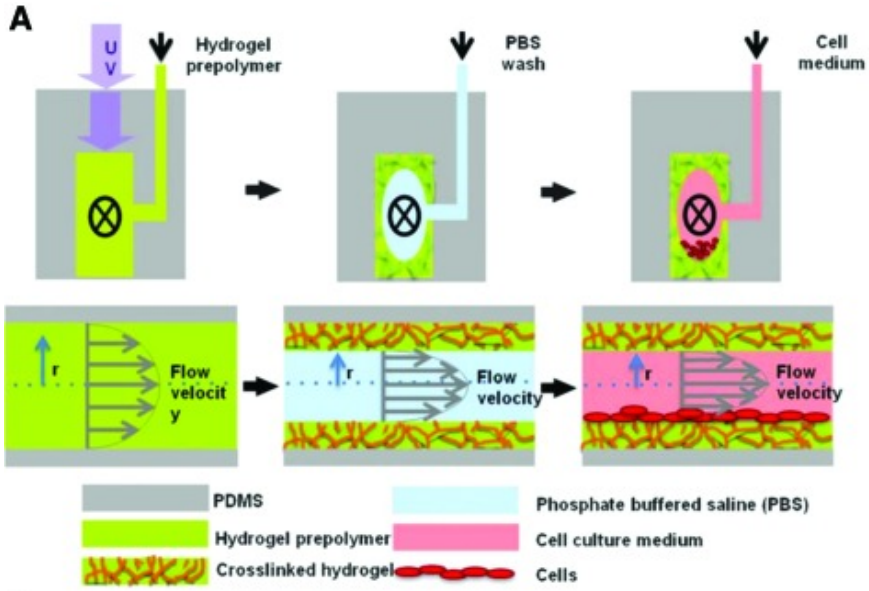

Figure 5: Diagram of microfluidic model for cultivating CM [13].

Grosberg et al. [14] employed a technique called muscular thin film (MTF) to fabricate a heart-on-a-chip model featuring cardiomyocytes (CMs) with anisotropic organization (Figure 6).

The MTF platforms were generated by microcontact printing fibronectin patterns on a thin, flexible polydimethylsiloxane (PDMS) film, which was subsequently seeded with primary neonatal rat ventricular CMs.

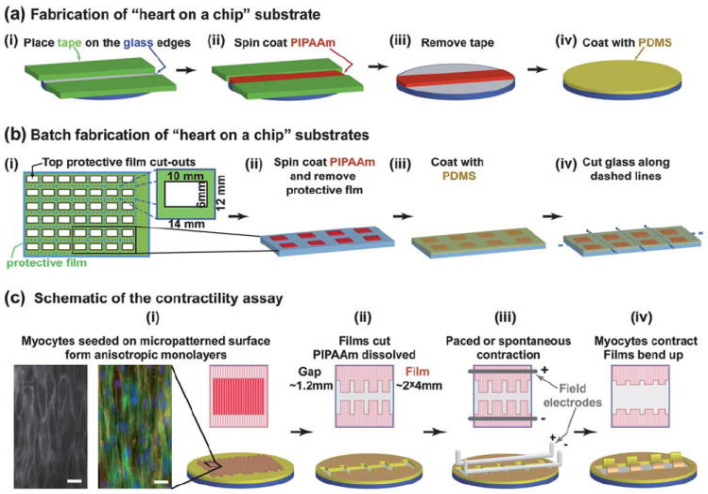

Figure 6: Grosberg et al. "Heart on a chip" assembly [15].

Additionally, the CMs on the functionalized surface were subjected to electrical stimulation through platinum electrodes. This electrical stimulation aimed to replicate the generation of electrical signals by pacing cells observed *in vivo*.

Furthermore, the electrical stimulation enhanced cellular alignment, differentiation, and functionality of the engineered cardiac tissue. The study successfully demonstrated the measurement of contractile behavior and electrophysiological properties, such as the morphology of action potentials, in the MTFs. Consequently, these measurements were used to assess the impact of pharmacological interventions on the contractile function of multiple cardiac microtissues by conducting a dose-range experiment to evaluate the effect of different epinephrine concentrations on contraction frequency based on the MTF contractility stress profiles. These findings showcased the potential of MTFs within a microfluidic chip to evaluate contractility in the presence of drugs or physiological cues like hydrodynamic, mechanical, and electrical stimuli. It is worth noting, however, that while this 2D monolayer of CMs allows for the analysis of cardiac microtissue deformation in a 3D-like manner, it cannot fully replicate the complex 3D microenvironment found in myocardial tissue.

An analogous MTF strategy was utilized to construct an aluminum-based microdevice designed for conducting high-throughput pharmacological assessments involving isoproterenol (Figure 7). This platform presented the benefit of employing a semi-automated manufacturing method that could be expanded and automated for enhanced screening of drugs. Additionally, the device integrated a metallic heating component, electrodes, and a transparent upper layer, enabling concurrent control of temperature, electrical field stimulation, and optical contraction analysis, respectively. Leveraging the microfluidic device's capacity for high-throughput analysis, the impact of isoproterenol on the contractile stress of MTFs was investigated.

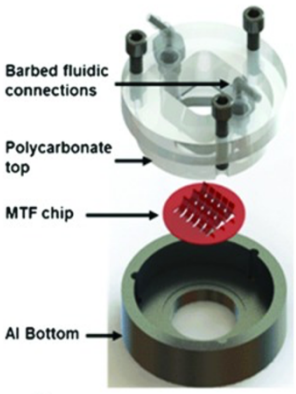

Figure 7: Heart-on-a-chip microdevice [16]

Furthermore, in 2020 was published an an Abulaiti et al. study called “Establishment of a heart-on-a-chip microdevice based on human iPS cells for the evaluation of human heart tissue function” [17], where a research team developed a heart-on-a-chip microdevice (HMD) as a novel bioassay system in ordet to evaluate the function of human iPSC-derived cardiac microtissues. It was done by integrating two different fundamental technologies, human iPSC technology and MEMS (Micro Electro-Mechanical System)-based organ-on-a-chip technology. The hypothesis was that the HMD recapitulates heart tissue function by validating the ability of the system to respond to electrical simulation and dose-dependent inotropic drug administration.

The microfluidic chip (Figure 8) made of polydimethylsiloxane (PDMS) and lacking check valves consisted of four main parts: the microchannel, chamber, diaphragm, and push bar. The microchannels were created using a replica molding technique and a silicon wafer, employing PDMS prepolymer (Silpot 184 W/C, Dow Corning Toray, Tokyo, Japan) and photoresist (SU-8 3050, Nihon Kayaku, Tokyo, Japan). The dimensions of the microchannels were approximately 200 µm in depth and width. The remaining components were constructed using PDMS sheets that were 1 mm thick.

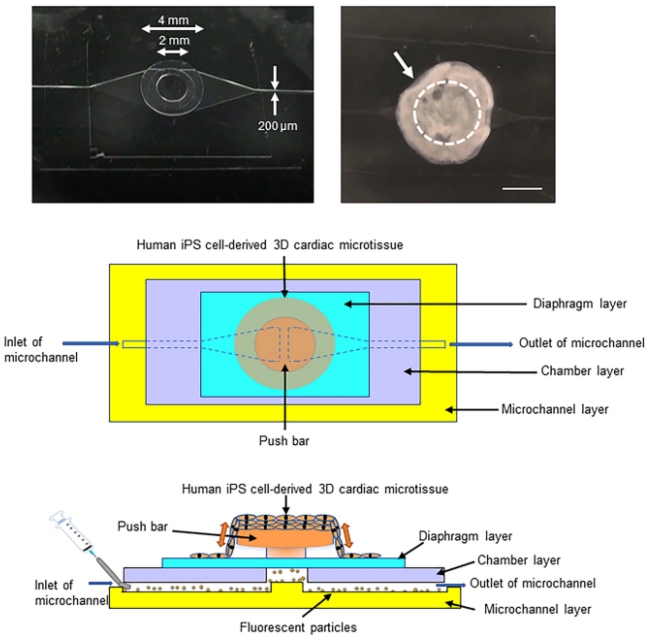

Figure 8: Preparation of HMDs [18]

The push bar was formed by cutting out cylinders with diameters of 2 mm and 4 mm from the PDMS sheet and stacking them together. This push bar was then assembled onto a 100-µm-thick diaphragm. The chamber was created by cutting a circle with a 3-mm diameter from a 100-µm-thick PDMS sheet. The different parts of the microchip were aligned and stacked in the desired arrangement. To bond all the components together, vacuum oxygen plasma treatment was performed at a power of 15 W and an oxygen flow rate of 5 mL/min for 0.5 minutes using a compact etcher (FA-1, SAMCO, Kyoto, Japan).

To enhance the adherence of 3D cardiac microtissues, they subjected the microfluidic chip to sterilization and coated it with a solution containing 50 µg/mL of fibronectin from bovine serum (Sigma, St. Louis, MO, USA) in phosphate-buffered saline (PBS) at 37 °C overnight. Once coated, the 3D cardiac microtissues were manually transferred onto the microfluidic chip and allowed to stabilize for 2 hours without medium. Subsequently, medium was added to create the heart-on-a-chip microdevice (HMD). The next day, they observed that the 3D cardiac microtissues displayed spontaneous beating and were well-attached to both the push bar (located at the center of the microtissue) and the diaphragm layer (situated at the periphery of the microtissue) of the microfluidic chip.

Finally, one of the most similar approximations of the microdevice that is proposed that can be found was shown in López-Canosa et al. article named "A microphysiological system combining electrospun fibers and electrical stimulation for the maturation of highly anisotropic cardiac tissue" [19]. They presented a microphysiological system designed to mature highly anisotropic cardiac tissue using a combination of electrospun fibers and electrical stimulation. The system was developed to address the limitations of traditional cell culture methods and can be used to model disease states and test drugs. The authors described the design and fabrication of the microphysiological system (Figure 9), which consists of a biocompatible electrospun scaffold that mimics the anisotropic structure of native cardiac tissue, and an electrical stimulation system that provides physiologically relevant cues to the cells. The system was evaluated using neonatal rat ventricular cardiomyocytes, and the authors found that the combination of the scaffold and electrical stimulation led to the maturation of highly anisotropic cardiac tissue. The authors also discussed the potential applications of the microphysiological system, including the modeling of diseases such as arrhythmias and the testing of drugs for cardiac toxicity.

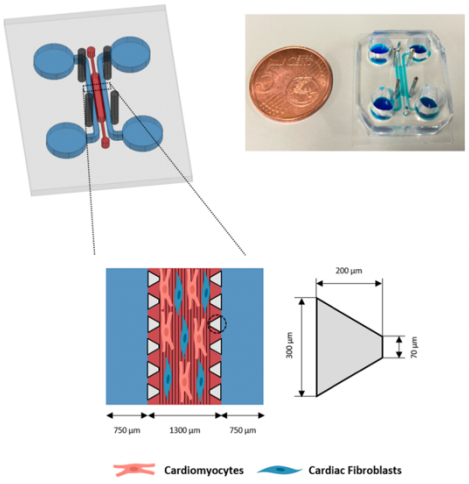

Figure 9: López-Canosa et al. microdevice [19]

The system has the potential to provide a more accurate representation of in vivo conditions and could lead to the development of more effective therapies for cardiac diseases. Overall, the article demonstrated the potential of combining biocompatible materials and electrical stimulation to create microphysiological systems that can be used to study and treat various diseases. The microchip was characterized by the assembly of external electrodes, as shown in Figure 10.

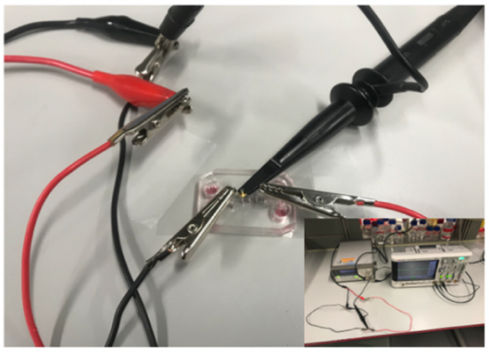

Figure 10: Setup to perform the voltage measurements [19]

2.3. State of the situation

This project is part of a big project carried by Dr. Oscar Castaño Linares, named "An Instrumented Microfluidic Platform as an Electrophysiologically Relevant Myocardium Model (uCardioChip)", supported and financed by the Ministry of Science and Innovation, the European Union, and the State Research Agency.

Over the past decade, the SIC-BIO group at the University of Barcelona (UB) and the research groups led by Prof. Elisabeth Engel and Prof. Josep Samitier at the Institute for Bioengineering of Catalonia (IBEC) in Barcelona have been pursuing two main research directions simultaneously:

1. They have been working on enhancing the potential of various biodegradable 3D biomaterials to enhance and regulate healing processes in different tissues, including the cardiac tissue.

2. Additionally, they have been developing novel Organ-on-a-Chip (OoC) devices specifically designed to assess the bioactivity of biomaterials.

Regarding the current project, they recently made advancements in two key areas. Firstly, they have developed a novel microphysiological system that combines electrospun fibers with electrical stimulation to promote the maturation of highly anisotropic cardiac tissue. This system has been used to investigate the effects of lactate ions as dedifferentiating signals.

Secondly, they have successfully designed and created a prototype microfluidic platform aimed at studying the impact of proangiogenic signals, such as calcium or lactate ions, on the neovascularization process. This platform allows for the investigation of how these signals influence the formation of new blood vessels.

Furthermore, two members of their research team have contributed to the development of a cardiac macrotissue that can apply continuous electrical stimulation. This stimulation has demonstrated the ability to align and synchronize cardiomyocytes, and the resulting processed signals resemble those observed in electrocardiograms. These studies have been conducted under both healthy and proarrhythmic conditions.

This previous work has been with a 2D cardiac cells matrix implementation and microdevice characterization carried out by using external electrodes.

The uCardioChip project aims to develop a more complex compact device that accurately replicates myocardium tissue, using internal electrodes and a 3D cardiac cells matrix. This project aligns with the primary thematic priority of "Health" outlined in the "Plan Estatal de Investigación Científica, Técnica y de Innovación 2021-2023". Specifically, it falls within the strategic line of "New Diagnostic Techniques" while also being relevant to the areas of "Precision Medicine and Therapeutics" and "Cancer and Geroscience: Aging, Degenerative Diseases".

3. Market analysis

3.1. Area of interest

Cardiovascular disease (CVD) stands as one of the primary causes of death, for instance the first one in the United States, affecting approximately 85.6 million individuals. This leads to a staggering a lot of deaths per day within, accompanied by an annual cost of billions of dollars, a figure that is expected to rise further. Consequently, there is an urgent requirement to develop new drugs that can either prevent or treat CVD. Despite this demand, the number of newly approved pharmaceutical compounds per research and development expenditure has shown a steady decline, halving every approximately nine years since 1950.

While scientific and technological fields have witnessed exponential progress, the field of drug development has not experienced a similar trend over the past six decades. Nonetheless, spending in pharmaceutical research and development continues to rise. These circumstances indicate a pressing need for a disruptive technology capable of enabling a more predictive and efficient drug discovery and development process. Such a technology has the potential to facilitate the discovery of novel and improved drugs for treating CVD, thereby alleviating the burden faced by patients at present.

Due to this diminishing number of approved new drugs and the difficulties encountered with preclinical models, there is a projected strong demand of cardiovascular organ-on-a-chip models from the pharmaceutical industry. Moreover, the use of microfluidic heart-on-a-chip platforms enables precise manipulation and regulation of the crucial elements involved. This advancement offers unique prospects for investigating cardiac physiology, pathology, and pharmacology. Specifically, these platforms show significant potential in the creation of high-throughput assays, which could prove invaluable in drug screening and toxicity assessments. [20]

3.2. Historical evolution of heart-celled microfluidic devices

As observed, there has been a growing trend in the development of new potential models aimed at simulating cardiac tissue in recent years in order to perform drug development and disease modeling research, as in recent years cardiovascular health problems have been growing and have gained increased attention [21].

During the beginning of the 21st century, Mike Shuler introduced the concept of utilizing cells from various human organs to construct tissue on a chip, aiming to replicate the human physiological environment. One notable advancement in this field was the development of the lung-on-a-chip by Huh et al. in 2010, which garnered significant interest. Subsequently, in the years that followed, successful fabrication of chips representing organs such as the liver, kidney, heart, gut, blood vessels, skin, bone marrow, and the blood-brain barrier (BBB) was also achieved.

In 2011, Grosberg et al. and their team introduced a heart-chip structure using muscle membrane technology. They placed neonatal rat CMs onto a flexible membrane, and electrical stimulation induced contractions in the CMs, causing the membrane to curl. The extent of curling provided

valuable information about the contractile behavior of the myocardial cells. Expanding on this work, Agarwal et al. and his team employed laser engraving techniques to create smaller muscle membrane chips. They also integrated optical cardiac contractility measurements with microfluidic devices, enabling efficient testing of cardiac function on a large scale. Marsano et al. further improved chip design by considering the physiological microenvironment of cardiac myocytes and incorporating biomechanical factors. Experimental findings demonstrated that cyclic stress played a significant role in strengthening the bonding within the chip, leading to exceptional physiological performance of the engineered heart tissue. With this background, heart-celled microfluidic devices started to be fabricated in 2015.

In recent years, the use of 3D printing technology and direct laser writing (DLW) photolithography has become increasingly prevalent in the field of microfluidics. Zhang et al. built upon previous work and utilized 3D bioprinting to fabricate endothelialized myocardial tissue. Human umbilical vein endothelial cells (HUVECs) were able to migrate around the microfiber scaffold, forming a vascular bed. Cardiomyocytes were then introduced into the scaffold to create an endothelialized myocardium, with this process taking place on a hydrophobic PDMS surface. This construct can be employed for drug screening when cultured in a microfluidic perfusion bioreactor.

Recently, Alan et al. discovered that alginate and cross-linking agent precursor solutions had detrimental effects on cardiomyocytes. The bio-ink used for bioprinting contains gelated alginate, but its impact on cardiomyocytes within microfluidic bioreactors remains to be fully understood. Meanwhile, Sun et al. developed a colored hydrogel by polymerizing non-close-packed colloidal arrays onto super-aligned carbon nanotube sheets (SACNTs). The anisotropic and electrically conductive properties of this structure contribute to the organization and beating of cardiomyocytes. Moreover, by combining the color hydrogel with a microfluidic device, visual heart sensing can be achieved, as the cell pulsations cause optical changes in the hydrogel deformation.

Jayne et al. designed a heart chip that integrates microfluidic actuators and mechanical sensors. The structure was created through DLW and soft lithography techniques. Notably, it features 3D self-assembly, customizable growth of heart tissue with specific shapes, and real-time monitoring of tissue stress. Furthermore, the chip's relatively small size allows for integration with standard 384-well or 24-well plates, offering the potential for high-throughput screening.

Despite the success of conventional two-dimensional (2D) animal (for instance, rats) cell cultures and animal disease models in advancing therapeutics, they often fall short in accurately replicating human *in vivo* conditions. That is why human cardiac cells began to be used in microdevice fabrication. While obtaining and working with human cardiac cells may be more challenging and require additional ethical considerations, they offer more precise and reliable outcomes. Even though it can replace animal models to a certain extent, 2D culture of human cells in vitro still has disadvantages at the time of simulating the real cell microenvironment and results in the loss of cell function.

The disparities between human biology and these animal models emphasize the need for improved and more predictive *in vitro* models based on human systems. Ideally, these models should encompass platforms that allow for the integration and control of biochemical, physical, and

electrochemical factors, enabling the replication of dynamic tissue microenvironments observed *in vivo* [22]. After years of development, various laboratories have successfully established and thoroughly characterized a range of different models, but there is yet a lot of research, design, fabrication and characterization to do before reaching a totally human heart-like microsystem [23].

3.3. Future perspectives

Research teams and companies are actively addressing several challenges in the field, including standardization, optimization, and scaling up for large-scale production. While the scientific community focuses on innovation and creating new platforms, the growth of companies in this area could lead to their optimization for standardized processes, reproducibility, and scalability. Successfully addressing these key challenges will enable the widespread use of cardiovascular organ-on-a-chip technology in drug discovery and facilitate regulatory endorsement. The potential impact of these technologies in drug discovery and development is expected to be significant (Figure 11). There are current opportunities to enhance performance in later stages of lead optimization and improve safety and efficacy in early stages of preclinical studies. Additionally, it can be anticipated that these technologies will have a substantial impact on preclinical stages soon and enable personalized medicine approaches at later stages.

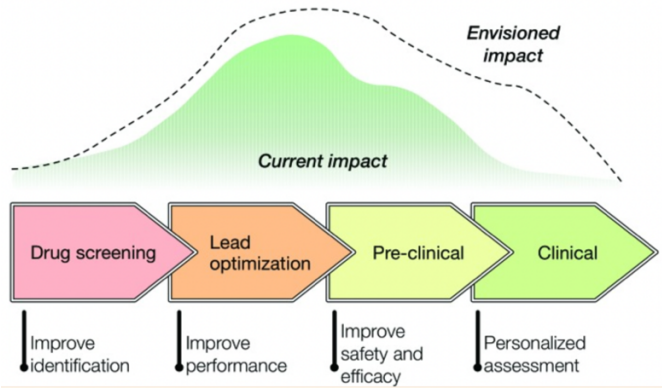

Figure 11: The influence of organs-on-a-chip technologies on the process of drug development

Concretely talking about heart-on-a-chip development, additional challenges involve determining the essential design criteria for the composition and arrangement of the extracellular matrix (ECM) necessary to accurately replicate the characteristics of the heart. This may entail conducting high-throughput screenings of various ECM compositions, among other methods. Moreover, while the 2D monolayer of CMs allows for the analysis of deformation in cardiac microtissue, it lacks the ability to replicate the 3D microenvironment of actual myocardial tissue. To address this limitation, a possible future solution would be to combine cellular encapsulation with microengineering techniques to create aligned 3D microtissues.

4. Concept engineering

4.1. Study of solutions

As demonstrated, the significance of modeling the heart has spurred the creation of diverse models and designs. However, this project specifically focuses on implementing a single model. To determine the most suitable model for this project, an additional investigation into potential solutions has been conducted. The proposed solution will be chosen not only based on the advantageous characteristics of the model itself but also taking into account practical considerations such as economic feasibility and time constraints.

This solutions study is divided into different parts, focusing on each part of the total microfluidic device and its characterization.

The review of existing literature in section 2.2 provides an overview of various models developed to simulate the heart or work with cardiac cells. These models exhibit differences not only in their design but also in their intended applications. Therefore, it is crucial to evaluate their strengths and weaknesses in order to make an optimal decision about the specific type of microfluidic organ-on-a-chip system suitable for cardiac tissue and cell applications that will be implemented in this project.

4.1.1. Electrodes

The first elements indispensable for this project are the microelectrodes, which have to be integrated into the microfluidic device. These electrodes must have a specific size and shape because of their electric properties. Depending on these two elements, the impedance, the resistance of the system can be changed.

4.1.1.1. Theoretical introduction

Before presenting the different options of the electrodes design, a theoretical introduction of which kind of electronic system is going to be created must be accomplished to better understand the options selected.

The system in question consists of different elements such as electrodes, medium and cardiac cells. As the complete system is too complex, a simpler model of it is proposed.

First, let's see a system between the electrodes (two electrodes) and the medium (liquid) (Figure 12):

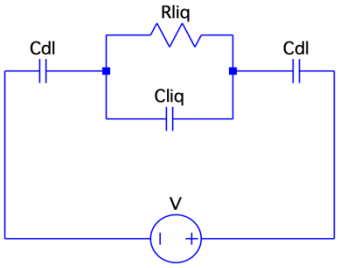

Cdl = double-layer capacity. This capacity always exists when leaving the electrode.

Rliq = liquid resistance

Cliq = liquid capacity

Figure 12: Circuit system electrode-medium

A system between the liquid and one cell would be the one shown in Figure 13. Thus, a complete system, considering the electrodes, the cell and the medium would be the one shown in Figure 14. This approximation is quite complicated and not real enough (there is actually only one cell, for instance) to make it worthwhile to fix it this way. There has to be found, then, a more realistic approximation; it has to be easier to solve.

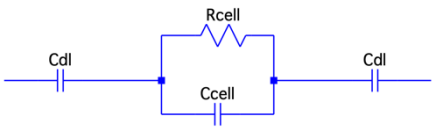

Figure 13: Circuit system cell-medium

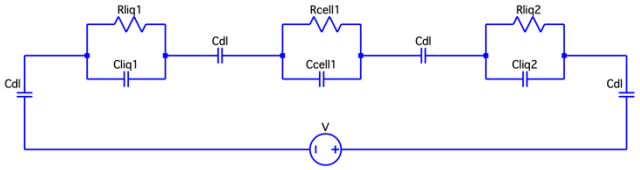

Figure 14: Circuit system cell-medium

As said before, two electrode plates act as a capacitor. The capacity (relationship between the charge Q on each of the plates and the potential difference V between them: C=Q/V) that appears between each one of the electrodes and the medium is called double-layer capacity (influence charge layer due to the presence of an electrode) (Figure 15).

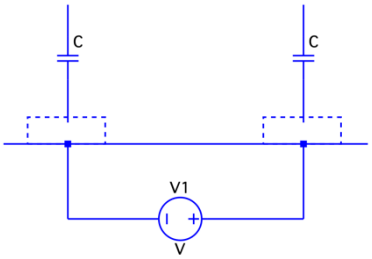

Figure 15: Capacitor (system of two electrodes in contact with the medium)

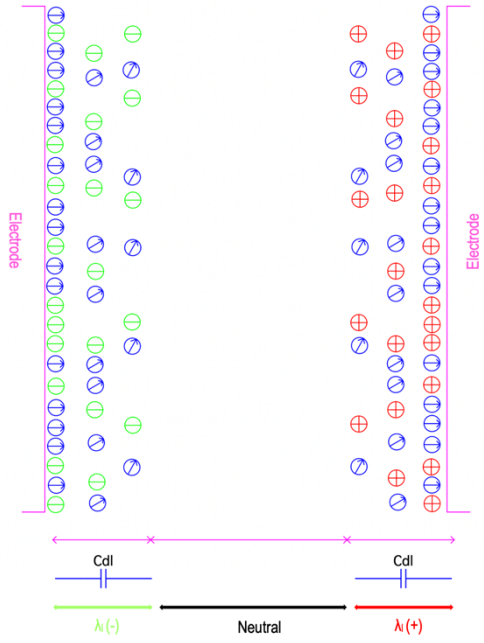

Figure 16: Capacitor effect on the medium charges

In this system, what happens is that there is a charge condensation on the electrode surface and near it. In one of the plates, the charges that accumulate are positive, and in the other one, the charges are negative. As the medium is a liquid and it is composed of water (dipolar molecule), its molecules are also located on the surface of the electrodes and near them in the form of a dipole. These molecules are oriented with the electric field and take up a lot of space on the surface. The structure can be better seen in Figure 16.

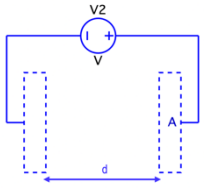

Figure 17: Plano-Parallel plates system

It must be also considered that in an ideal case of two-faced electrodes (Plano-Parallel plates) system (Figure 17), the capacity is the one shown in Equation 1. If the area of the electrode increases, the capacity does it too, but the dissociation impedance decreases, as shown in Equation 2.

$$C = \frac{A \cdot \varepsilon_o}{d} \quad (1) \qquad Z_c = \frac{j}{wc} \quad (2)$$

A simpler model, then, is released (Figure 18). We also must take into account that the parasitic capacity of the system, it is, everything that is capacitive but that does not go through the circuit (what goes through the glass of the microchip, for instance). Then, the system would be the one shown in Figure 19. In this model, the parallel RC circuit composed of Rm and Cm behaves as a single R.

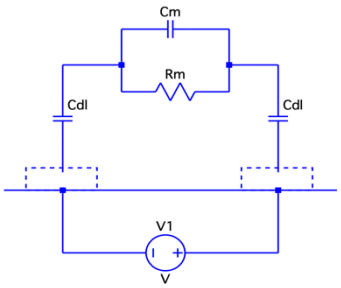

Figure 18: Circuit electrode-medium with cells

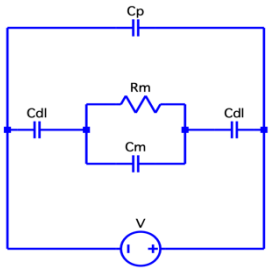

Figure 19: Completed modeled system

Cm = Medium capacity

Rm = Medium resistance

Medium = Cells + liquid

Cp = Parasitic capacity

Once achieved the total system, it is modeled in two different parts: The first one is shown in Figure 20, and the second one, in Figure 21.

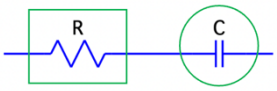

Figure 20: Part 1. RC series circuit

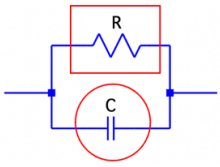

Figure 21: Part 2. RC parallel circuit

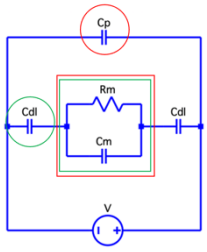

Figure 22: Completed modeled system

Part 1: RC in series circuit

The equivalent impedance of a RC in series system is computed and its module is calculated for low (Equation 4) and high (Equation 5) frequencies.

$$Z_{eq} = R - \frac{j}{wc} \Rightarrow |Z_{eq}| = \sqrt{R^2 + (\frac{1}{wc})^2} \quad (3)$$

For low frequencies: $\omega \to 0 \Rightarrow |Z_{eq}| = \sqrt{R^2 + (\frac{1}{wc})^2} = \frac{1}{wc} \Rightarrow C$; only the capacity intervenes. (4)

For high frequencies: $\omega \to \infty \Rightarrow |Z_{eq}| = \sqrt{R^2 + (\frac{1}{wc})^2} = \sqrt{R^2} = R \Rightarrow R$; only the resistance intervenes. (5)

In order to do the graphical representation, it is transformed into a logarithmic scale:

Capacitive component

$$log|Z_c| = -log(w) - log(C) \quad (6)$$

Resistive component

$$Z_R = R \quad (7)$$

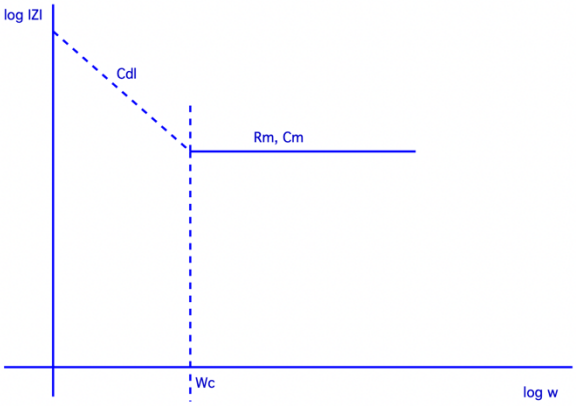

As it can be seen in Figure 22, if there is a concrete Zc, as higher is the resistance (R), lower the ωc would be (the lines would intersect sooner). Depending on the C value, the intersection between the lines would be before or after (considering, for instance, that R doesn't change).

Figure 22: Schematic of the RC in series circuit

Part 1: RC in parallel circuit

The equivalent impedance of a RC in parallel system is computed and its module is calculated for low (Equation 4) and high (Equation 5) frequencies.

$$\frac{1}{Z_{eq}} = \frac{1}{R} + jwc = \frac{1+jwRC}{R} \Rightarrow Z_{eq} = \frac{R}{1+jwRC} = \frac{R}{1+w^2R^2c^2} + j\frac{wR^2c}{1+w^2R^2c^2} \Rightarrow \quad (8)$$

$$\Rightarrow |Z_{eq}| = \sqrt{\frac{R^2}{(1+w^2R^2c^2)^2} + \frac{w^2R^4c^2}{(1+w^2R^2c^2)^2}} \Rightarrow |Z_{eq}| = \frac{R}{\sqrt{1+w^2R^2c^2}} \quad (9)$$

For low frequencies: $\omega \to 0 \Rightarrow |Z_{eq}| = \frac{R}{\sqrt{1+w^2R^2c^2}} = R$; only the resistance intervenes. (10)

For high frequencies: $\omega \to \infty \Rightarrow |Z_{eq}| = \frac{R}{\sqrt{1+w^2R^2c^2}} = \frac{1}{wc} \Rightarrow C$; only the capacity intervenes. (11)

In order to do the graphical representation, it is transformed into a logarithmic scale:

Capacitive component

$$log|Z_c| = -log(w) - log(C) \quad (12)$$

Resistive component

$$Z_R = R \quad (13)$$

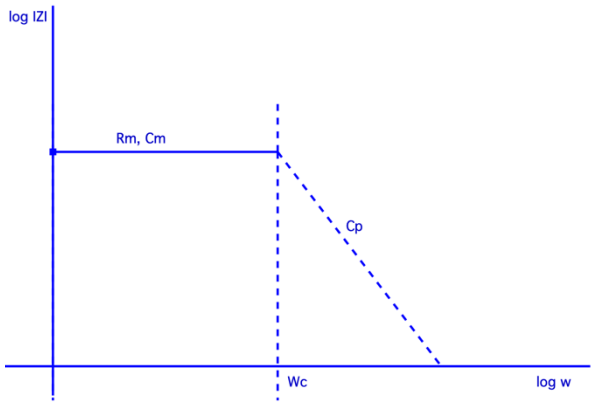

As it can be seen in Figure 23, like what happens in Part 1, if there is a concrete Zc, as higher is the resistance (R), lower the ωc would be (the lines would intersect sooner). Depending on the C value, the intersection between the lines would be before or after (considering, for instance, that R doesn't change). In this case, though, the first line is the one corresponding to the resistive part.

Figure 23: Schematic of the RC in parallel circuit

Finally, if the two parts (two circuits, Figure 22 and Figure 23) are joined, the total schematic of the system is the one shown in Figure 24.

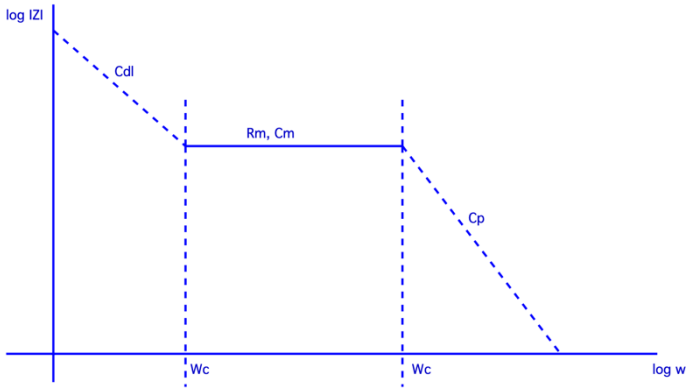

Figure 24: Schematic of the total modeled system

The resistance of the system is the one given by Equation 14. Thus, the more distance (L) between electrodes, the more resistance the system has. Moreover, the more area of the electrodes (A), less resistance the system has.

$$R = \frac{L}{A \cdot \sigma} \quad (14)$$

4.1.1.2. Design

The design of the electrodes is the first step to follow for its posterior fabrication. There have been two different options in terms of number of electrodes and their consequent distribution. Different elements that contribute to this election must be considered:

- Size of the coverslip.
- Size of the microchannels and the space they occupy in the coverslip.
- Size of the ends of the electrodes, which have to be placed on the coverslip but out of the microchannels scaffold.

Thus, there have been proposed the following options:

Full electrode-covered chamber design

This first design (Figure 25) consists of placing the maximum number of electrodes as possible covering all the central chamber (Figure 25, a). The electrodes are of a size of 50 µm, and there is a space of 150 µm between each one of them (Figure 25 b). There is a total amount of 45 electrodes with their respective ends. Going from left to right of the microchannels design, the electrodes go from a little before the first channel to a little further than the second channel. Moreover, the ends of the electrodes (Figure 25, c) are squares of 2 mm of side, the distance between them is of 50 µm and the separation from the end of the coverslip is of 60 µm.

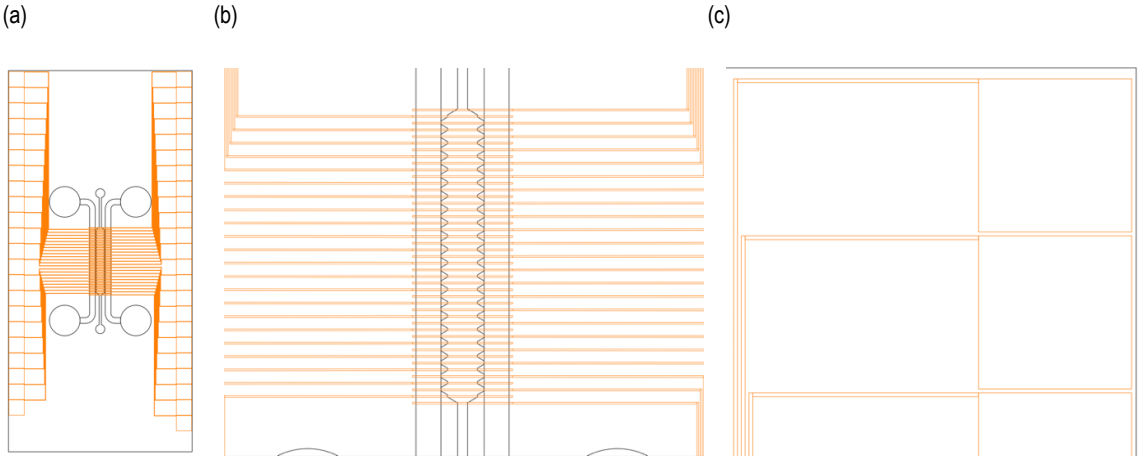

Figure 25: First option of the electrodes design. a) View of the coverslip and the total electrode design. b) View of the size of the electrodes and the distance between them. C) View of the ends of the electrodes and the distance between them.

Eight-modelled electrode design

The second design (Figure 26) consist of placing only eight electrodes in the zone of the central chamber (Figure 26, a). These eight electrodes are divided into two different groups. The first group is located at the upper side of the central chamber and the second group is located at the lower part of it (Figure 26, b). The principal idea of this design is that it allows different configurations, even maintaining the structure just mentioned. That is, that there can be different electrode sizes, different distances between electrodes and different distances between the two different groups of the electrodes (going from the lower end of the last electrode of the first group to the upper end of the first electrode of the second group). Furthermore, there is no distance left between the end of the electrode and the end of the coverslip (Figure 26, c).

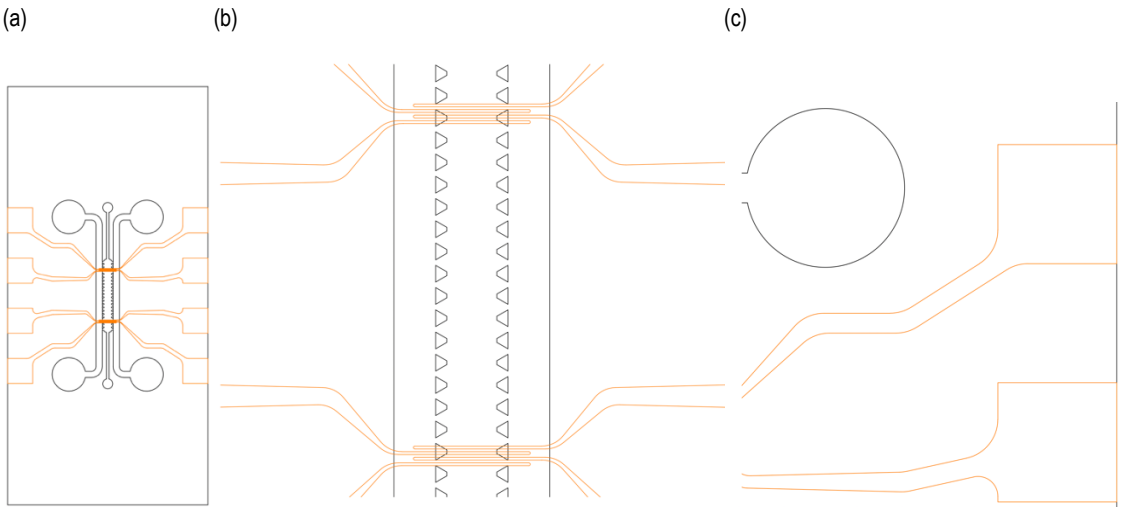

Figure 26: Second option of the electrodes design. a) View of the coverslip and the total electrode design. b) View of the size of the electrodes and the distance between them. C) View of the ends of the electrodes and the distance between them.

4.1.1.3. Materials

Traditional microelectrodes are typically fabricated using arrays of microwires or micro-electromechanical system (MEMS) arrays. Microwires are often made of metals such as gold, tungsten, and stainless steel, which are coated with insulating materials [24]. The choice of metal is based on the need for direct contact with biological tissue, resulting in reduced resistance [25]. Therefore, the microelectrodes must be biocompatible and suitable for long-term implantation. Among the most common electrode materials are gold (Au), silver/silver chloride (Ag/AgCl), platinum (Pt), iridium oxide (IrOx), and platinum-iridium oxide (Pt/IrOx) (Figure 27).

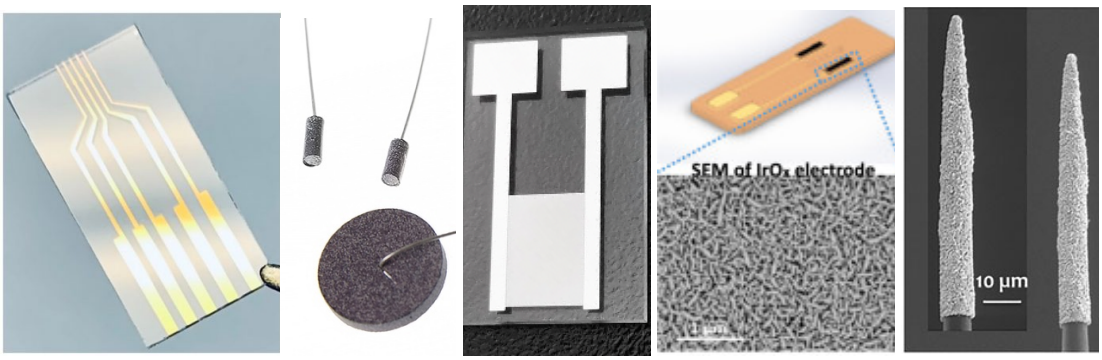

Figure 27: Different electrodes depending on the materials they are made of: a) Au [26]. b) Ag/AgCl [27]. c) Pt [28]. d) IrOx [29]. e) Pt/IrOx [30].

Ag/AgCl is considered the optimal material for DC-ECoG signal recording due to its nearly ideal non-polarization liquid-solid interface. However, biocompatibility studies have shown that it can cause extensive tissue necrosis, making it unsuitable for long-term in vivo monitoring and clinical applications.

Platinum (Pt) is widely used as an electrode material due to its low impedance and high charge storage capacity. However, some tests have revealed that gold (Au) electrodes exhibit greater stability in terms of reversible charge and capacitive behavior compared to Pt electrodes [31].

4.1.2. Microfluidic channels

4.1.2.1. Design

The design of the microfluidic channels has been partially reused from a previous design of some researchers of the group. Concretely, the design from a study called “A microphysiological system combining electrospun fibers and electrical stimulation for the maturation of highly anisotropic cardiac tissue” [19]. It has to be decided if the design remains the same (Figure 28) of if some modifications have to be done.

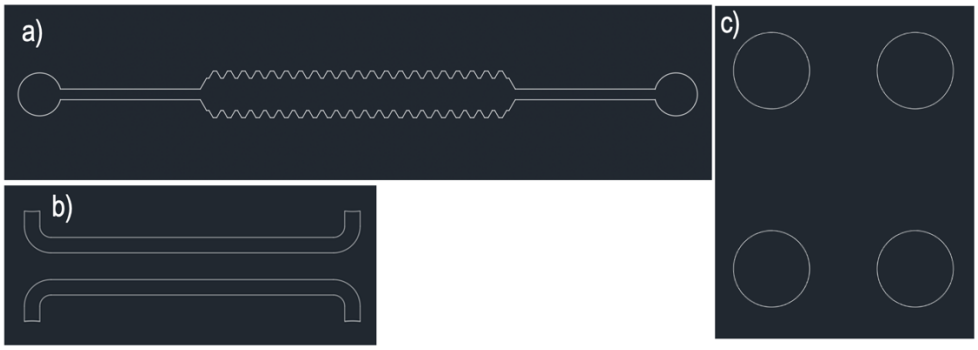

Figure 28: Microchannels previously done design: a) Central chamber b) Middle channels. c) Reservoirs.

This design, though, has too large reservoirs if we consider that the microdevice that has to be fabricated has to incorporate electrodes. As said before, the ends of the electrodes have to be placed outside the scaffold but inside the coverslip limits, and they must have a minimum size. With this minimum size, the ends of the reservoirs of this design would end up being cut off. For that reason, the new proposal is to reduce de size of this reservoirs, going from a size of 6mm of diameter to a size of 4mm of diameter. That way, the reservoirs would be inside the scaffold.

The design of the central chamber and the middle channels would be, more or less, the same, only changing in size in order to adapt them to the reservoirs size.

4.1.2.2. Materials and techniques

To achieve a realistic model that accurately reproduces all the characteristics of in vivo cardiac tissue, it is crucial to make specific material choices during the fabrication of the microdevice. Thus, the scaffold material used to perform the replica of the mold of the design carried out. There are different options to choose:

- **PDMS (Polydimethylsiloxane)**: it is known for its cost-effectiveness, malleability, biocompatibility, and optical transparency, and allows for easy visualization through imaging methods. Furthermore, it is non-toxic, non-flammable, permeable to gases and water, and possesses a considerable level of flexibility. PDMS is frequently used in the creation of Organ-on-a-chip Systems due to its biocompatible, non-toxic, and affordable properties. Moreover, PDMS is an elastomeric and transparent substance that can be quickly prototyped and tailored into a microfluidic system using soft and photolithography techniques. Nevertheless, the hydrophobic characteristics of PDMS impose restrictions on cell attachment and spreading. This issue can be overcome by treating the PDMS surface with proteins such as fibronectin, which promote cellular adhesion [32].

- **PET (Polyethylene terephthalate)**: this material has been explored in various studies as a scaffold material [33]. As a member of the polyester family, PET exhibits high flexibility and appears colorless and semi-crystalline in its original form. Its rigidity can vary depending on the processing method employed, ranging from semi-rigid to rigid. PET assumes a semi-crystalline structure once it stabilizes. Notably, PET is recyclable and

possesses resistance against impact, moisture, alcohols, and solvents. Moreover, PET is well-suited for transparent applications when quenching is applied during processing [34].

- **PTFE (Polytetrafluoroethylene)**: it is an incredibly versatile plastic fluoropolymer with an ivory-white and opaque appearance. It is created through the free-radical polymerization of numerous tetrafluoroethylene molecules and finds utility across a wide range of applications. Researchers have conducted studies [35] involving microchannels constructed from this material. PTFE boasts remarkable flexibility, resistance to chemicals and heat, non-stick properties, and electrical resistance. It exhibits high flexural strength, even in low temperatures, and possesses exceptional electrical resistance and dielectric strength. Its resistance to water is attributed to the high electronegativity of fluorine, and it also exhibits a low coefficient of friction. Furthermore, it has a high-density of 2200 kg/m3. However, it is not resistant to high-energy radiation, which can lead to the breakdown of PTFE molecules [36].

- **PMMA (Polymethyl methacrylate)**: it is a thermoplastic material that offers transparency and improved light transmission compared to other materials, like PDMS. It also exhibits greater chemical stability and compatibility with organic solvents. However, a limitation of PMMA is its challenging processability when it comes to creating intricate micro or nano structures [37].

- **ECM (gels)**: When it comes to ECM gels, collagen is a highly viable material choice. By altering the materials used, such as the degree of crosslinking, polymer composition, and treatment method, the properties of hydrogels can be readily adjusted. This includes modifying biocompatibility, porosity, and stiffness. Hydrogels are well-suited for co-culture systems as they can be loaded with astrocytes, pericytes, and neurons [38].

4.2. Chosen solution

In this section all the chosen options of the different elements presented in the last section are represented in Table 2. It shows which options are for each element and the one highlighted is the one selected.

Table 2: Schematic comparison of the suggested solutions and highlighting of the chosen one.

CHARACTERISTIC	OPTIONS				
ELECTRODES DESIGN	Full electrode-covered chamber design			**Eight-modelled electrode design**	
ELECTRODES MATERIAL	**Au**	Ag/AgCl	Pt	IrOx	Pt/IrOx
MICROCHANNEL DESIGN	Already done design model			**Modified design model**	
SCAFFOLD MATERIAL	**PDMS**	PET	PTFE	PMMA	ECM gels

Moreover, in order to better understand the structure the microdevice must have to store the cardiac cells and the medium, a schematic has been done and shown in Figure 29. The surface of the coverslip where the central chamber is placed on is covered with electrospun fibers, placed one next to the other parallelly. Then, the CMs are introduced to the central chamber, and they are expected to be aligned with the fibers and placed on them.

In this project, though, not only fibered cell-filled microdevices are fabricated, but also chips without fibers with cells, chips with fibers without cells and chips without fibers without cells.

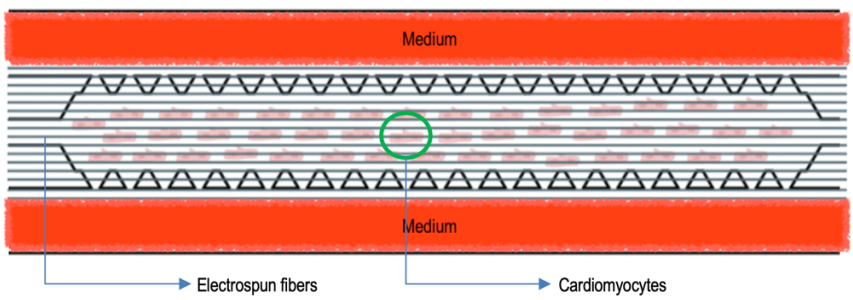

Figure 29: Design of the components of the desired microfluidic OoC

After conducting a comprehensive analysis of all potential solutions, carefully considering their attributes and drawbacks, a final decision has been reached. This decision considers the specific application of the project and how well each option aligns with its requirements. Moreover, economic and time aspects have influenced the final decision.

The design of the electrodes has to be chosen considering that, as mentioned before, as their geometric area decreases, the electrode impedance increases, making the corresponding potential drift more prominent. The electrodes must be as large as possible while being at a distance as small as possible. But too many electrodes are not wanted so that there isn't so much margin for error due to interference. It is also wanted to see the difference in impedance measurements between electrodes that are quite far away, to corroborate what has just been discussed. For these reasons, the design chosen to be used in this project is the Eight-modelled electrode design.

As previous explained, Gold (Au) electrodes demonstrate enhanced stability in terms of reversible charge and capacitive behavior. So, for what concerns the election of the electrodes material, the winner option has been Gold material. The material and its properties are totally in line with the desired microdevice functionality, but it has to be also said that the decision of this choice has been made considering economic and time aspects, and material and machines availability.

On the other hand, for the microchannels design it has to be considered that the previously design done has a reservoirs size too for them to fit inside the scaffold material, as the wanted microchannels have to be placed on the electrodes placed on the coverslip. That is the reason why the selected design of this project is a modified design model, it is, it has to change and incorporate smaller reservoirs.

For the decision of the scaffold material it has to be chosen one of the options presented before. Even though, for instance, PMMA offers improved light transmission than PDMS, this last material is frequently used in the creation of Organ-on-a-chip Systems due to its biocompatible, non-toxic, and affordable properties. In this project, the used scaffold material is also PDMS, because of these properties and because is the one that was available for the research group.

Finally, different microdevice scenarios have been created. This means that not all the microchips have been filled with cells, and also means that not all the microdevices filled with cells contain fibers for them to be attached. The ones that don't are filled with a specific protein that has adhesion properties. PLA material has been used to cover the coverslip with fibers for the cardiac cells to attach to them, and it has been done with an electrospinning process. On the other hand, Fibronectine has been used to do the coating of the cells (of other chips different from the ones containing the PLA fibers) in order for them to be placed on the surface of the chips and see the difference compared to the fibered chips.

5. Detail engineering

To effectively execute the project and bring the theoretical concept into practical realization, a set of procedures needs to be undertaken. This section provides a comprehensive explanation of all the essential processes and protocols that must be adhered to in order to successfully create a microfluidic device.

As previously stated in this paper, the objective is to fabricate and sense a microdevice that incorporates electrodes and involves the introduction of cells into a microfluidic system. The intention is to create a structure in which the properties, structure, and functions of these cells closely resemble those of the heart.

First, the design of the microchip must be done. It includes de design of the microchannels and also of the microelectrodes. Everything has to be precise because the coverslip has a determinate size and all the components have to fit in there, without crossing the limits. Once the designed is done, the following step is to fabricate the different elements that conform the microdevice. On one hand, the mold of the microchannels has to be done for its consequent replication. This replication is done by introducing a semi-solid material into the mold; this way, the design becomes a 3D structure. On the other hand, the electrodes have to be fabricated on the surface of the coverslip. Then, the replica has to be detached from the mold and placed on the electrodes (on the coverslip containing them).

Parallelly, the cardiac cell culture has to be maintained during the days. The medium has to be periodically changed, and only a fraction of the cells than grow every day has to be moved to another container. Then, the day of cell seeding, the process has to be the same but there has to be one more step to do: their introduction to the microchannels.

Finally, to assess the electrical properties of the system and characterize the microchip, an impedance study has to be realized. This characterization is done by using a concrete machine and the results have to be saved for their discussion.

A summary of all the processes that have to be performed is shown in the following list:

- Design of the elements of the microdevice.
- Fabrication of the elements of the microdevice.
- Coupling of the different elements.
- Cell maintenance.
- Cell seeding.
- Characterization of different devices.

The next sections explain all these processes in detail and show the results that have been obtained, with their corresponding discussion.

5.1. Design

5.1.1. Electrodes

The first step of the microdevice realization is to design the electrodes. As mentioned in the last section of this project, the electrodes design chosen to be used in this project is the Eight-modelled electrode design.

This task has been realized by using AutoCAD, a computer-aided design program and drafting software application developed and marketed by Autodesk. The design has consisted of two separated zones with 4 electrodes in each part. The electrodes are placed at the middle of the design in order to be placed at the same zone as the central chamber of the microchannel part of the device. Then, each electrode has a prolongation that goes to a square end, right up to the limit of the coverslip.

There have been designed different models of this configuration. It means that the structure has been the same in all models, but the size and distances have varied. Three things have been changed:

- The width of the electrode itself (Figure 30, a).
- The distance between the electrodes (between two electrodes) (Figure 30, b).
- The distance between the two groups of electrodes (Figure 30, c).

For the electrode's width, there have been two different options, one of 50 µm and one of 100 µm. Then, for each one of them, there have been two different options considering the distance between the two groups of electrodes, one option of 4650 µm of distance, and the other of 6500 µm of distance. Finally, for each one of these models, there have been three different options considering the distance between electrodes. This last characteristic has been different depending on the first one (the width of the electrode), it is, for the model of 50 µm electrode width, the three options of distance between electrodes have been of 50 µm, 100 µm and 150 µm. For the model of 100 µm electrode width, the distances have been of 100 µm, 200 µm and 300 µm (it can be seen that these measures have been decided by taking firstly the size of the electrode, then multiplying by 2 for the second one, and multiplying by 3 for the last one). Each electrode has been related to a title indicating all these measures.

If we do the calculus, in total twelve models of electrodes have been designed. All the different models are shown in Annex D.

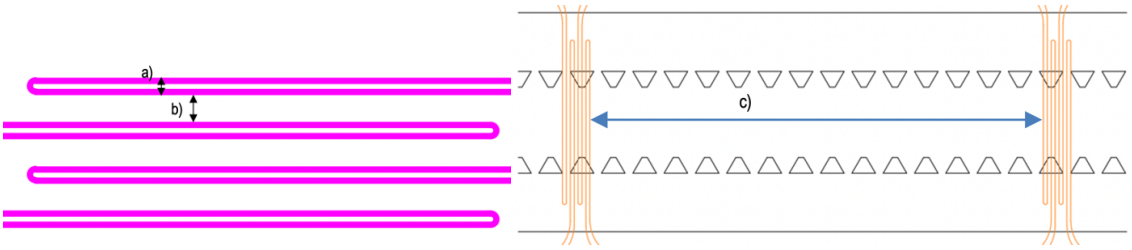

Figure 30: Different distances that have varied of the electrodes design. a) Width of the electrode. b) Distance between the electrodes. c) Distance between the two groups of electrodes.

5.1.2. Microchannels

As mentioned in the last section of this project, the design chosen to be used in this project is the modified design model.

This task has been also realized by using AutoCAD. The design consists of a central chamber with an inlet and an outlet, two lateral channels and four reservoirs (two for each lateral channel). The central chamber and the lateral channels are connected. That is because there are apertures at both sides of the chamber, the sides seem like they are isosceles trapezoids (Figure 30) one next to the following one. This way, the medium can go from the channels to the central chamber by diffusion.

There have been designed two different models of microchannels, only differing in the width of the central chamber. The first model has a central chamber size (Figure 31, a) of 1300 µm, and the second one, a size of 2600 µm. The reservoirs has a size (Figure 31, b) of 4 mm of diameter and the inlet and outlet (Figure 31, c) of the central chamber has a diameter size of 1 mm. Moreover the size

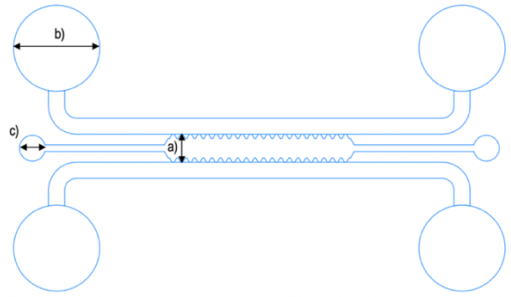

Figure 31: Designed model of microchannels. a) Central chamber size. b) Size of the reservoirs. C) Size of the inlet and outlet.

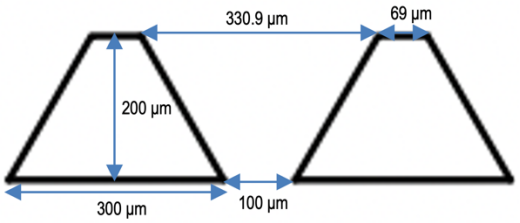

Figure 32: Size of the isosceles trapezoids

5.1.3. DinA4

Once the electrodes design and the microchannels design have been done, they have been placed in the same DinA4 for them to be ready to send to print. The twelve electrodes models have been duplicated, as there has been space in the DinA4 to do it, and there have been placed six microchannels designs with a chamber width of 1300 µm, and six others with a chamber width of 2600 µm. Each group of six has been placed inside a circle (it is useful to do for its posterior replica fabrication). Figure 33 shows the final total design for the microdevice. Moreover, this figure is enlarged in the Annex 2.

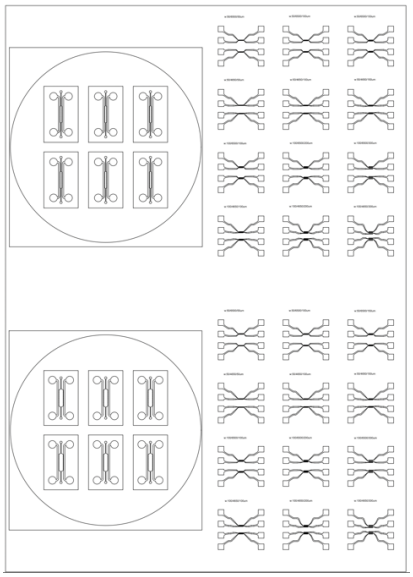

Figure 33: Total microdevice design

5.2. Fabrication

5.2.1. Electrodes

The fabrication of microelectrodes is a complex undertaking, demanding the utilization of highly precise techniques and specialized equipment. Their fabrication has taken place inside a clean room located at the IBEC.

5.2.1.1. Materials and machines

As mentioned in the last section of this project, the material chosen to be used in this project for the electrodes fabrication is the gold material.

Furthermore, the materials needed for the fabrication of the electrodes wanted are coverslips, an acetate mask with the pattern, MR-DW2 resin, gold, titanium, resin developer, isopropanol, acetone, tweezers, Petri dishes, and support materials like rags and soap. Moreover, there have been used different types of machines: a mask aligner, a plasma cleaner, a spinner and hot plates for the photolithography process; an evaporator-sputtering for the gold placement; an ultrasonic sonicator for the lift-off and a nitrogen gun for the cleaning process. Also, a profilometer and an optical microscope have been used for the process characterization.

5.2.1.2. Fabrication technique

In this section the fabrication process of the electrodes is detailed. As said before, the fabrication has been done in a clean room, with a previous security tour and a training of the techniques. Photographs of the process, materials and machines are shown in Annex 3.

First of all, the design, together with the microchannels design, has been sent to a photomask printing company named Output City [39]. This company has sent back the design printed on an acetate photomask. The design is sent with the printing information. In this case, about the polarity, the outside area (DinA4) has been white and the emulsion has been placed on the back side. The change of color from white to black and vice versa happens when there is a new closed area, from the outside to the inside. Figure 34 shows the color pattern of the printed design. There is a logical reason why the patterns are white or black, and it's explained next.

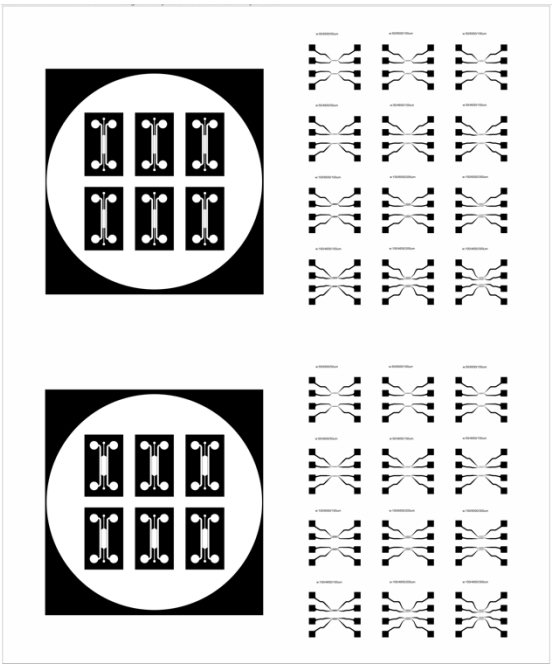

Figure 34: pattern of the photomask

There has been used a concrete photoresist in order to carry out a photolithography process. This resin has been a negative one. So, as the result of a UV light exposure, the negative resist

remains on those parts the light has impacted. With a chemical bath process, the parts of the resist that has not been exposed to light will be lifted off. For the electrodes, the gold material has to be placed on the surface where this resist has been lifted off, it is, on the holes of the coverslip surface covered with resin. For this reason, the color of the electrodes of the acetate mask has to be black, in order to not letting the UV light to go through them and thus form holes with their shape.

Once got the acetate mask, as mentioned previously, the fabrication process can start. The first step is very important for the optimal result of the hole process, and it consist of the cleaning of the coverslips where the electrodes have to be placed on. Firstly, the glasses are cleaned with soap and put into a plastic recipient filled with acetone. This recipient is placed in an ultrasonic sonicator for 10 minutes. Then, it is emptied, refilled with acetone and placed again in the sonicator 10 minutes more. Once cleaned, the coverslips are dried with a nitrogen gas gun and placed 15 minutes on a 90ºC hot plate. The next step is placing them in a plasma cleaner for 30 seconds at 0.8 torr.

When everything is cleaned, the photolithography process is carried out. First of all, 2 µm of a negative resin called MR-DWL2 are placed on the coverslips by a spinning process (two phases of the spinning process: one of 10''/500rpm/100acc, and one of 30''/3000rpm/300acc). When finishing this, the soft bake is done by placing them on a 50ºC hot plate for 2 minutes and after on a 90ºC hot plate for 4 minutes. Then, they are subjected to a UV light exposition using a mask-aligner machine, at 120mJ/cm^2 of intensity for few seconds. Next, they post bake is done by placing them again on the hot plate (the same time an Tº as before). Finally, the coverslips are placed on a recipient with resin developer for 1 minute for the resin that has not been exposed to the UV light to be detached from the coverslip surface. As said before, the resin that is going to be detached is the one that has adopted the shape of the electrodes; that's why the shape of the electrodes are holes in the resin.

Now the coverslips are ready to be put inside the evaporator to incorporate the gold layer by the sputtering technique. The evaporation consists of a two-material deposition on the coverslips. As the gold does not attach well to the glass surface, before its deposition there is a titanium layer placement on the coverslip of 20 nm of thickness. Then, two phases of 50 nm gold deposition are carried out to obtain a total gold thickness of 100 nm. Finally, the coverslips are put again in a recipient filled with developer and placed in the ultrasonic sonicator. This way the lift-off process is started, making the resin with gold on it to detach and only leaving the gold that has been placed on the glass. The fabrication process is represented in Figure 35.

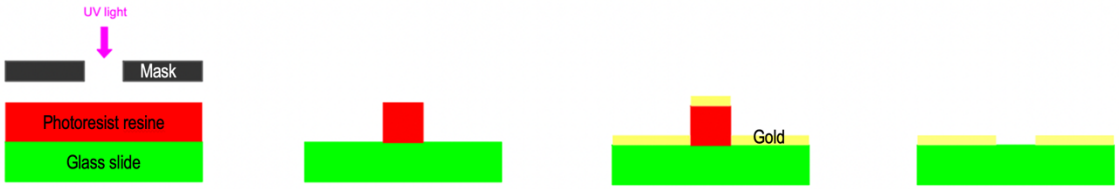

Figure 35: Electrodes fabrication process

5.2.1.3. Results

During and after the electrodes fabrication process, there have been different results to be considered and that have been characterized in order to assess whether the processes have been giving the optimal results expected. Figure 36, a), shows the resulting pattern of the initial design on the acetate mask. After doing one photolithography test to see how the mask patter transmits to the resin, it has been seen that, as the edges of the electrodes' ends are transmitted just on the also edges of the coverslip, at the end the holes made in the resin communicate each one with the others. That is because the resin never places uniformly at the edges of the surface where it is on. That is the reason why Figure 36, b), shows the real acetate mask used in this project, it is, the same mask but with the lateral edges a little bit cut. Furthermore, Figure 36, c), shows the pattern on the coverslip after the light exposure and the first resin detachment and Figure 36, c), shows the final result of the gold electrodes on the coverslip surface. In total, there have been fabricated 16 different electrodes, 4 replicas of 4 different designs (w:50/4650/100um, w:50/6500/100um, w:10/4650/100um and w:100/4650/100um).

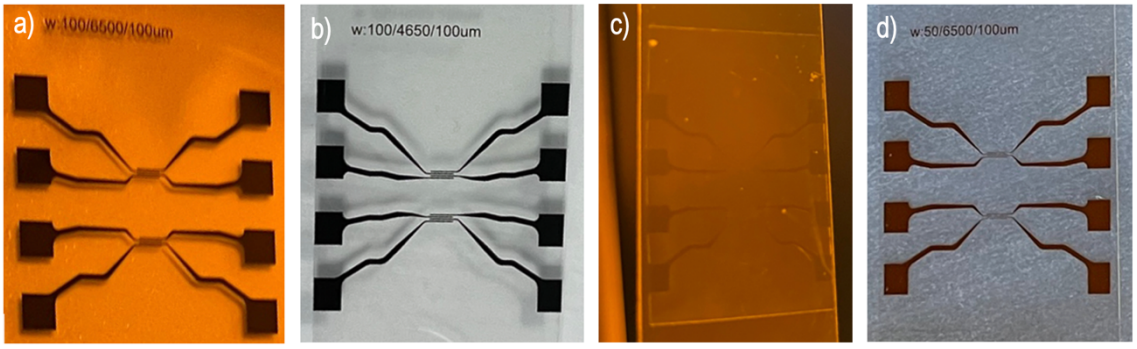

Figure 36: Electrodes fabrication results. a) Pattern of acetate mask. b) Pattern of acetate mask after cutting the borders. c) Pattern on coverslip after the UV exposure and the 1st resin detachment. d) Gold electrodes on the glass coverslip surface.

For the characterization of these fabrication results, as said before, a profilometer and an optical microscope have been used. The profilometer has given the real thickness of the gold layer (remember that it has to be of 120 nm: 20 nm of titanium layer and 100 nm of gold layer), and the optical microscope has given the real measures of the electrodes.

For instance, Figure 37 is an optical microscope image that shows the sizes of a w:100/4650/100 electrode after its total fabrication. As it can be seen, the sizes match with the designed ones: 100 µm between electrodes and 100 µm of electrode's width.

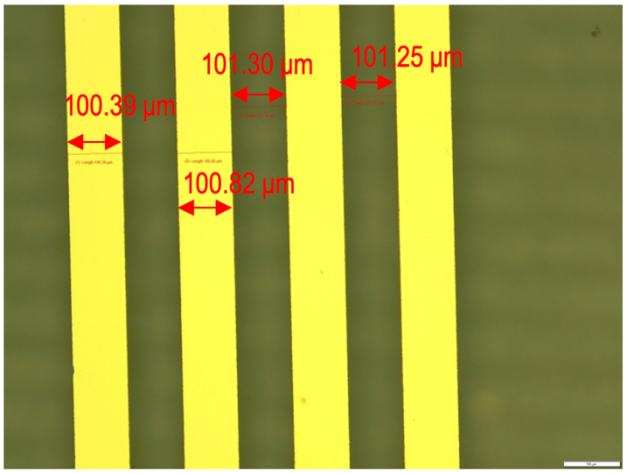

Figure 37: Electrodes: gold.100.4650.100 10X_Meas

5.2.2. Microchannels

The fabrication of the microchannels is also a complex process, demanding the utilization of highly precise techniques and specialized equipment too. Their fabrication has also taken place inside a clean room located at the IBEC.

5.2.2.1. Materials and machines

As mentioned in the last section of this project, the material chosen to be used in this project for the microchannels fabrication is the PDMS. Also, the master to be replicated with this PDMS has been a silane wafer.

Furthermore, the materials needed for the fabrication of the microchannels wanted are an acetate mask with the pattern, SU-8 resin, resin developer, PDMS, isopropanol, acetone, tweezers, Petri dishes, and support materials like rags and soap. Moreover, there have been used different types of machines: a mask aligner, a plasma cleaner, a spinner and hot plates for the photolithography process; a vibrating platform for the chemical bath; a nitrogen gun for the cleaning process; and a vacuum chamber for the silinization process and also for the soft-lithography process, which also requires an oven. Also, a profilometer, a contact angle machine, and an optical microscope have been used for the process characterization.

5.2.2.2. Fabrication technique

In this section the fabrication process of the the microchannels is detailed. As said before, the fabrication has been done in a clean room, with a previous security tour and a training of the techniques. Photographs of the process, materials and machines are in Annex 4.

First of all, the design has been transferred to an acetate mask just the same way as the electrodes previously explained. Then, the fabrication of the microchannels has been done by following two different processes: photolithography and soft lithography (replica), schematically shown in Figure 38.

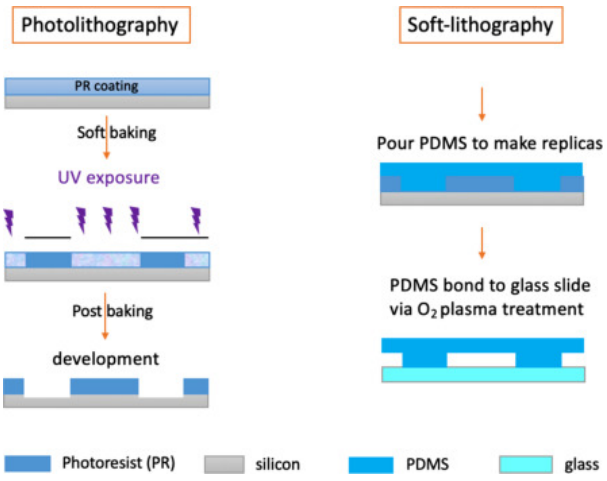

Figure 38: Photolithography and soft lithography processes [40]

Photolithography

First of all, two silane circular masters (two because there have been fabricated 12 designs, 6 in each one) have been placed on a 200ºC hot plate for 15 minutes. Then, they have been subjected to a plasma treatment for 30 seconds at 0.8 torr. Next to that, the SU-8 negative resin have been placed on the surface of the master, and through two different spinning process (each process has had two phases of spinning: one of 10"/500rpm/100acc, and one of 30"/1900rpm/300acc) this resin has formed a 150 µm layer on the master. After the first process,

the masters have had to be placed on a 95ºC hot plate for 40 minutes (soft bake), and after the second process, it has been done the same.

After the resin deposition, the exposition has been carried out. The masters have been placed in the mask-aligner and they have been exposed to UV light at 120mJ/cm^2 of intensity for 21.95 seconds (120mJ/12.3mW = 21.95s. This 12.3 has been extracted from the calibration of the mask-aligner machine). Once finished this process, the masters have been reposed for 10 minutes for the acids' liberation. Then, a post bake has realized by placing the masters on a 65ºC hot plate for 5 minutes and then on a 95ºC hot plate for 12 minutes. After this time, the masters have been introduced in two Petri dishes filled with SU-8 developer and placed on a vibrating platform for 15 minutes. Then, the masters have been transferred to another two Petri dishes filled with Isopropanol and few time later cleaned and dried off with a nitrogen gas gun.

Once cleaned, the masters have been placed again on a 95ºC hot plate for 30 minutes and after that on a 65ºC hot plate for 10 minutes (hard bake). Finally, they have been introduced into a vacuum chamber with silane molecules for 1 hour. This process is done in order to make the silane master surface hydrophobic to avoid the PDMS to attach to the silane surface when doing the soft-lithography process. Inside the vacuum chamber, the silane molecules places on the master's surface and create covalent bonds with it. These molecules also have a fluor tail that provides the hydrophobic characteristic needed to the surface. The mold of the microchannels then have been ready to be used for the soft-lithography process.

Soft-lithography

Soft-lithography is a mechanical process that allows the processing of elastomeric polymers and patterning of surfaces using PDMS to create the replicas of the resulting molds of the photolithography.

Soft lithography implies several steps. The first one is already done: the creation of the hard master. This master has been placed and taped on a Petri dish surface for it to be fixed and for the optimal extraction of the PDMS after the process. Then, the PDMS has to be poured into this Petri dish. This PDMS solution has been previously prepared. There are two reagents needed: the silicon elastomer and the curing agent (Sylgard 184), and they have a ratio of 1/10. Thus, to obtain a thickness of 1.1 cm, for the Petri dish used, the quantities needed are 120g of the elastomer and 12 of the curing agent. Then, the Petri dishes have been placed into a vacuum chamber for at least 30 minutes to get the bubbles removed. Finally, the Petri dishes have been placed on a 65ºC oven for at least 2 hours to solidify.

5.2.2.3. Results

Once the fabrication is done, there have been used some techniques to characterize the results obtained in order to assess whether the processes have been giving the optimal ones expected. There has been only fabricated one of the two models of microchannels (according to central chamber width), the one with a central chamber of 1300 µm of width, 12 of them, it is, 2 masters of 6 each one.

Figure 39: Microchannels molds fabrication results. a) Pattern of acetate mask. b) Pattern on the silane wafer after the UV exposure and the resin detachment. c) Final resulting pattern on the silane wafer after de salinization.

A profilometer has been used in order to determine if the resin has been uniformly placed everywhere and that it has a thickness of 150 µm. There have been 5 different measurements for each master, four points in the corners and one in the middle. The different measures are shown in Table 3 and Figure 40 is an example of how the resulting graphic of the machine is.

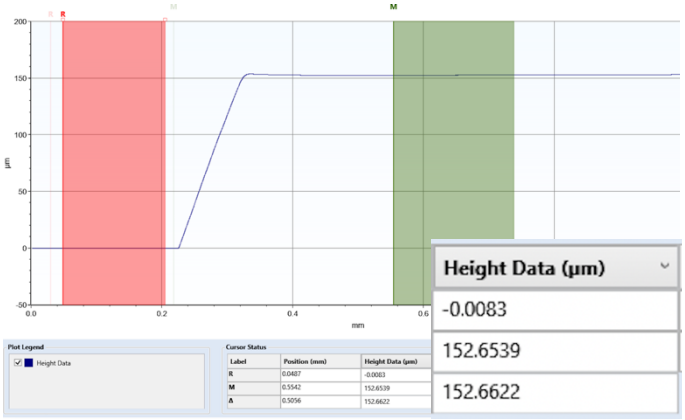

Figure 40: Profilometer resulting graphic. 152.65 µm.

Furthermore, using a contact angle machine it has been possible to determine if the silane master's surface have been correctly hydrophobized. A water drop is placed on the surface and if the angle it forms with the surface is bigger than 100º, it is considered to be hydrophobic. In all the points measured, the angle is bigger than 100º, as seen in Figure 41, so it can be said that the silinization process has been successful.

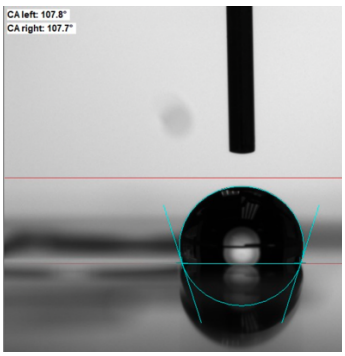

Figure 41: Contact angle result. 107.8º

Table 3: Results of the profilometer of both masters.

POINT	MASTER 1	MASTER 2
1	152 µm	152 µm
2	159 µm	153 µm
3	148 µm	158 µm
4	152 µm	158 µm
5	146 µm	153 µm

Lastly, an optical microscope has been used in order to see if the chamber isosceles trapezoids of the central chamber have the expected size. The two sets of 6 microchip channels have been visualized and measured. The measures have been taken after doing the photoresist detachment. Figure 42 shows the results.

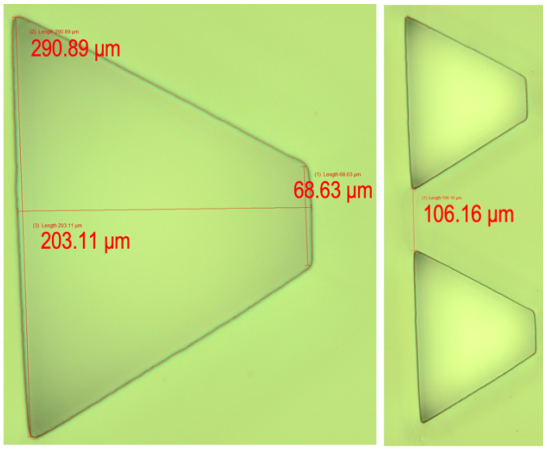

Figure 42: Results of trapezoids measurements of Mater 1.

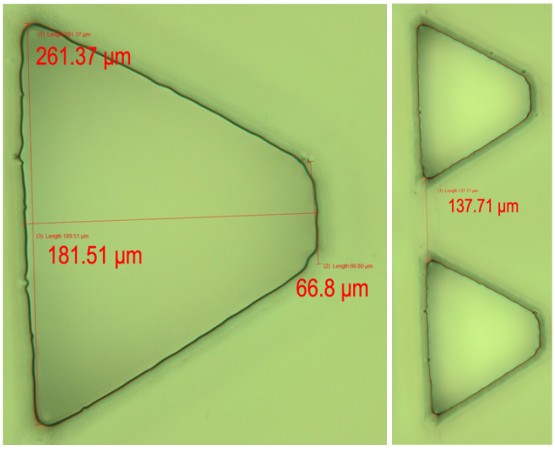

Figure 43: Results of trapezoids measurements of Mater 2

As it can be seen, the results of the Master 1 match the design, but something has happened with the Mater 2, as the distances are not even close to the ones designed (Figure 32) (taking into account that the measurement unit is the µm, differences at the macroscale that could be considered small, here suppose changes). This could be due to a wrong alignment of the mask with the wafer, maybe placing the side of the ink the wrong way. Even though, some of the microchannels taken from the Master 2 have been posteriorly used to do the characterization of the complete chips.

5.3. Cardiac cells

5.2.1. Cell and medium composition

The cardiac cells employed in this study are HL-1 cells. Derived from the atrial tissue of mouse hearts, the HL-1 cell line represents a type of cardiac muscle cells. Widely utilized in cardiac research, this cell line closely replicates the characteristics of primary cardiac myocytes and exhibits the ability to exhibit spontaneous rhythmic contractions.

The cells have been cultured following the protocol recommended by the Sigma-Aldrich laboratory. Claycomb medium has been used and supplemented with 10% FBS (Fetal Bovine Serum), 100 µg/ml of penicillin/streptomycin, 0.1 mM of norepinephrine, and 2 mM of L-glutamine (Table 4). The addition of norepinephrine is crucial for preserving the contractile phenotype of the cells.

Table 4: Supplemented Claycomb Medium

Product Name	mL	Final Concentration
Claycomb Medium	87	
Fetal Bovine Serum	10	10%
Penicillin/Streptomycin	1	100 U/mL:100 µg/mL
Norepinephrine (10 mM stock)	1	0.1 mM
L-Glutamine (200 mM stock)	1	2 mM

5.2.2. Cell maintainance

The cells have been taken from an existing cell culture from the research group that is supporting this project, and there has been the need of carry out medium change processes periodically. Also, in one of these processes, it has been taken only a fraction of the cells that have grown between two processes of changing the medium. Sometimes, in addition to changing the medium, this medium has had to be prepared.

The process of changing the medium includes different steps, like the trypsinization of the cells for them to detach from the surface of the flask they are into, the posterior addition of Soybean Trypsin Inhibitor to inhibit the trypsin effect once the detachment is done, the introduction of fibronectin to the new flask in order to make the surface adhesive for the new cells that have to be placed there, the counting of cells, the different centrifugation processes, the posterior redissolution of the pellet of cells and the visualization of the cells with an inverted phase contrast optical microscope. Figure 44 shows a microscope picture of the cardiac cells before introducing the trypsin. It can be seen that there are a lot, that they are attached to the surface and that even have created aggregates. Moreover, the colour of the medium liquid that is originally red has changed to an orange colour, which means that the nutrients have run out. On the other hand, Figure 45 shows another microscope picture of the cardiac cells after introducing the trypsin. It can be seen that they are not attached to the surface anymore, they are suspended in the liquid medium.

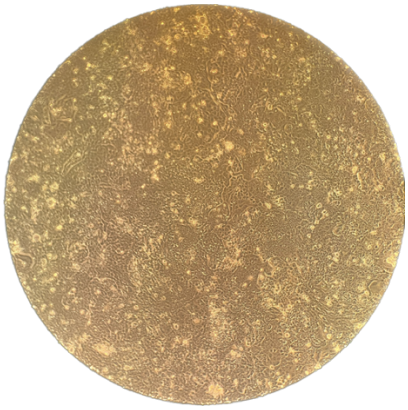

Figure 44: Cardiac cells before trypsinization

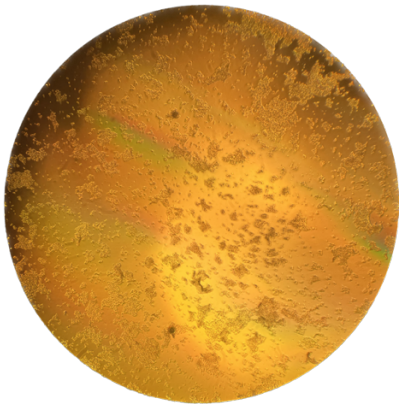

Figure 45: Cardiac cells after trypsinization

Explicative pictures from all the trypsinization process can be found in Annex 5. The protocol where the steps to follow and the materials that must be used are clearly explained are shown in Annex 6, provided by the same research group mentioned before.

5.4. Final coupling

This section explains how the coupling of the different elements of the microfluidic device have been carried out. As a reminder, those elements are the coverslips with the gold electrodes on their surface and the PDFS scaffolds with the microchannels sunk in them.

5.4.1. Electrospinning

First of all, the microchip thought for this project incorporates, at the surface of the glass coverslip with the electrodes on it, a layer of fibers for the cells introduced to be able to attach to the surface and align. As one objective is to characterize the microchip in different conditions, not all the chips have incorporated these fibers. From the 16 fabricated electrodes, only 8 (4 replicas of 2 different models) have been used to fabricate the chips, and only 4 of them have incorporate the fibers (2 of each model).

The fibers are made off a polymer called PLA (polylactic acid) 70/30. An 8% solution of PLA 70/30 in 2,2,2-trifluoroethano has been used. This PLA solution has been loaded into a 5ml syringe and delivered through a hand-held electrospinning machine.

Before start doing the electrospinning process, the coverslips have been cleaned with acetone, then placed on a sheet of aluminum foil and fixed with adhesion tape, as shown in Figure 46. Then, the aluminum sheet has been placed by using again adhesive tape on the collector of the electrospinning machine. This collector has a diameter of 90 cm, the needle of the syringe containing the PLA solution is approximately 10 cm away from it and it rotates at 1000 rpm. The syringe has been squeezed by hand until creating a bubble at the needle tip that has caused the continuous exit of the fibers, which have been collected by the collector, as well as deposited on the coverslips.

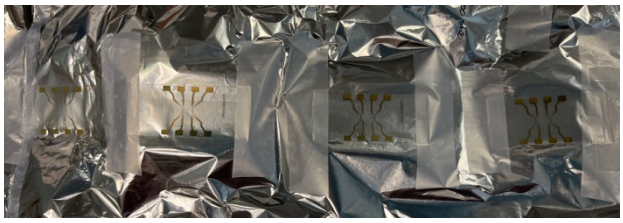

Figure 46: coverslips with electrodes placed on a sheet of aluminum foil.

Once the electrospinning process has been done, the coverslips have been removed from the aluminum foil by using acetone to break the fibers to only have at the end fibers remaining on the part of the electrodes where the central chamber is placed on.

5.4.2. Bonding

The next step is preparing the different elements to do their bonding. The coverslips with the electrodes have been cleaned up with acetone in a clean room. On the other hand, the PDMS has to be also prepared.

Firstly, a PDMS square containing the 6 designs has been extracted from the Petri dish where it was into. Then, each design has been cut and separated from it. Next, the holes of the inlet, outlet and the 4 reservoirs have been done using a punch. Once this done, they have been cleaned with soap, distilled or milli-Q water and stored in a new Petri dish. Then, these PDMS microchannels and the cleaned coverslips have been taken to the clean room of the Faculty of Physics and have been placed inside a plasma cleaner. This process is done for both surfaces to activate and leave the OH groups free to form a covalent bond between them and thus perfectly adhere. Finally, the bounded microchip has been placed on a hot plate during at least 2 hours.

5.4.3. Seeding of cells

From the total of 8 microchips coupled, 4 with PLA fibers and 4 without, only 4 microchips have incorporated cells inside. That is because in this project it is wanted to see if there are differences in impedance in different conditions. Moreover, only 2 of these 4 cell-filled microchips have PLA fibers. So, summing up, cells have been introduced into 2 fibered chips and into 2 non-fibered chips. Furthermore, these 2 non-fibered chips have been filled with fibronectin 45 minutes before the cell seeding. That is because, as the chips don't contain fibers, the cells can't attach to the surface and align. Fibronectin is a protein that gives adhesion to the surface, so when it is removed after those 45 minutes, the cells can attach to the surface of the coverslips.

Once all the microchips have been ready to be used, cell seeding has been carried out. Firstly, the cells have been introduced into the central chamber using a pipette. In each microchip have been introduced 10 µl of medium solution containing 150,000 cells. To do this solution, a cell counting has been carried out using a Neubauer chamber, then the cells have been centrifuged and redissolved in a new medium (of the wanted volume).

After 30 minutes of waiting after the cell seeding, medium has been introduced into 2 of the 4 reservoirs and suctioned from the other 2 to it to fill all the channels. Then, the 4 reservoirs have been filled again until their top, trying to avoid bubble formation.

Finally, the 4 microchips have been visualized with the microscope and then placed inside an incubator. Figure 47 shows the cells seeded inside a PLA-fibered microchip. This figure can be compared with Figure 29, the schematic done before. Figure 48 shows the cells seeded inside a non-PLA-fibered microchip (previously filled with fibronectin). It can be observed that cells have adhered more to the chip that has fibers than to the one that doesn't have.

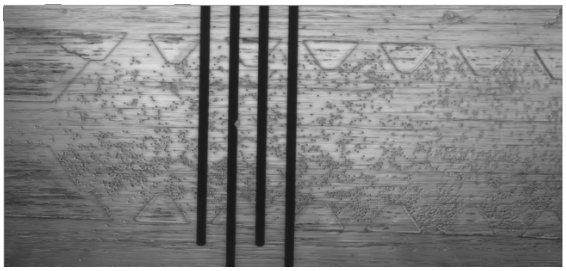

Figure 47: Cells seeded inside a PLA-fibered microchip.

Figure 48: cells seeded inside a fibronectin-filled microchip

After 35 hours incubating, the microchips with cells have been visualized again.

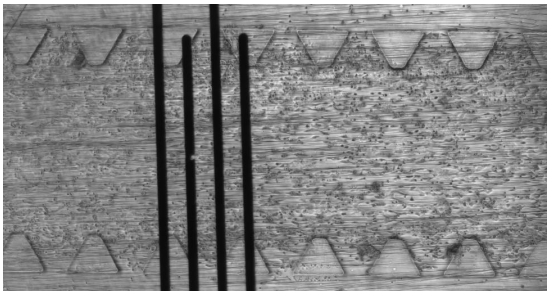

Figure 49: Cells inside a PLA-fibered microchip after 35h.

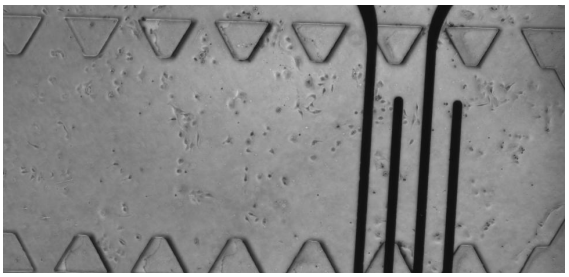

Figure 50: cells inside a fibronectin-filled microchip after 35h.

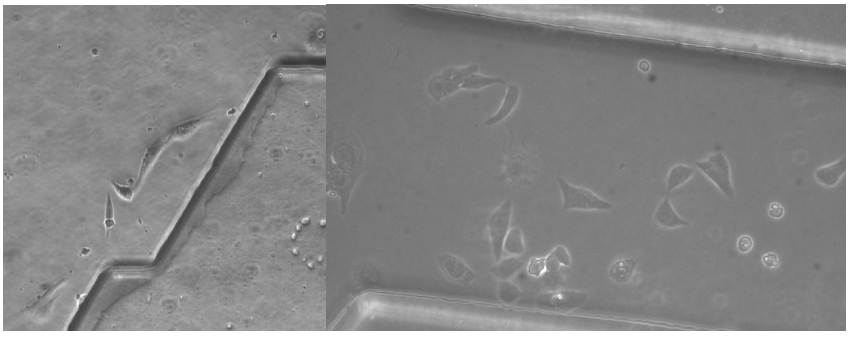

Figure 51: Cardiac cells well proliferating (coated chip)

As it can be seen in Figures 49, the cells have adhered to the fibers of the fibered microchip, and they are expected to be also aligned on them. This chip also has a lot of cells. On the contrary, not that many cells have been visualized in the non-celled microdevices, as shown in Figure 50. Maybe the reason of that is not waiting enough time from the introduction of the fibronectin inside the channels to the extraction of it in order to put the cells inside. Even though, it is also expected for them to grow, as the shape of some of the cells that have already been able to properly grow is what is being looked for, as shown in Figure 51.

After getting these results, it has been decided not to characterize these chips withs cells because the cells have not grown enough. It is important to note that once the microchips that contain cells are taken from the incubator and taken from the inside of the Petri dish, the sterile environment disappears. It means that after characterizing the device, all the cells inside are dead. For that reason, it has been decided to prolongate the waiting time to let the cells grow inside the microdevice. On the other hand, the remaining medium has been extracted from the reservoirs and new medium has been introduced before placing the microchips again in the incubator.

5.5. Device characterization

Once the microdevice design and fabrication have been done, the last part of this project has been carrying out a microdevice characterization. As mentioned before, at the end only two different microchips have been characterized. The first one is a w:50/6500/100 with electrospun fibers on the surface of the electrodes where the central chamber is placed on (50 µm of electrode's width, 6500 µm between the two groups of electrodes and 100 µm between electrodes) and the other is the same w:50/6500/100 but without electrospun fibers.

The characterization has consisted of determining which has been the electrical impedance of the system, and it has been done using an EIS machine, concretely the Agilent 4294A Machine. Firstly, in order to prepare the chips for its sensing, different wires have been stuck on the ends of the electrodes by using silver paint, as shown in Figure 52. Then, the microchips have been sensed by hooking them with alligator clips to the machine sensor, as shown in Figure 53.

Figure 52: Silver paint on electrodes.

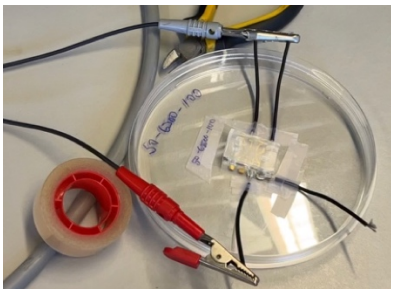

Figure 53: Electrodes connected to EIS.

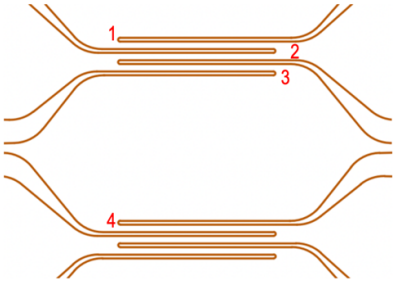

Figure 54: reference number of electrodes.

For each microchip, there have been carried out 4 different electrode configuration measures of the electrical impedance, it is, four different combinations of two electrodes. The reference number given to each electrode is shown in Figure 54, and the different combinations have been 1-2, 1-3, 2-4 and 2-3. Moreover, these four measurements have been done 3 times for each microchip: one

time with empty channels (open system), one time with the channels filled with PBS, and the last time with channels filled with Claycomb medium.

The impedance has been measured along frequency, with a maximum frequency value of 10MHz, as for larger frequencies the machine doesn't work well. The units of frequency are Hz and Impedance units are Ohms, for the modulus, and grades (º) for the phase.

The first characterization done is shown in Table 5. It has consisted of comparing the electrical impedance modulus and phase of the 4 electrodes configuration for each one of the situations for each microchip. As it has been predicted when the electrical circuit of the microdevice system has been modeled, the electrode configuration that has resulted in a lower impedance has been the one in which the electrodes are the closest one to each other (it can be seen in the modulus graphics). For this reason, the next results study has been done only considering this pair of electrodes (1-2 configuration) for the different microdevice environment.

Table 6 shows the results of this just mentioned study. As it can be seen, for the three environments, the microchip with the fibers has resulted in the one with lower impedance. For this reason, the last study has consisted on determining which of the three environments of the microchip with the fibers results in the one with lowest impedance. This last study is shown in Table 7, where it can be seen that the environment in which the electrical impedance is lower is the one with PBS, followed by the one with the medium.

Table 5: Characterization results differenced by modulus/phase and what is inside the microchannels

	MODULUS	PHASE
Fibers open system	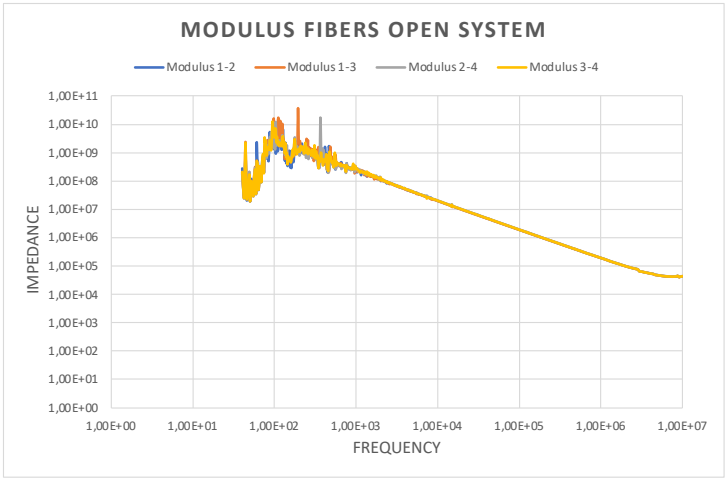	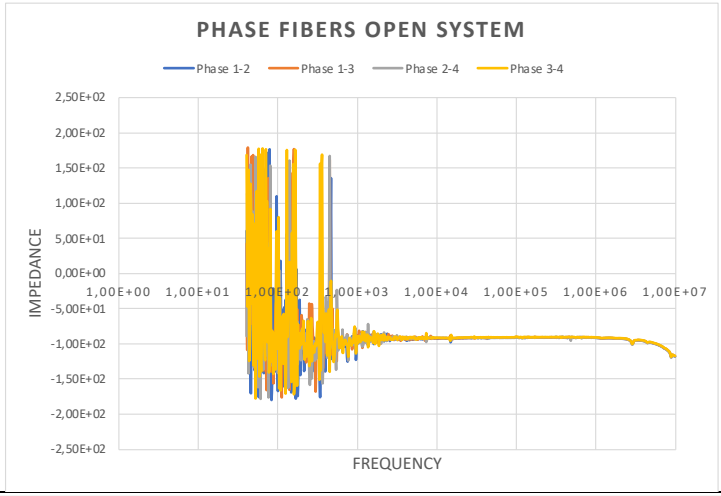
Fibers PBS	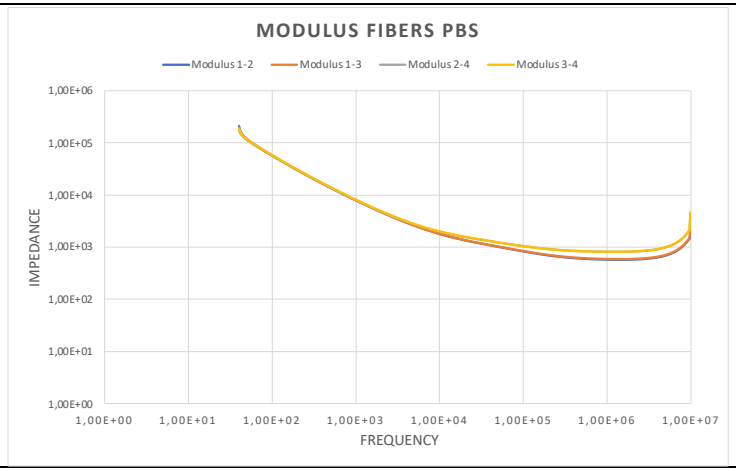	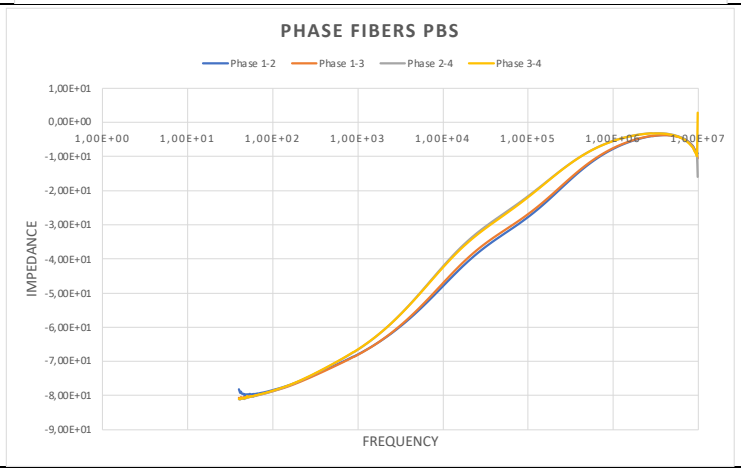

Fibers medium	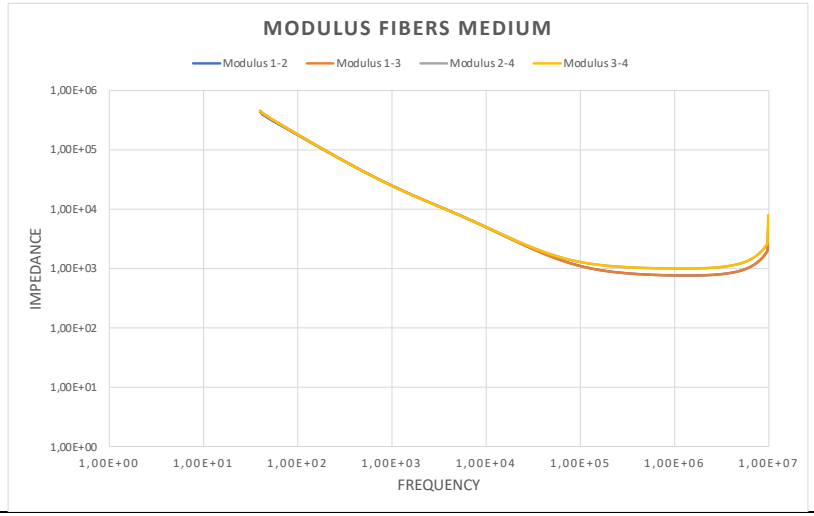	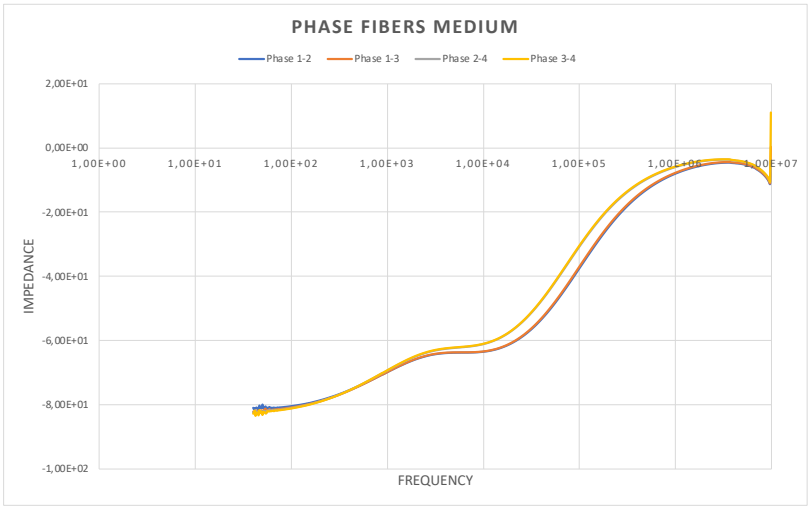
NO Fibers open system	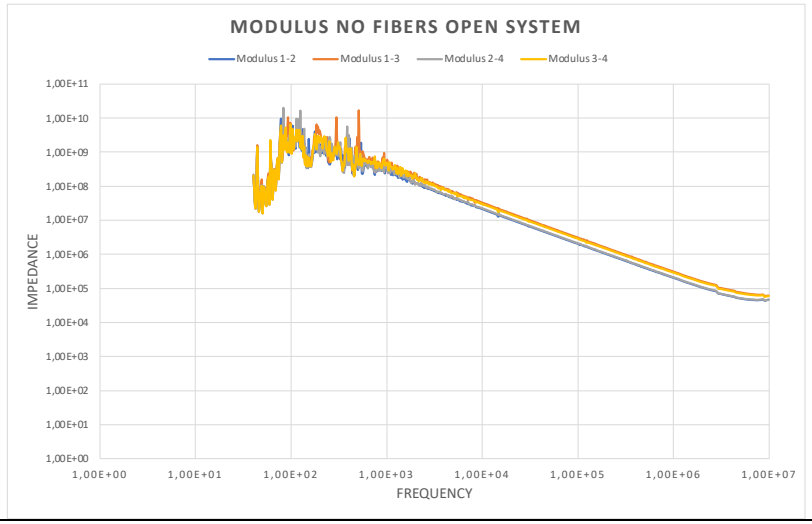	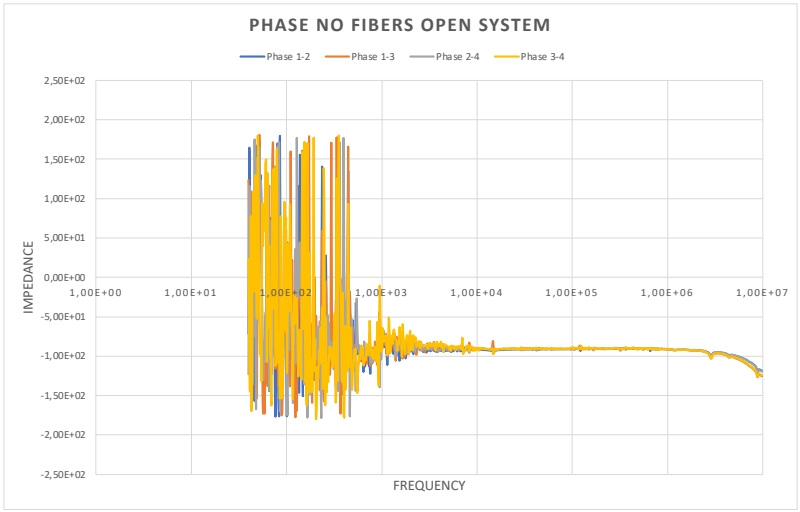

NO Fibers PBS	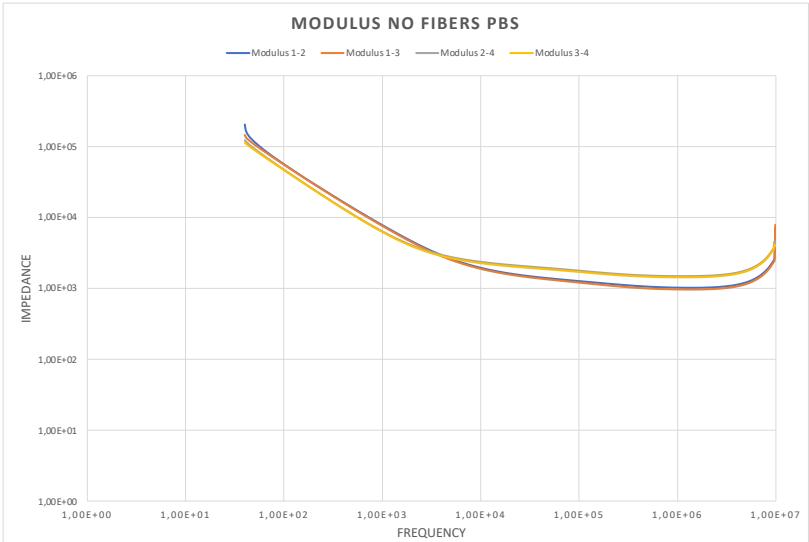	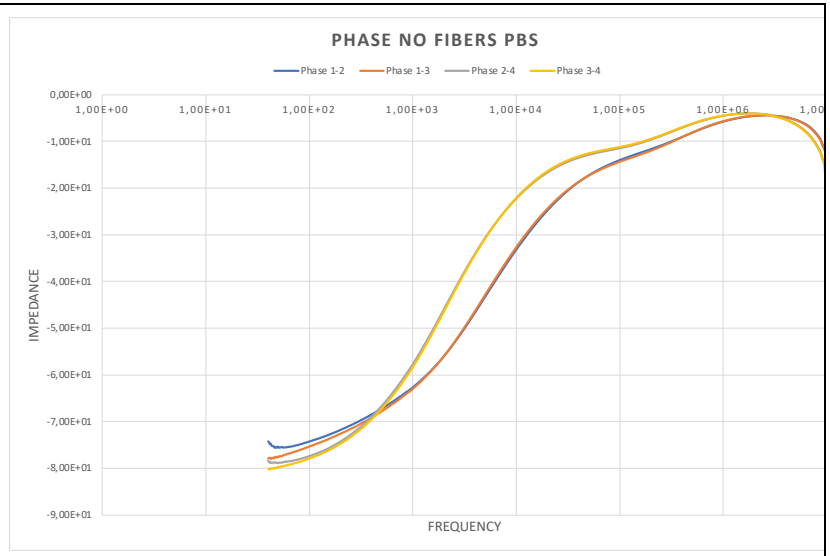
NO Fibers mediu m	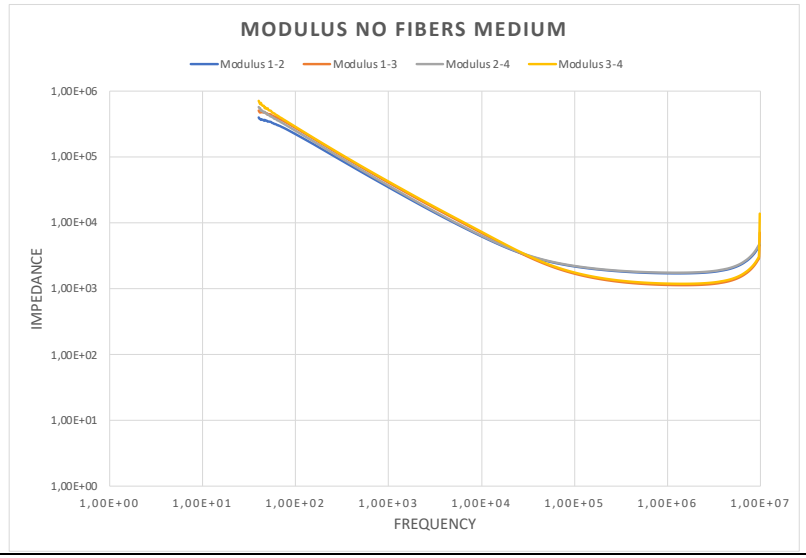	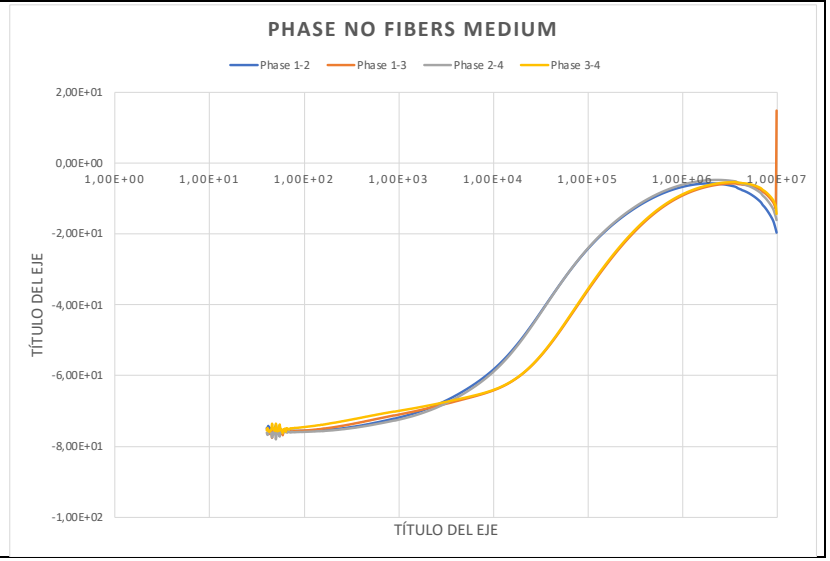

Table 6: Characterization results differenced by modulus/phase for 1-2 electrode configuration for different environments

	MODULUS	PHASE
Open system	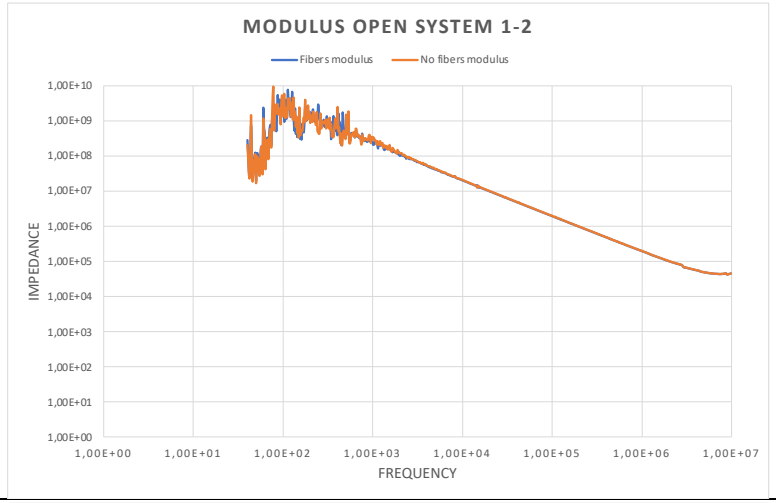	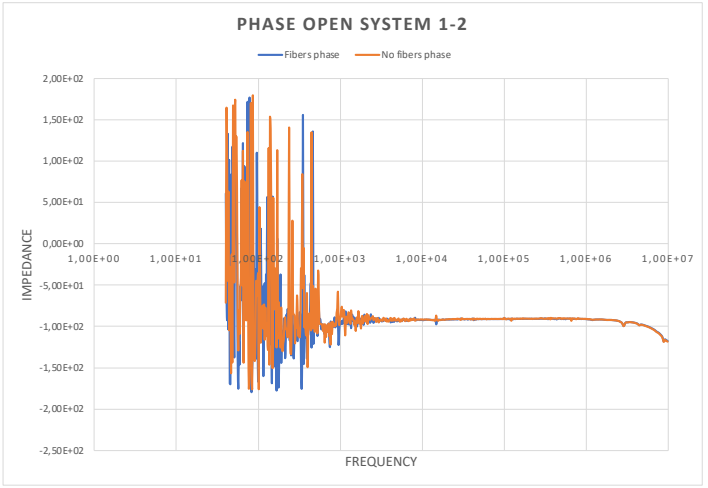
PBS	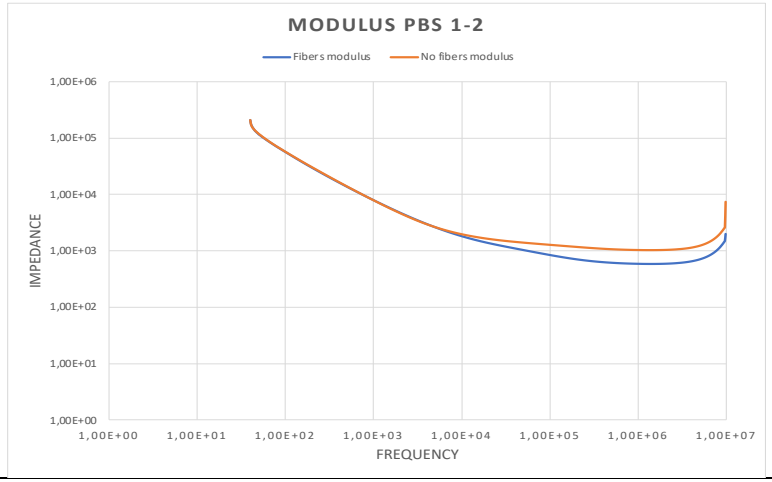	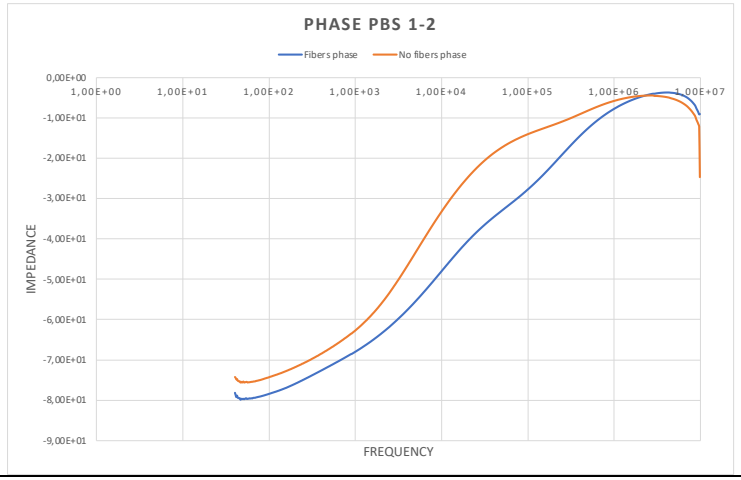

Medium	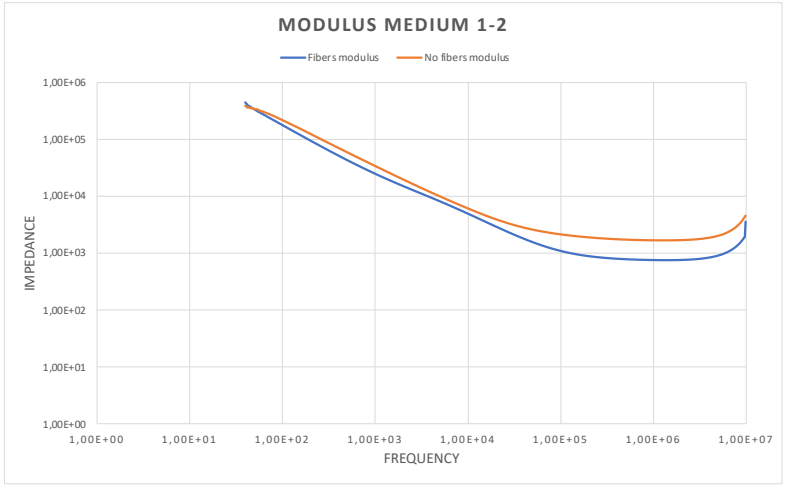	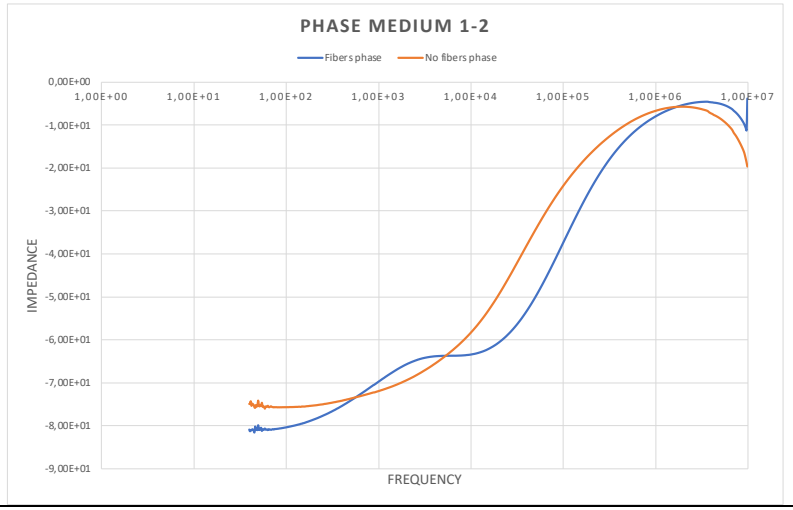

Table 7: Characterization results of the fibered microchip (1-2)

	MODULUS	PHASE
Fibered microchip	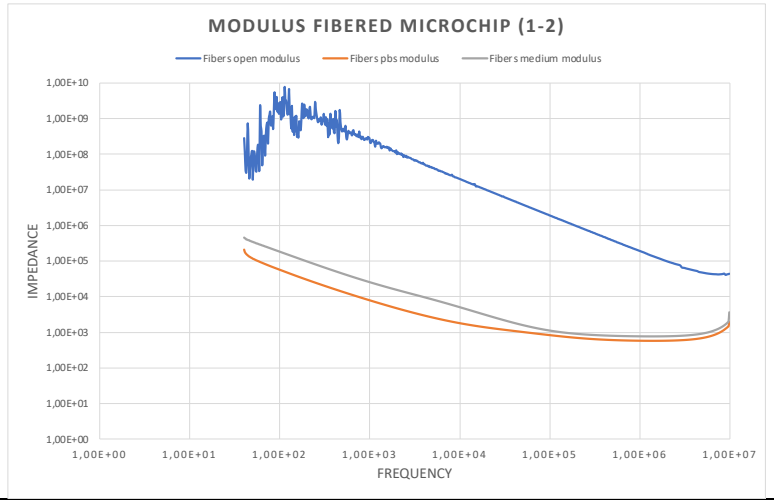	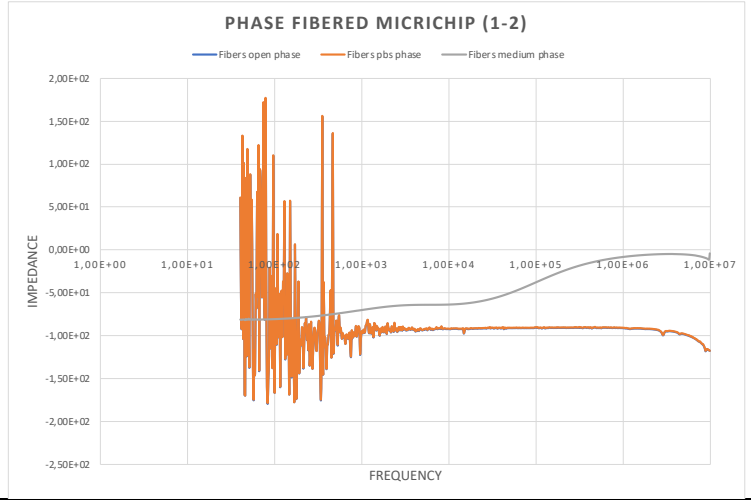

6. Execution chronogram

6.1. Work Breakdown Structure (WBS)

A work breakdown structure (WBS) is used to break down the complete scope of the project into smaller, more manageable tasks. It involves identifying and listing all the specific activities that need to be performed to accomplish the project objectives. This hierarchical structure aids in creating a phased schedule of tasks, where each phase can be systematically planned, executed, and monitored. The WBS provides a clear overview of the project's components and allows for effective management of resources, timelines, and dependencies. By breaking down the project into smaller tasks, it becomes easier to assign responsibilities, track progress, and ensure that all aspects of the project are addressed in a structured manner. Figure 55 dhows the WBS diagram of this project.

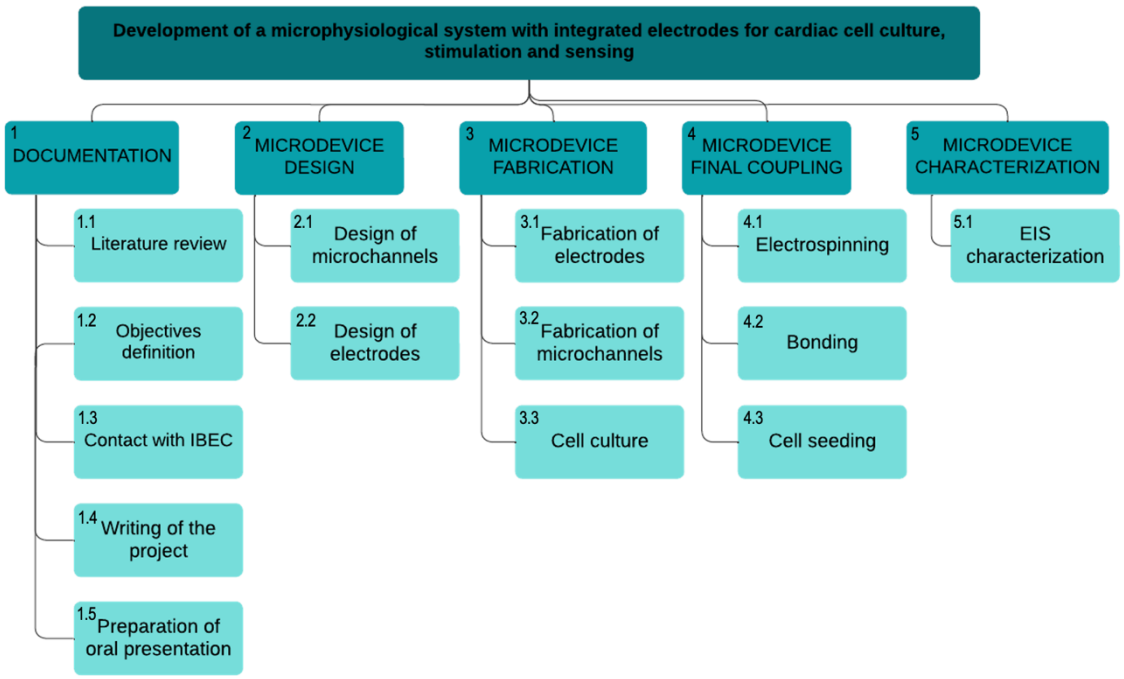

Figure 55: WBS diagram of the project

All the different tasks have been step by step explained s the writing of the report of this project has progressed.

Furthermore, Table 8 shows the different tasks mentioned, with their pertinent WBS ID, their letter reference, their previous tasks and the total number of days they have been carried out. The previous tasks of one concrete task are the ones that if are not finished, this concrete task cannot be started.

Table 8: Table of tasks. Previous tasks and timings.

	Activity	ID WBS	Ref	Previous task	Time (days)
Documentation	Literature review	1.1	A	-	15
	Objectives definition	1.2	B	-	2
	Contact with IBEC	1.3	C	B	3
	Writing of the project	1.4	D	-	45
	Preparation of oral presentation	1.5	E	D	5
Microdevice design	Design of microchannels	2.1	F	C	7
	Design of electrodes	2.2	G	F	25
Microdevice fabrication	Fabrication of electrodes	3.1	H	G	2
	Fabrication of microchannels	3.2	I	F	1
	Cell culture	3.3	J	B	5
Microdevice final coupling	Electrospinning	4.1	K	H	1
	Bonding	4.2	L	I, K	1
	Cell seeding	4.3	M	L	1
Microdevice Characterization	EIS characterization	5.1	N	M	1

6.2. Execution Chronogram of the global project (GANTT)

The GANTT diagram provides a visual representation of the project's timeline, showcasing the sequence of tasks and their durations. This diagram allows us to clearly observe the start and end dates of each activity, the expected duration of each task, any instances of overlapping activities, and most importantly, it helps in establishing the overall start and finish dates for the entire project. By displaying the tasks against time in the GANTT diagram, a comprehensive understanding of the project's temporal progression is gained and the project's schedule can effectively be planned and managed.

Figure 56 shows the GANTT diagram of this project and an ampliated image of the table with the initial times and the ending times (days).

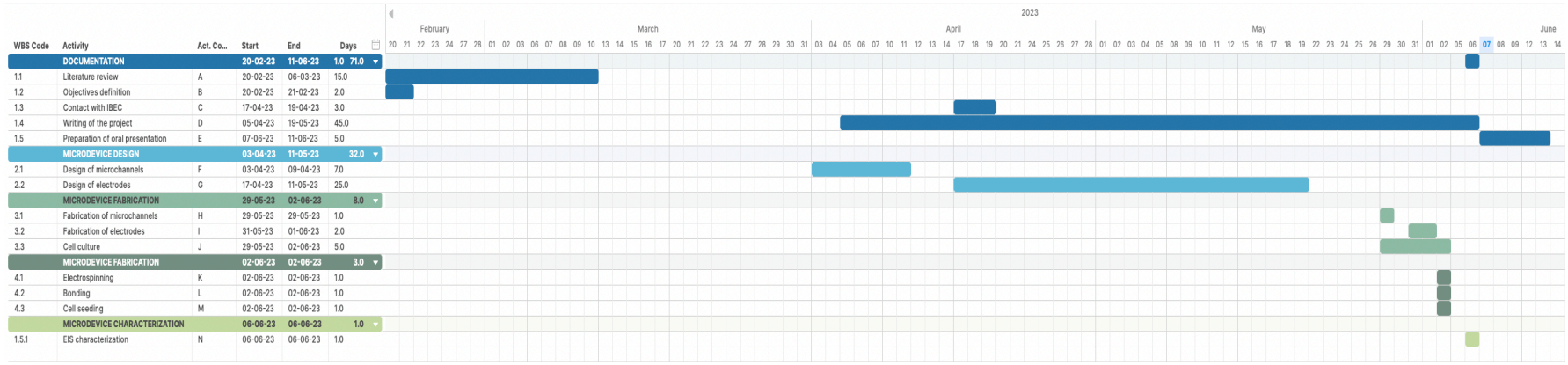

WBS Code	Activity	Act. Co...	Start	End	Days
	DOCUMENTATION		20-02-23	11-06-23	1.0 71.0
1.1	Literature review	A	20-02-23	06-03-23	15.0
1.2	Objectives definition	B	20-02-23	21-02-23	2.0
1.3	Contact with IBEC	C	17-04-23	19-04-23	3.0
1.4	Writing of the project	D	05-04-23	19-05-23	45.0
1.5	Preparation of oral presentation	E	07-06-23	11-06-23	5.0
	MICRODEVICE DESIGN		03-04-23	11-05-23	32.0
2.1	Design of microchannels	F	03-04-23	09-04-23	7.0
2.2	Design of electrodes	G	17-04-23	11-05-23	25.0
	MICRODEVICE FABRICATION		29-05-23	02-06-23	8.0
3.1	Fabrication of microchannels	H	29-05-23	29-05-23	1.0
3.2	Fabrication of electrodes	I	31-05-23	01-06-23	2.0
3.3	Cell culture	J	29-05-23	02-06-23	5.0
	MICRODEVICE FABRICATION		02-06-23	02-06-23	3.0
4.1	Electrospinning	K	02-06-23	02-06-23	1.0
4.2	Bonding	L	02-06-23	02-06-23	1.0
4.3	Cell seeding	M	02-06-23	02-06-23	1.0
	MICRODEVICE CHARACTERIZATION		06-06-23	06-06-23	1.0
1.5.1	EIS characterization	N	06-06-23	06-06-23	1.0
					115.0

Figure 56: GANTT diagram of the project. Zoom up of tasks table

7. Technical feasibility

This project has turned out to be more challenging than expected. Furthermore, during the fabrication and testing of the chip, specific technical hurdles have emerged. These challenges must be considered to conduct a comprehensive assessment of the product's feasibility.

First, this project has required working in specific clean rooms where regulations are strictly stablished. Moreover, these installations are not always disponible, as more people have the right to book the different machines whenever they want and are free. This has led to a situation in which not all the things wanted to do have been actually carried out.

On the other hand, the cell culture maintenance and the cell seeding have needed a sterile environment with rigorous cleaning protocols. Even a minor error during cell manipulation or medium handling can result in contamination of the entire sample. If the sample is contaminated, the most probable following step is to repeat all the processes again. Thus, the project prolongates along the time and more money has to be invested. These are the reasons why working with cells results into a very significant challenge.

Considering the materials used, the construction of the microchip has involved the submission of the coverslip to an electrospinning process, where they are very likely to be broken, and the attachment of a fragile glass coverslip to a PDMS structure. This step is crucial to ensure that the cells remain within the device and can be observed under a microscope. However, this assembly introduces a higher risk of chip breakage during handling due to the delicate nature of the required thin glass coverslip. As the chips require regular manipulation, including daily medium changes (which unavoidably involve applying pressure to the glass coverslip) they potentially lead to its breakage.

Several fabrication processes involved in constructing the device entail extended waiting periods. For instance, both processes of fabricating the electrodes and the microchannels require for the researchers to be waiting for hours while the elements are in the hot plates, the sonicator, the evaporator, and other machines. Moreover, the PDMS structures nedds considerable time to solidify in the oven, the bonding of the structures to the glass coverslip in the clean room also requires a significant duration. These processes are time-consuming and disruptive since subsequent fabrication steps cannot start until the preceding one is completed. Consequently, the waiting hours become unproductive because, most times, doing something else implies getting out of the clean room, and that also wastes time (putting on and taking off the safety suit).

Considering these technical aspects, which are actually drawbacks of the project, the SWOT analysis presented below (Table 9) details the technical feasibility of the project on a global scale.

Table 9: SWOT analysis of the designed product

STRENGTHS	WEAKNESS
- *Integrated electrodes for sensing* - *Great materials for good bonding* - *Fiber deposition thanks to electrospinning* - *Different states of characterization for comparison* - *Great cell growing*	- *Doesn't incorporate 3D cellular matrix* - *Device fragility* - *Large waiting process time* - *Inefficient workflow* - *Lack of availability of machinery* - *Clean room conditions* - *Sterile conditions*
OPPORTUNITIES	**THREATS**
- *Market potential* - *Evasion of testing with animals* - *Produced in laboratories* - *Growth of research related to the topic.*	- *New technology* - *Lack of standards about it* - *Room for design and fabrication improvements*

As it can be observed, the first section (upper row, left column) of the table shows the strengths the microdevice has. One of the most advances has been the integration of the electrodes inside the microdevice, so the characterization measurements can be directly done. Moreover, the inclusion of electrospinning allows for efficient fiber deposition, enhancing cells introduced inside the microdevice can be attached to them. Furthermore, the microdevice possesses other strengths that contribute to its effectiveness. It incorporates integrated electrodes for sensing purposes, enhancing its functionality; it utilizes high-quality materials that enable strong bonding between its components, ensuring durability; multiple states of characterization are employed, enabling effective comparisons and analysis; and the microdevice facilitates optimal cell growth, promoting successful biological applications. Conversely, the second section (upper row, right column) of the table shows the weakness of the microdevice. They have been previously described, as they have been significant.

Furthermore, the third section (lower row, left column) of the table shows the microdevice's opportunities, as its future market potential when improved, the investigation evolution to a non-animal testing research, the advantage of being able to be produced in laboratories and the high growing of technologies it incorporates.

Finally, the fourth section of the table (lower row, right column) shows its threats. For instance, even though, as mentioned before, the technologies the microdevice incorporates are constantly improving, they are relatively new. Moreover, there's no concrete standardization for this kind of devices yet. For all these reasons, it can be said that there's a room for this microdevice's design and fabrication improvements.

8. Economic feasibility

Completing this project entails a financial investment. Even though it can't be so much specific, as there has been used a lot of materials and during the process some cost information can have been lost, whether for the reason that some of them are not sold individually or because they have not been considered. Thus, to obtain an understanding of the approximate magnitude and sources of this expenditure, an examination of the project's economic aspects has been undertaken.

First of all, for this project, the design of the microdevice has been done with a free trial of the AutoCAD design software, but the normal fee is of 2,342.00 € per year. For the printing of the design into an acetate mask, the Output City budget for one DinA4 printing is shown in Table 10. It can be observed that the total cost of the acetate mask has been 175.00$, which means a cost of 163.34€, considering that at this moment 1$ equals 0.93€.

Table 10: Output City printing budget

Description	Quantity	Price ($)
Translation	1	25.00
10x12 20k mask	1	76.00
Ship Express Saver	1	74.00
Total		**175.00**

Regarding all the fabrication processes, Table 11 shows the budget of the IBEC cleaning room that their researchers have provided. It includes the costs of 2 silicon masters of 150um and 16 Ti/Au electrodes fabrication, it is, the Si master fabrication, the electrodes fabrication, the silanization and characterization of the masters, the characterization of the electrodes and the technical support for training and fabrication. This last cost wouldn't be necessary if the person who has to carry out all these processes already has permission to do it alone without supervision.

Table 11: budget of the IBEC cleaning room for the fabrication process

Description	Quantity	UOM[1]	Unit Price (€)	% Dct	Total (€)
4" Si wafer	2	unit	14.16	0%	28.32
Plasma	4	proc	9.70	20%	31.04
Chemical bath	3	h	55.30	20%	132.72
Photolithography service	8	h	129.00	20%	825.60
Silanization	1	proc	25.00	20%	20.00
Optical Microscope	2.5	h	14.00	20%	28.00
Profilometer	0.5	h	33.30	20%	13.32
Contact angle	0.25	h	43.00	20%	8.60
Thermal evaporatio	1	proc	148.50	20%	118.80
Additional layer	1	proc	33.90	20%	27.12
Thermal Au	100	nm	3.52	0%	352.00
E-beam Ti	20	nm	0.43	0%	8.60

[1] UOM: Unit Of Measurement

Specialist Technician	8	h	65.00	20%	416.00
Total without IVA (€)					2,010.12
IVA (21%) (€)					422.13
Total cost (€)					**2,432.25**

As it can be observed, the total cost of the IBEC cleaning room for the fabrication process has been 2,432.25 €.

In terms of the personnel involved in the project, it has been necessary to have a biomedical engineering student to execute the project and a supervisor who has provided guidance and advice to the student. The cost of the student has been estimated based on the average annual salary of a junior engineer, which is approximately 20€ per hour [41]. Similarly, the cost of the supervisor was estimated considering the average annual salary of a senior engineer, which amounts to 30€ per hour [42]. Table 12 shows the total cost for human resources allocation. It can be seen that this total cost is 6,450.00 €.

Table 12: Budget for human resources allocation

Technician	Total time (hours)	Cost (€/hour)	Total Cost (€)
Biomedical Engineering student	300	20.00	6,000.00
Director	15	30.00	450.00
Total cost (€)			**6,450.00**

Finally, for the chip characterization, the Agilent 4294A Machine has been used. It cost is approximately 25,000 € [43].

Calculating the sum of all the previously mentioned budgets, the total cost of the project, including the one-year AutoCAD subscription, results in 36,387.59 €.

9. Regulations and legal aspects

All aspects of this project, including its development and execution, have taken place in Barcelona. Consequently, the applicable legislations and regulations are those mandated by the Spanish Government.

The product created in this project falls under the category of 'organ-on-chip' devices. As a relatively new technology, there are significant gaps in the legislation and regulation surrounding these products. One of the most urgent gaps is the lack of specific standardization that governs their characterization, including aspects such as shape, tissue types, size, methods of use, and materials. Additionally, there is a lack of consensus on the definition of 'organ-on-chip' and its associated terminology, as well as agreed-upon requirements for their production. Despite these existing gaps in regulation, it is worth noting that certain standards applicable to other devices can be extended to Organ-on-Chip (OoC) technologies due to the overlapping nature of their fields. For instance, ISO-IWA 23 - 2016 [44] is a standard that presents a classification system for microfluidic devices, and ISO 10991-2009 [45] provides definitions for terms such as 'microfluidics' and 'lab-on-chip'. These established standards offer a framework that can be utilized in the absence of specific regulations for OoCs.

Even though, given the immense potential of such devices in transforming biomedical research and drug development, the establishment of standards would greatly facilitate the acceptance of Organ-on-Chip (OoC) technologies in regulatory contexts. Standardization would enable a comprehensive and systematic characterization of various types of OoC devices based on their structural and functional attributes. It would also regulate the qualification processes necessary to demonstrate their technological and biological significance. Ultimately, standardization would propel the progress of these technologies by positioning them as commercial products and facilitating their integration into the healthcare industry.

On the other hand, this project has involved the storage and usage of cells, which raises ethical concerns regarding the legislation governing the collection of cells for biomedical research. Several legal regulations exist that outline requirements for obtaining consent, authorization, and licensing for research involving any form of human tissue or cells. The process and quality requirements for establishment, maintenance and characterization of cell lines are reported in ISO 21709:2020 standard [46]. The ISO/TS 23511:2023 [47] also is necessary to know the general requirements and considerations for cell line authentication. It describes the general principles, detection strategies and analytical methods for cell line authentication. It specifies requirements and key considerations for method selection, quality control parameters, data analysis and reporting.

Apart from the mentioned regulations, this project has had a fabrication process that has been carried out inside the IBEC clean room. For that reason, its usage normative has to be also considered. These regulations are defined in ISO 14644-15:2017 [48], which describe the requirements and guidelines for cleanrooms and associated controlled environments.

10. Conclusions and future work

The elaboration of this project has allowed the development of a microfluidic device with integrated electrodes that has been used for cell seeding and impedance sensing. This microchip has been designed, fabricated, and characterized in different conditions.

The design and fabrication of the microchip has been challenging because of the objective of incorporating gold electrodes inside it. Even though, it has been possible to characterize it with an EIS machine. Moreover, another reason why some things to be done in this project have changed along the time is the unpredictability of working with cells and working in very regulated installations.

Although the different drawbacks, the design of the microelectrodes and microchannels and, consequently, the design of the hole microchip has been successful and functional. Their fabrication has been carried out and its results have been mostly the expected ones. It is true that not all the elements fabricated have been perfectly obtained and that along the time some of them have been removed from the workflow of the project. For this reason and for lack of time, at the end only two microdevices have been sensed. Even though, it has been possible to see the differences between microchips with electrospun fibers on the surface of the coverslip where the microchannels are placed on and microchips without them. It has been determined that the best configuration is the fibered microchip filled with PBS. For future work, the optimal option is to characterize more microchips in order to have a more realistic result.

On the other hand, even though one of the objectives was to incorporate a 3D cardiomyocyte matrix, the reality is that, for the moment, it has not been possible. More students and researchers have been working on the project where this thesis belongs and have tried to build a hydrogel matrix. Future objectives fall to get a functional 3D matrix; this way, the microdevice of this project could incorporate it and accomplish the original objectives.

For now, as mentioned before, it has been worked with a 2D layer of cells, but due to the short time between the cells seeding and the moment of microdevice sensing, these cells haven't been able to grow enough, so it has been decided not to characterize its electrical impedance yet. The idea is that in an imminent future time, the cells of these chips have grown and then their characterization could be done. This way, it will be possible to determine the difference between the microchips with electrospun fibers and the ones with fibronectin fibers, both containing cells.

11. Bibliography

[1] MEMORIA CIENTÍFICO-TÉCNICA DE PROYECTOS INDIVIDUALES Convocatoria 2021 - «Proyectos de Generación de Conocimiento», Memoria-cientifico-tecnica-individual-2021-uCardioChip_Intro+WPs. Given document.

[2] ROTH, A. Human microphysiological systems for drug development, Shibboleth authentication request. Available at: https://www-science-org.sire.ub.edu/doi/10.1126/science.abc3734.

[3] Groff, K. et al. (2014) Review of evidence of environmental impacts of animal research and testing, MDPI. Available at: https://www.mdpi.com/2076-3298/1/1/14

[4] Nanobioengineering and biomaterials unit (2023) IN2UB. Available at: https://www.ub.edu/in2ub/grup-de-recerca/nanobioengineering-and-biomaterials-unit/

[5] Kartha, C.C. (1970) Structure and function of Cardiomyocyte, SpringerLink. Available at: https://link.springer.com/chapter/10.1007/978-3-030-85536-9_1

[6] Cardiac muscle tissue: Structure and function - getbodysmart (no date) Get Body Smart. Available at: https://www.getbodysmart.com/heart-anatomy/cardiac-muscle-tissue/

[7] Cardiac action potential (2023) Wikipedia. Available at: https://en.wikipedia.org/wiki/Cardiac_action_potential

[8] Ripa, R., George, T. and Sattar, Y. (no date) Physiology, cardiac muscle - statpearls - NCBI bookshelf, National Library of Medicine. Available at: https://www.ncbi.nlm.nih.gov/books/NBK572070/

[9] Picture: Niculescu AG, Chircov C, Bîrcă AC, Grumezescu AM. Fabrication and Applications of Microfluidic Devices: A Review. Int J Mol Sci. 2021 Feb 18;22(4):2011. doi: 10.3390/ijms22042011. PMID: 33670545; PMCID: PMC7921936. Available at: https://www.ncbi.nlm.nih.gov/pmc/articles/PMC7921936/

[10] Niculescu AG, Chircov C, Bîrcă AC, Grumezescu AM. Fabrication and Applications of Microfluidic Devices: A Review. Int J Mol Sci. 2021 Feb 18;22(4):2011. doi: 10.3390/ijms22042011. PMID: 33670545; PMCID: PMC7921936. Available at: https://www.ncbi.nlm.nih.gov/pmc/articles/PMC7921936/

[11] Ribas J, Sadeghi H, Manbachi A, Leijten J, Brinegar K, Zhang YS, Ferreira L, Khademhosseini A. Cardiovascular Organ-on-a-Chip Platforms for Drug Discovery and Development. Appl In Vitro Toxicol. 2016 Jun 1;2(2):82-96. doi: 10.1089/aivt.2016.0002. PMID: 28971113; PMCID: PMC5044977. Available at: https://www.ncbi.nlm.nih.gov/pmc/articles/PMC5044977/

[12] Annabi N, Selimović Š, Acevedo Cox JP, Ribas J, Afshar Bakooshli M, Heintze D, Weiss AS, Cropek D, Khademhosseini A. Hydrogel-coated microfluidic channels for cardiomyocyte culture. Lab Chip. 2013 Sep 21;13(18):3569-77. doi: 10.1039/c3lc50252j. PMID: 23728018; PMCID: PMC3744594. Available at: https://pubmed.ncbi.nlm.nih.gov/23728018/

[13] Picture: Annabi N, Selimović Š, Acevedo Cox JP, Ribas J, Afshar Bakooshli M, Heintze D, Weiss AS, Cropek D, Khademhosseini A. Hydrogel-coated microfluidic channels for cardiomyocyte culture. Lab Chip. 2013 Sep 21;13(18):3569-77. doi: 10.1039/c3lc50252j. PMID: 23728018; PMCID: PMC3744594. Available at: https://pubmed.ncbi.nlm.nih.gov/23728018/

[14] Grosberg A, Alford PW, McCain ML, Parker KK. Ensembles of engineered cardiac tissues for physiological and pharmacological study: heart on a chip. Lab Chip. 2011 Dec 21;11(24):4165-73. doi: 10.1039/c1lc20557a. Epub 2011 Nov 10. PMID: 22072288; PMCID: PMC4038963. Available at: https://www.ncbi.nlm.nih.gov/pmc/articles/PMC4038963/

[15] Picture: Grosberg A, Alford PW, McCain ML, Parker KK. Ensembles of engineered cardiac tissues for physiological and pharmacological study: heart on a chip. Lab Chip. 2011 Dec 21;11(24):4165-73. doi: 10.1039/c1lc20557a. Epub 2011 Nov 10. PMID: 22072288; PMCID: PMC4038963. Available at: https://www.ncbi.nlm.nih.gov/pmc/articles/PMC4038963/

[16] Picture2: Annabi N, Selimović Š, Acevedo Cox JP, Ribas J, Afshar Bakooshli M, Heintze D, Weiss AS, Cropek D, Khademhosseini A. Hydrogel-coated microfluidic channels for cardiomyocyte culture. Lab Chip. 2013 Sep 21;13(18):3569-77. doi: 10.1039/c3lc50252j. PMID: 23728018; PMCID: PMC3744594. Available at: https://pubmed.ncbi.nlm.nih.gov/23728018/

[17] Abulaiti, M., Yalikun, Y., Murata, K. et al. Establishment of a heart-on-a-chip microdevice based on human iPS cells for the evaluation of human heart tissue function. Sci Rep **10**, 19201 (2020). Available at: https://www.nature.com/articles/s41598-020-76062-w

[18] Picture: Abulaiti, M., Yalikun, Y., Murata, K. et al. Establishment of a heart-on-a-chip microdevice based on human iPS cells for the evaluation of human heart tissue function. Sci Rep 10, 19201 (2020). Available at: https://www.nature.com/articles/s41598-020-76062-w

[19] Adrián López-Canosa, Soledad Perez-Amodio, Eduardo Yanac-Huertas, Jesús Ordoño, Romen Rodriguez-Trujillo, Josep Samitier, Oscar Castaño and Elisabeth Engel, 2021, A microphysiological system combining electrospun fibers and electrical stimulation for the maturation of highly anisotropic cardiac tissue.

[20] Valentina Paloschi (no date) Organ-on-a-chip technology: a novel approach to investigate cardiovascular diseases, Oxford Academic. Available at: https://academic.oup.com/cardiovascres/article/117/14/2742/6174689

[21] Li Z, Hui J, Yang P, Mao H. Microfluidic Organ-on-a-Chip System for Disease Modeling and Drug Development. Biosensors (Basel). 2022 May 27;12(6):370. doi: 10.3390/bios12060370. PMID: 35735518; PMCID: PMC9220862. Available at: https://www.ncbi.nlm.nih.gov/pmc/articles/PMC9220862/

[22] Chan, A.H.P. and Huang, N.F. (2021) Engineering cardiovascular tissue chips for disease modeling and Drug Screening Applications, Frontiers. Available at: https://www.frontiersin.org/articles/10.3389/fbioe.2021.673212/full

[23] Li Z, Hui J, Yang P, Mao H. Microfluidic Organ-on-a-Chip System for Disease Modeling and Drug Development. Biosensors (Basel). 2022 May 27;12(6):370. doi: 10.3390/bios12060370. PMID: 35735518; PMCID: PMC9220862. Available at: https://www.ncbi.nlm.nih.gov/pmc/articles/PMC9220862/

[24] Gulino, M. et al. (2019) Tissue response to neural implants: The use of model systems toward new design solutions of implantable microelectrodes, Frontiers. Available at: https://www.frontiersin.org/articles/10.3389/fnins.2019.00689/full

[25] Khandpur, R.S. (no date) Microelectrodes, Shibboleth authentication request. Available at: https://onlinelibrary-wiley-com.sire.ub.edu/doi/10.1002/9781119288190.ch234

[26] Maloney, J. (2023) Using patterned electrodes for chemical sensors, Platypus Technologies. Available at: https://www.platypustech.com/patterned-electrodes-chemical-sensors

[27] Disk & Pellet Ag/AgCl Electrode (no date) M systems. Available at: https://www.a-msystems.com/p-384-disk-pellet-agagcl-electrode.aspx

[28] 12 pieces/pack 4μm platinum interdigitated electrodes ide transparent ... Available at: https://www.amazon.com/Interdigitated-Electrodes-Transparent-Microelectrode-Biosensor/dp/B0975J1DTN

[29] Author links open overlay panelTao Sun a et al. (2023) Flexible Irox neural electrode for mouse vagus nerve stimulation, Acta Biomaterialia. Available at: https://www.sciencedirect.com/science/article/pii/S1742706123000260 (Accessed: 07 June 2023).

[30] della Valle, E. et al. (2021) Electrodeposited Platinum Iridium enables microstimulation with carbon fiber electrodes, Frontiers. Available at: https://www.frontiersin.org/articles/10.3389/fnano.2021.782883/full (Accessed: 07 June 2023).

[31] Cui, H., Xie, X., Xu, S. et al. Electrochemical characteristics of microelectrode designed for electrical stimulation. BioMed Eng OnLine 18, 86 (2019). Available at: https://doi.org/10.1186/s12938-019-0704-8

[32] Jastrzebska E, Zuchowska A, Flis S, Sokolowska P, Bulka M, Dybko A, Brzozka Z. Biological characterization of the modified poly(dimethylsiloxane) surfaces based on cell attachment and toxicity assays. Biomicrofluidics. 2018 Jul 10;12(4):044105. doi: 10.1063/1.5035176. PMID: 30034568; PMCID: PMC6039296. Available at: https://www.ncbi.nlm.nih.gov/pmc/articles/PMC6039296/

[33] Yin Z, Cheng E, Zou H, Chen L, Xu S. Fabrication of two dimensional polyethylene terephthalate nanofluidic chip using hot embossing and thermal bonding technique. Biomicrofluidics. 2014 Nov 25;8(6):066503. doi: 10.1063/1.4902945. PMID: 25553203; PMCID: PMC4247375.].

[34] Comprehensive guide on polyethylene terephthalate (PET) (no date) Polyethylene Terephthalate (PET) - Uses, Properties & Structure. Available at: https://omnexus.specialchem.com/selection-guide/polyethylene-terephthalate-pet-plastic

[35] Paloschi, V. (no date) Whole-teflon microfluidic chips | PNAS, PNAS. Available at: https://www.pnas.org/doi/10.1073/pnas.1100356108 (Accessed: 07 June 2023).

[36] The properties and advantages of PTFE (2016) AFT Fluorotec. Available at: https://www.fluorotec.com/news/blog/the-properties-and-advantages-of-polytetrafluoroethylene-ptfe/

[37] PMMA – POLYMETHYLMETHACRYLATE (no date) Resinex. Available at: https://www.resinex.co.uk/polymer-types/pmma.html

[38] Caliari SR, Burdick JA. A practical guide to hydrogels for cell culture. Nat Methods. 2016 Apr 28;13(5):405-14. doi: 10.1038/nmeth.3839. PMID: 27123816; PMCID: PMC5800304. Available at: https://www.ncbi.nlm.nih.gov/pmc/articles/PMC5800304/

[39] Services (no date) CAD/Art Services :: outputcity, photomasks, photomask services, phototools, photolithography. Available at: https://www.outputcity.com/services.html

[40] Soft lithography (no date) Soft Lithography - an overview | ScienceDirect Topics. Available at: https://www.sciencedirect.com/topics/materials-science/soft-lithography

[41] Castillo, E. (2018, April 10). Analista de datos, el puesto más demandado (y mejor pagado) por las empresas. Cinco Días. Retrieved June 5, 2022, from https://cincodias.elpais.com/cincodias/2018/04/09/midinero/1523274767_631043.html

[42] BOLETÍN OFICIAL DEL ESTADO. (2019, May). MINISTERIO DE TRABAJO, MIGRACIONES Y SEGURIDAD SOCIAL.

[43] Keysight Technologies (agilent HP) 4294A used or new for sale at used-line (no date) used. Available at: https://www.used-line.com/list-analyzers/impedance/agilent-hp-4294a

[44] IWA 23:2016 (2022) ISO. Available at: https://www.iso.org/standard/70603.html

[45] ISO 10991:2009 (2020) ISO. Available at: https://www.iso.org/standard/46546.html (Accessed: 07 June 2023).

[46] ISO 21709:2020(EN), biotechnology Biobanking process and quality ... (no date a) Online Browsing Platform (OBP). Available at: https://www.iso.org/obp/ui/#!iso:std:71382:en

[47] ISO/TS 23511:2023 (2023) ISO. Available at: https://www.iso.org/standard/75854.html

[48] *ISO 14644-15:2017(en) Scc.isolutions.iso.org*. Available at: https://scc.isolutions.iso.org/obp/ui#!iso:std:iso:14644:-4:ed-1:v1:en

Annexes

Annex 1: Electrode model designs

1300 um channel: width of the central chamber of the microfluidic device.

4x2_ends_2_zones_4x50um_electrodes: Electrodes of 50 µm of width.

- 6500um_externDistance: Distance between the two groups of electrodes.

  - 50um_distance4electrode: Distance between electrodes (two by two).

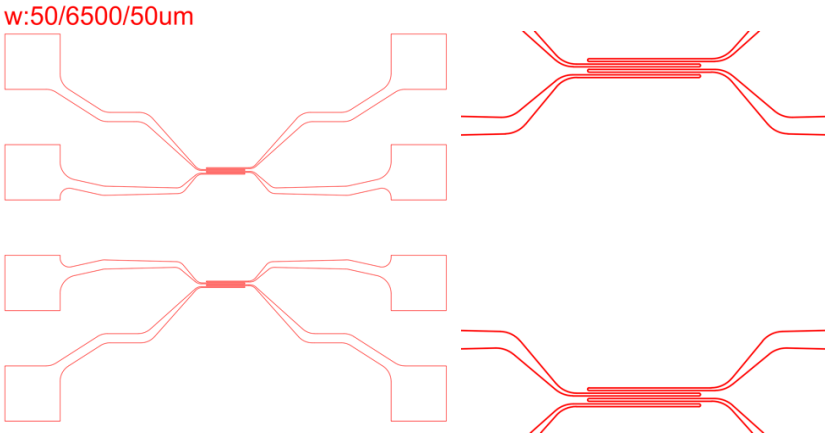

  - 100um_distance4electrode

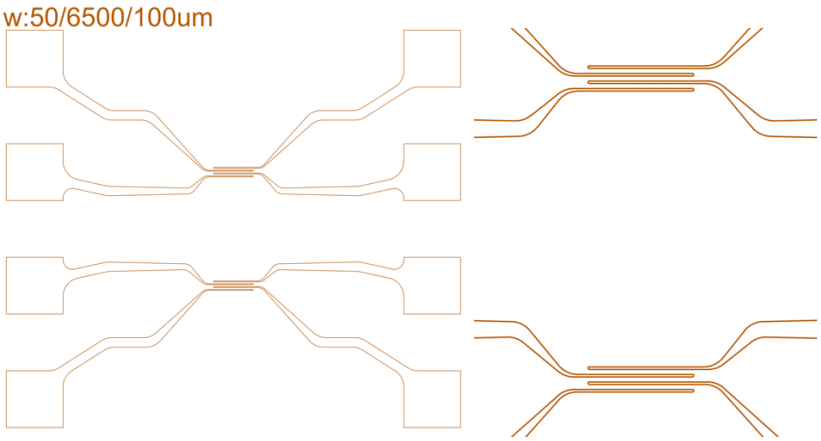

- 150um_distance4electrode

w:50/6500/150um

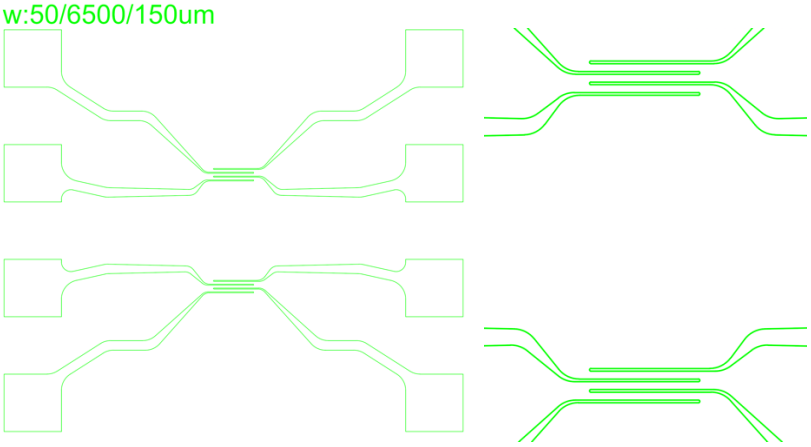

- 4650um_externDistance:

- 50um_distance4electrode

w:50/4650/50um

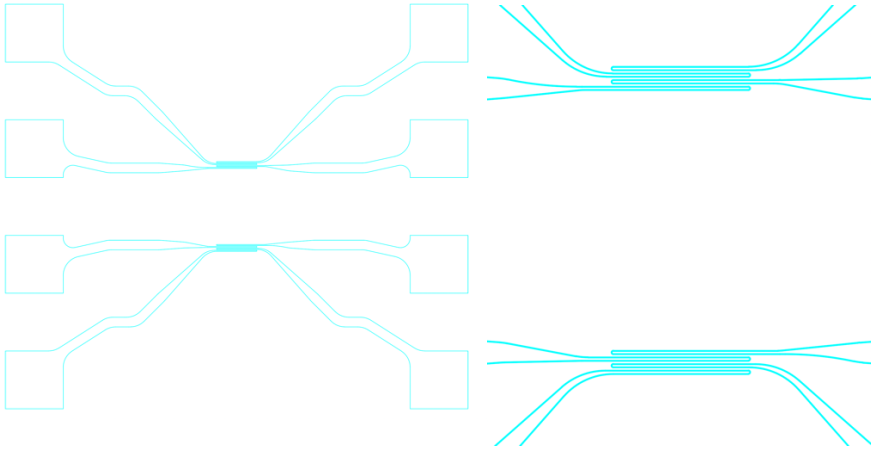

- 100um_distance4electrode

w:50/4650/100um

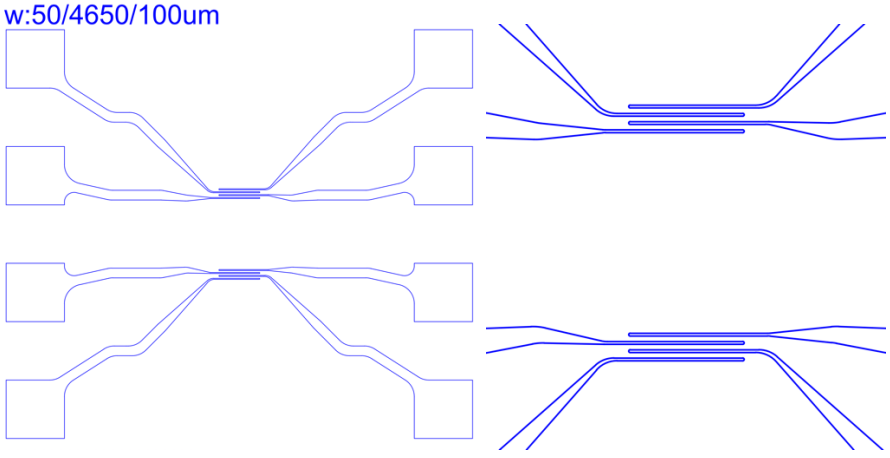

- 150um_distance4electrode

w:50/4650/150um

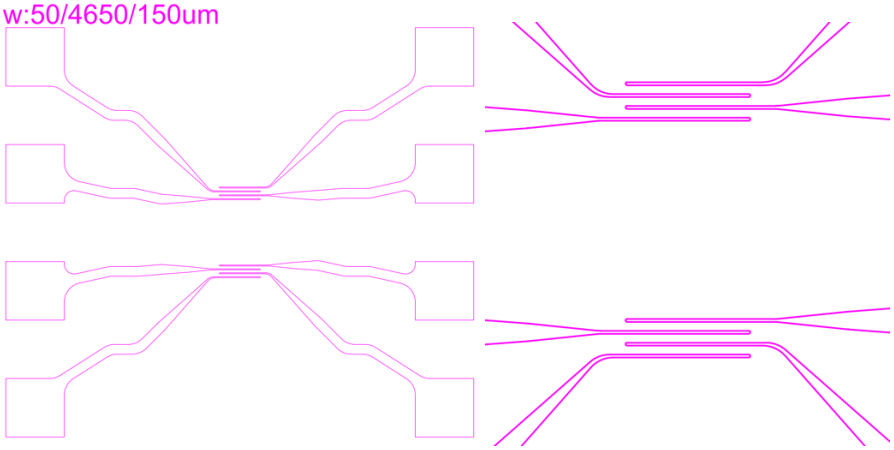

4x2_ends_2_zones_4x100um_electrodes:

- 6500um_externDistance:

  - 100um_distance4electrode

w:100/6500/100um

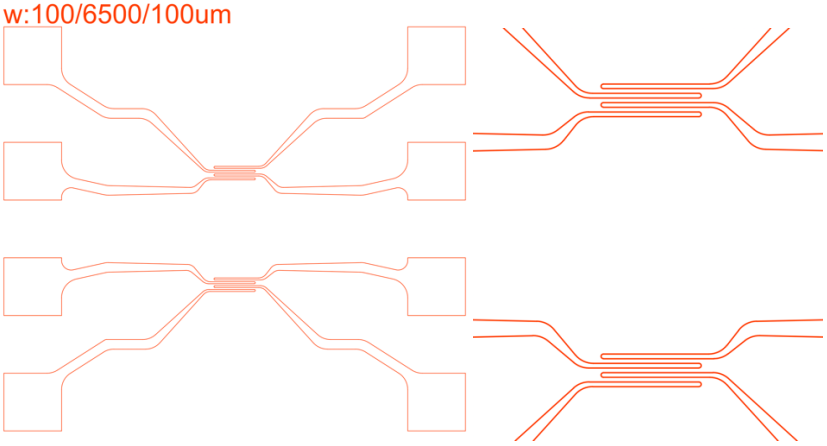

  - 200um_distance4electrode

w:100/6500/200um

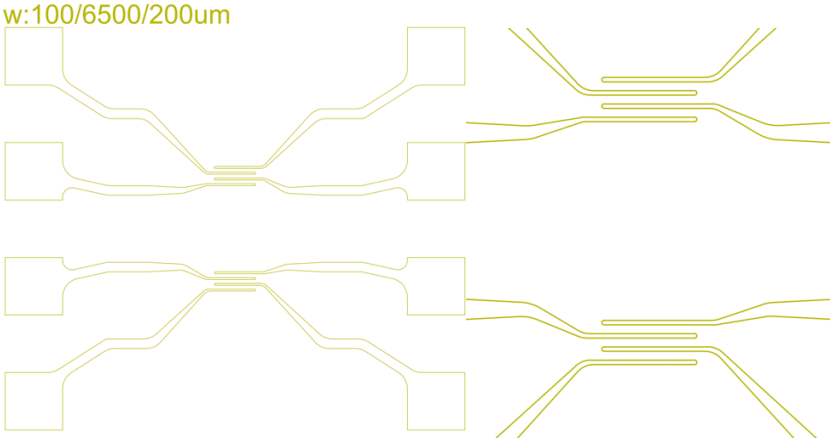

- 300um_distance4electrode

w:100/6500/300um

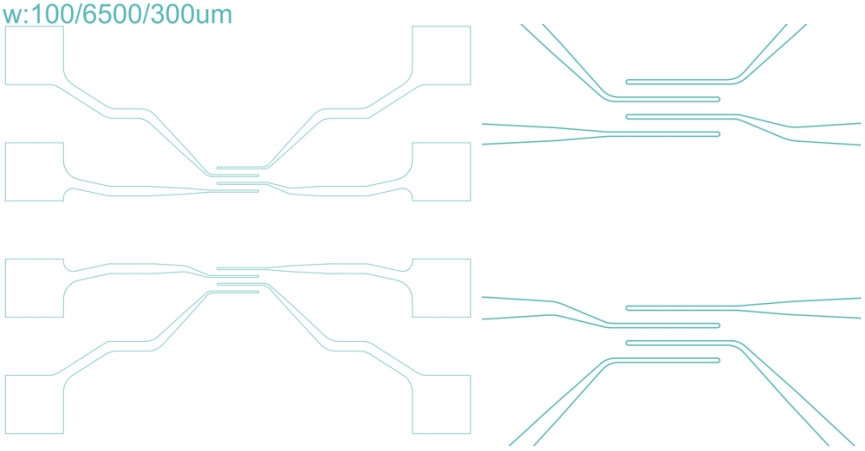

- 4650um_externDistance:

- 100um_distance4electrode

w:100/4650/100um

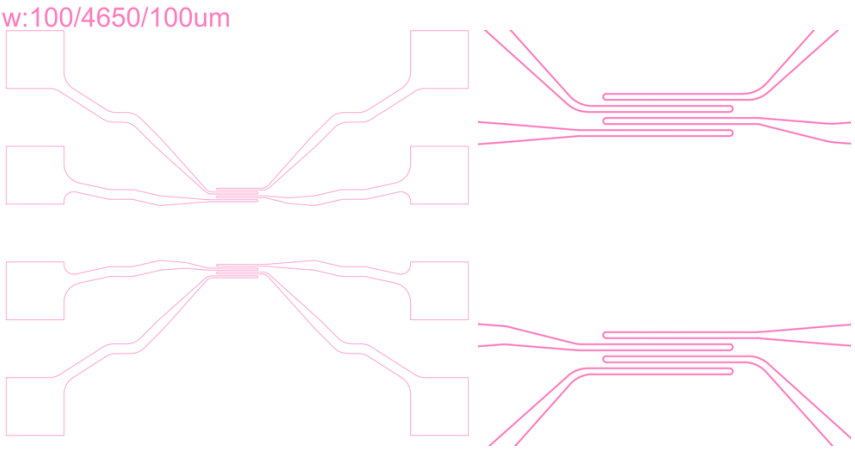

- 200um_distance4electrode

w:100/4650/200um

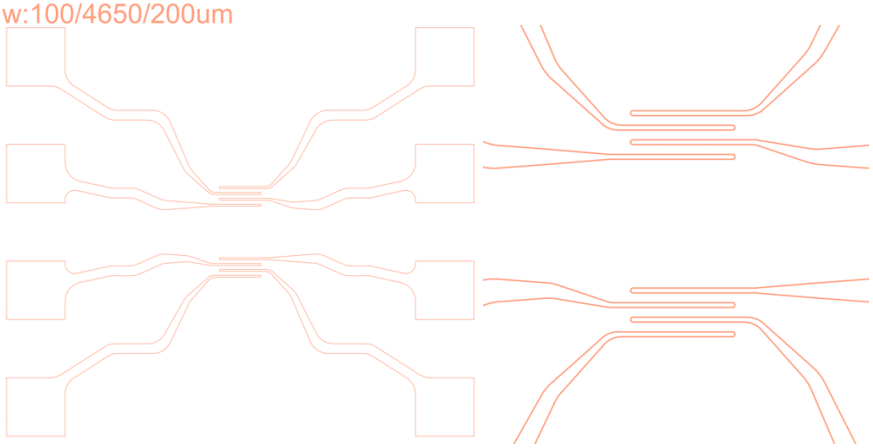

- 300um_distance4electrode

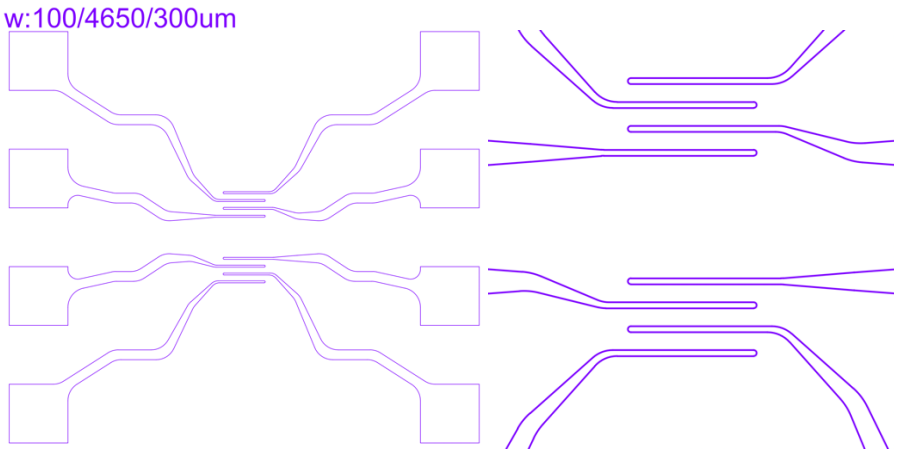

Note: the length of all the electrodes from the tip of the electrode to the beginning of the extension of it is the same. Do not have in consideration the difference of size of the different captures. The only important thing to consider here is the difference of distances in width between electrodes. To understand it better, remember that the width of the electrodes of each case is said before and it can be taken as a reference: 50 micrometers for the six first models and 100 micrometers for the last six.

Annex 2: DinA4 total design of the microdevice elements

Here is shown the DinA4 used to create the masks. At the left side, there are the microchannels, and at the right side there are the electrodes. Twelve electrodes have been placed at the upper right part of the sheet, and then they have been duplicated and placed at the right bottom of the sheet.

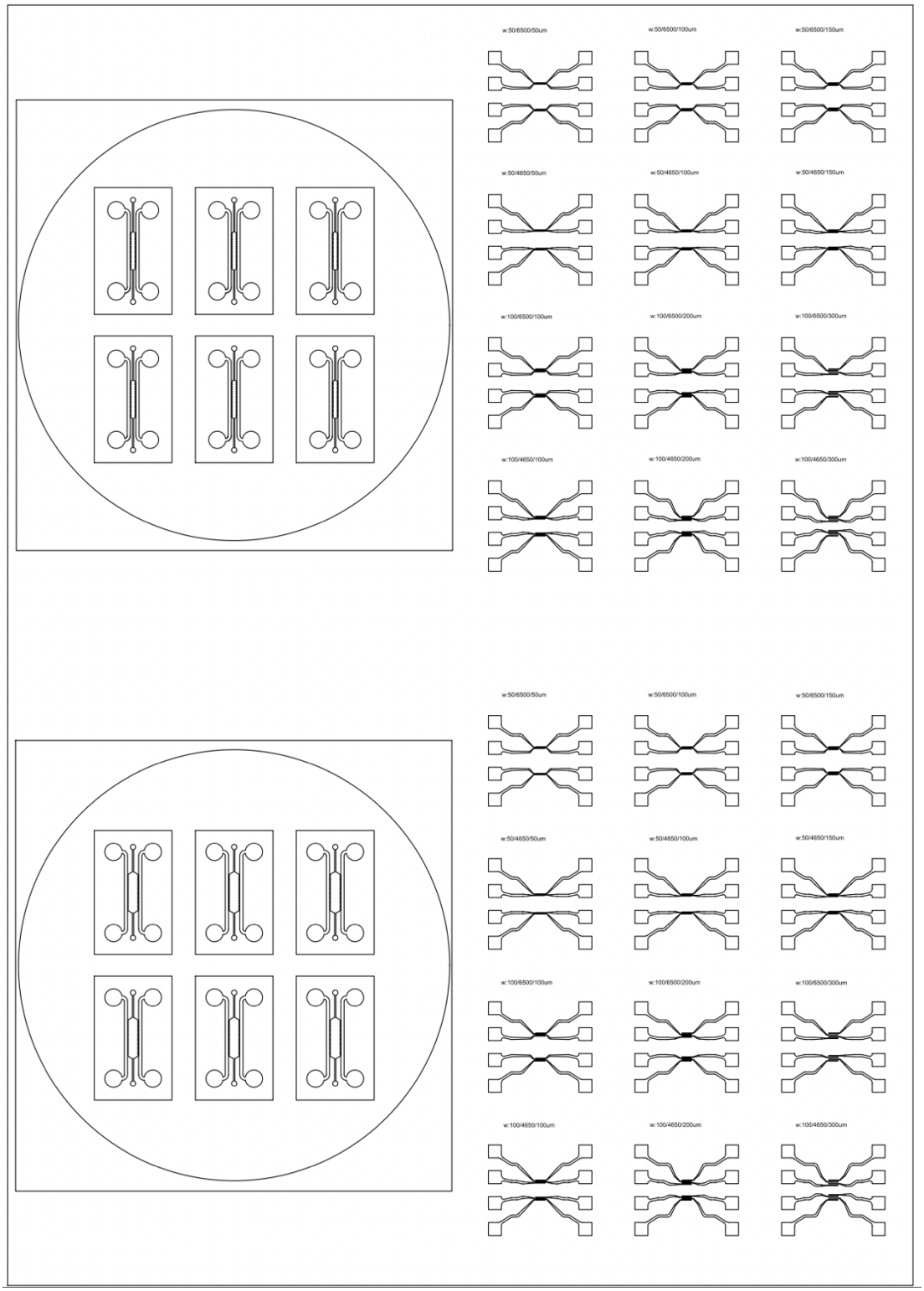

Annex 3: Electrodes fabrication machines and materials

Resin deposition on the coverslip inside a spinner machine.

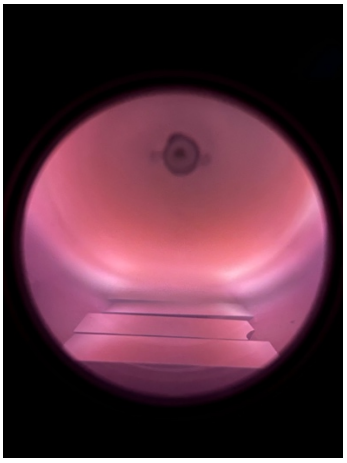

Plasma cleaner

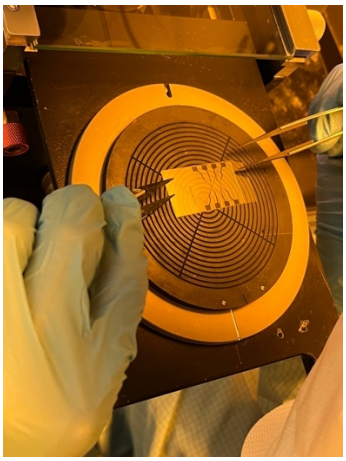

Mask alignment

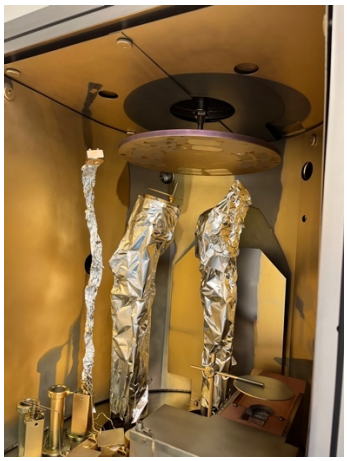

Evaporation-sputtering machine

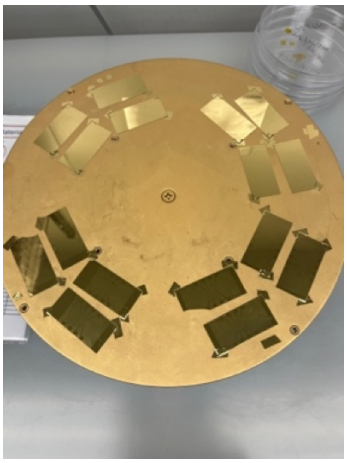

Gold deposited on the coverslips

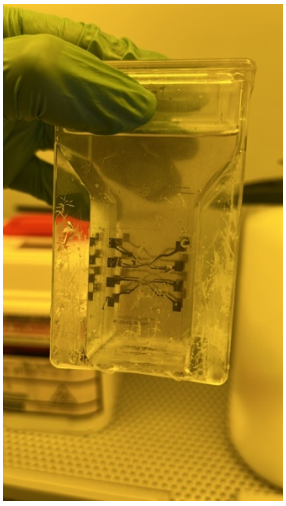

Lifting-off of the leftover gold

Annex 4: Microchannels fabrication machines and materials

Resin deposition on the wafer inside a spinner

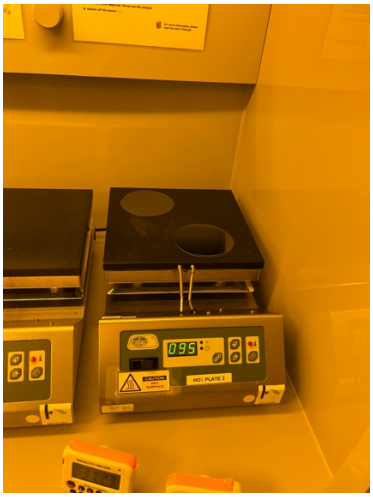

Wafers on a 95ºC hot plate

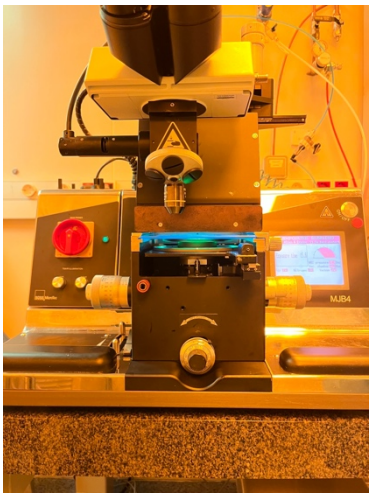

Mask aligner

Vacuum chamber for silinization

Annex 5: Cell culture and seeding machines and materials


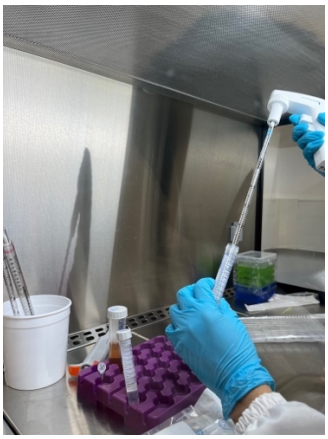
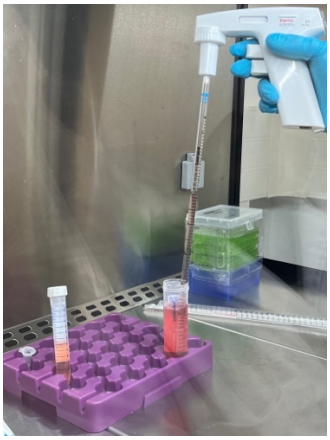

Medium changing of the cell culture

Cell culture hood

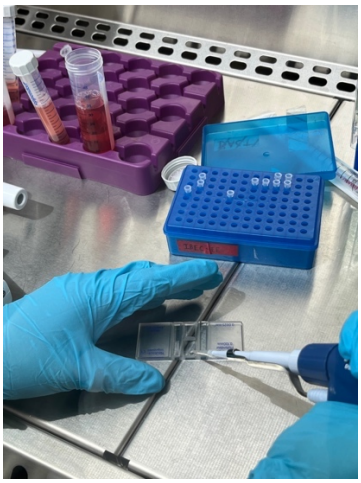

Neubauer chamber

Incubator

Annex 6: Cell maintenance protocol and cell counting technique

General Procedures

1. Take solid waste and liquid waste containers in the entrance. In the case that the latter is almost full, empty and put a small quantity of bleach.
2. Turn on the cabin and activate the UV light for 10 min.
3. Pick all the required reagents and warm them in the 37 ºC bath.
4. Once the cabin is ready, sterilize the floor of the cabin and all the material with ethanol.
5. After finishing all the procedures, close all the recipients (such as falcons, reagents bottles, etc.) with parafilm.
6. Clean the working space with ethanol.
7. Turn off the cabin.

Pre-Preparation

Norepinephrine (10 mM)

Materials

- 147.5mg Abscorbic Acid
- 25 ml Distilled water
- 80mg Norepinephrine
-
- Filter-sterilize using a 0.2 µm syringe filter.
- Aliquot in 1 ml volumes into sterile microtubes with screw caps, and store at -20°C.
- Norepinephrine needs to be made up fresh month

Soybean trypsin inhibitor

- 25mg Soybean trypsin inhibitor
- 100ml Dulbecco's Phosphate buffered Saline (PBS; Ca2+-free and Mg2+-free)
-
- Filter-sterilize, using a 0.2 µm syringe filter, into a 100 ml bottle.
- This is good for a month at 4°C

Gelatin 0.02%

- 0.1g Gelatin Bobine
- 500ml Distilled water

Pre-Coating

Flask

- 1ml Fibronectin (1mg/ml)
- 199ml Gelatin 0.02%

Chip

- 5ul Fibronectin (1mg/ml)
- 0.995ml Gelatin 0.02%

- Mix gently, and immediately aliquot 6ml/100ul.
- Freeze aliquots at -20°C.

Medium Preparation

Materials

- Falcons of 50 ml
- Pipettes of 10 ml and pipetboy
- Pipette of 100-1000 µl and tips
- Reagents (depending on desired medium, see below)
- Norepinephrine (10 mM)

Protocol

1. Generally 50 ml of medium are prepared and put into a 50 ml falcon. Depending on the cell type the composition is the following:
   - **HL-1 Medium (Mouse Atrial Cardiac Muscle Cell Line)**
     - ✓ 87 % Claycomb medium → 43.5 ml
     - ✓ 10 % FBS → 5 ml
     - ✓ 1 % L-glutamine → 0.5 ml
     - ✓ 1 % penicillin/streptomycin → 0.5 ml
     - ✓ 1 % Norepinephrine (10 mM)→ 0.5 ml
   - **HL-1 Wash Medium (Mouse Atrial Cardiac Muscle Cell Line)**
     - ✓ 93 % Claycomb medium → 46.5 ml
     - ✓ 5 % FBS → 2.5 ml
     - ✓ 1 % L-glutamine → 0.5 ml
     - ✓ 1 % penicillin/streptomycin → 0.5 ml
   - **Cardiac-Fibroblasts (Mouse Cardiac Fibroblasts)**

- ✓ 88 % Advanced DMEM (Dulbecco's Modified Medium) → 44 ml
- ✓ 10 % FBS (Fetal Bovine Serum) → 5 ml
- ✓ 1 % L-glutamine → 0.5 ml
- ✓ 1 % penicillin/streptomycin → 0.5 ml

Thawing and Plating

Materials

- Cryotube with cells
- Recipient with dry ice
- Flasks of 25 ml or 75 ml
- Coating Flask
- Pipettes of 10 ml and pipetboy
- Pipette of 100-1000 µl and tips
- Falcons of 50 ml

Protocol

1. Gelatin/fibronectin-coat a T75 tissue culture flask for at least an hour in a 37°C incubator. (Only for HL-1)
2. Remove the gelatin/fibronectin from the culture flask, and replace with 10 ml of supplemented Claycomb Medium. Place this flask back into incubator
3. Transfer 10 ml wash medium into an empty 15 ml centrifuge tube. Incubate tube in a 37°C water bath.
4. Take the cells either from the -80ºC freezer or liquid nitrogen tanks and put them in a recipient with dry ice.
5. Quickly thaw the cells in a 37°C water bath (about 2 min), and transfer into the 15 ml centrifuge tube containing the wash medium (be careful not to spend too much time, as the cell medium contains DMSO, which is toxic to the cells).
6. Centrifuge for 5 minutes at 500×g
7. Remove the tube from the centrifuge and remove the wash medium by aspiration.
8. Gently resuspend the pellet in 5 ml supplemented Claycomb Medium, and add to the 10 ml of medium already in the T75 flask
9. Replace the medium with 15 ml of fresh supplemented Claycomb Medium 4 hours later (after cells have attached).
10. In the subsequent days change the medium every days.

Medium Change

Materials

- Falcon with cell medium
- Falcon rack
- Flask with cells
- Tips of 100-1000 µl
- Pasteur glass pipettes

Protocol

1. Connect the vacuum tubing to the Pasteur pipette using as an adaptor a pipette tip of 10-1000 µl.
2. Open carefully the vacuum valve.
3. Open the cell flask and gently aspirate the old medium.
4. Add 5 ml (for flasks of 25 ml) or 10 ml (for flasks of 75 ml) of cell medium.
5. Put the fresh medium in the flask and close it.
6. Take cell flask back to the incubator.

Passaging

Materials

- Flask with cells
- Falcon with cell medium
- Falcon with cell wash medium
- Trypsin/EDTA
- HL-1 Wash Medium
- Soybean Trypsin Inhibitor
- Falcons of 15 ml
- Falcon rack
- Pipettes of 10 ml and pipetboy
- Pipette of 100-1000 µl and tips
- Pipette of 1-10 µl and tips
- Pasteur pipettes
- Hemocytometer and counter

Protocol

1. Gelatin/fibronectin-coat a T75 tissue culture flask for at least an hour in a 37°C incubator. (Only for HL-1)
2. Remove the gelatin/fibronectin from the culture flask, and replace with 10 ml of supplemented Claycomb Medium. Place this flask back into incubator
3. Transfer 10 ml wash medium into an empty 15 ml centrifuge tube. Incubate tube in a 37°C water bath.
4. Connect the vacuum tubing to the Pasteur pipette using as an adaptor a pipette tip of 10-1000 µl.
5. Open carefully the vacuum valve.
6. Open the cell flask and gently aspirate the old medium.
7. Add 2.5 ml (for flasks of 25 ml) or 5 ml (for flasks of 75 ml) of Wash Medium (PBS tor the Cardiac Fibroblast) pipetting onto the wall of the flask in order not to damage the cells. The goal of this step is to wash and remove as many dead cells as possible.
8. Aspirate Wash Medium (PBS for Cardiac Fibroblast) and add 2 ml of trypsin/EDTA (trypsin for Cardiac Fibroblast) for flasks of 5 ml or 5 ml for flasks of 75 ml.

9. Put the flask in the incubator for 5 min.
10. Gently tap cell flask to make sure that virtually all the cells are detached. Check it in the microscope before proceeding further.
11. Take a 10 ml pipette to aspirate the content of the flask and put it into a 15 ml Falcon. Put 3 ml of Wash Medium (PBS for Cardiac Fibroblast), wash, aspirate and transfer to the Falcon in order to make sure that remaining cells are collected.
12. Add 2 ml of Soybean Trypsin Inhibitor (FBS for Cardiac Fibroblast) (for flasks of 25 ml) or 5 ml (for flasks of 75 ml) to the Falcon in order to inhibit trypsin effect.
13. Centrifuge the Falcon for 5 min at 500 G (for Cardiac Fibroblast use 5 min at 300 G). It is necessary to fill another Falcon with the same volume of distilled water in order to compensate the centrifugal force and avoid vibrations of the machine.
14. Take the Falcon back to the cabin and aspirate very carefully the liquid content using at the beginning a 10 ml pipette and in the end a 1 ml pipette until only the final pellet is left.
15. Add 1 ml of medium and resuspend the cells gently pipetting up and down.
16. Take 10 µl and put in the hemocytometer for counting. If needed, dilute more the cells to make counting easier.
17. Depending on the number of cells and subsequent experiments, divide the volume accordingly.

Counting

Materials

- Flask with cells
- Falcon with cell medium
- Falcon with cell wash medium
- Coating Flask
- Trypsin (TrypLE or Trypsin/EDTA)
- PBS (Phosphate-Buffered Saline)
- FBS (Fetal Bovine Serum)
- Falcons of 15 ml
- Falcon rack
- Pipettes of 10 ml and pipetboy
- Pipette of 100-1000 µl and tips
- Pipette of 1-10 µl and tips
- Pasteur pipettes
- Hemocytometer and counter

Protocol

1. Perform passaging protocol.
2. Take a hemocytometer (Neubauer chamber) with its coverglass and clean with ethanol.

3. Put the 10 µl of cell suspension in the space between the chamber and the coverglass.
4. Go to the microscope and using the 10*x* objective to look for something as the following:

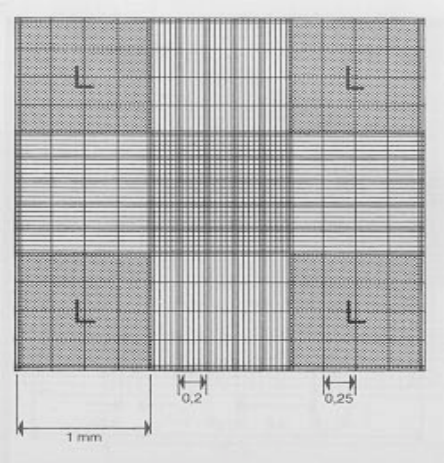

5. Use a counter and check the number of cells within the area *L* (4x4). Two of the sides of the square can also be considered (they have to be adjacent, that is, we cannot consider the two parallel sides). For instance:

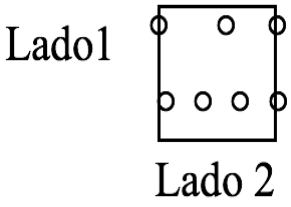

Number of cells = 3 (inside) + 2 (side 1) + 0 (side 2)

6. Repeat the same procedure for all of the four areas marked with an *L* and average the number of cells counted in each of them.
7. The real number of cells/ml can be estimated as $c = n\ x10^4$. This is due to the fact that each *L* region is 1x1 mm^2 and 1 mm in height (1 $mm^3 = 1 * 10^{-4}$ ml). To know the total number of cells we have to multiply this number by the total volume we have in the original solution.

Freezing

Materials

- Flask with cells
- Falcon with cell medium
- Falcon with cell wash medium
- Trypsin (TrypLE or Trypsin/EDTA)
- PBS (Phosphate-Buffered Saline)
- FBS (Fetal Bovine Serum)
- Falcons of 15 ml

- Falcon rack
- Pipettes of 10 ml and pipetboy
- Pipette of 100-1000 µl and tips
- Pipette of 1-10 µl and tips
- Pasteur pipettes
- Hemocytometer and counter
- Cryotubes
- Mr. Frosty

Protocol

1. Perform passaging technique till step 11 (pellet formation).
2. Depending on the number of cells, resuspend in appropriate quantity of medium. Essentially, the freezing medium has to be composed of:
   - **Cardiac fibroblasts**
     - ✓ 90 % FBS
     - ✓ 10 % DMSO
   - **HL-1:**
     - ✓ 95 % FBS
     - ✓ 5 % DMSO

   Note: for instance, if we have 1 million cells and we want 500.000 in each cryotube, we should resuspend the cells in 1.8 ml of FBS and put 0.9 ml in each cryotube and then add 0.1 ml of DMSO to the cell suspension.
3. Put the cryotubes in a Mr. Frosty and leave it for 24 h in the -80ºC freezer to progressively freeze the cells.
4. If the cells are planned to be used in the short term (maximum 1-2 weeks) leave in the -80ºC freezer. Otherwise, take to the liquid nitrogen containers.

3D Culture

Materials

- Flask with cells
- Falcon with cell medium
- Falcon with cell wash medium
- Trypsin (TrypLE or Trypsin/EDTA)
- PBS (Phosphate-Buffered Saline)
- FBS (Fetal Bovine Serum)
- Coating Flask

- Coating Chip
- Falcons of 15 ml
- Falcon rack
- Pipettes of 10 ml and pipetboy
- Pipette of 100-1000 µl and tips
- Pipette of 10-100 µl and tips
- Pipette of 1-10 µl and tips
- Pasteur pipettes
- Eppendorfs of 0.5 ml
- Hemocytometer and counter
- Microfluidic chips
- PTFE tubing (ID =0.5, OD = 1 mm)
- Precision tips (orange colour)
- Syringes of 5 ml or 10 ml
- Pump (Chemyx Fusion 200)

Protocol

1. Perform passaging and counting techniques.

   Note: before performing the process, put microfluidic chips in the plasma chamber for 30 s at HIGH to hydrophilize them. Wait for around 1 h 30 min before starting passaging the cells.

2. Then, take volume correspondent to the cells needed for each replica from the stock cell solution. This number will depend on cell type, but generally we will load around 120.000 cells.
3. Then, put correspondent volume in the 0.5 ml Eppendorfs (as many as the number of replicas) and centrifuge them again for 5 min at 500 G (for Cardiac Fibroblast use 5 min at 300 G). For Co-culture HL-1 and Fibroblast use 5 min at 400G.
4. Prepare hydrogel: our 3D cultures will be performed in a fibrin gel scaffold, which will be injected in each microfluidic chip (a total of 10 µl per device). To create the gel, we have to prepare a 2.5 mg/ml fibrinogen solution and a 100 U/ml thrombin solution (both in sterile DPBS).
5. Aspirate cell media from the 0.5 ml Eppendorf by using first the pipette of 10-100 µl and then the 1-10 µl one.
6. Create gel by mixing 50 µl of the fibrinogen solution with 0.5 µl of thrombin solution (final concentration of 1 U/ml).
7. Mix well, aspirate 10 µl and resuspend the cells in that volume.

8. Inject the cell suspension in the chip using one of the cell chamber ports. The process should be performed quickly, as the gel is only injectable during the first 30-40 s after mixing.
9. Make sure there was no leakage to the side channels and put chip in the incubator at 37 ºC for 15 min to perform polymerization.
10. After polymerization is complete, perform hydration of lateral channels. In the case of having media reservoirs, start by putting 100 µl of media in one of the upstream reservoirs and then, take a 100-1000 µl and cut it to fit the size of the downstream reservoir. Make sure the pipette forms a tight seal with it and aspirate gently till liquid start flowing through the channel. Repeat the procedure with the other channel.

    Note: in the case of using the design without reservoirs (just ports of 1 mm to connect the tubing), hydrate by placing a 1-10 µl pipette tip with media on the upstream reservoir and aspirating from the opposite side with a pipette of the same volume.
11. Completely fill the reservoirs with media, put the chips in a Petri and take to the incubator.

    Note: in the case of using the design without reservoirs (just ports of 1 mm to connect the tubing), connect first the two inlet ports to the media reservoirs (Falcons of 15 ml with the amount of media required for the experiment) using PTFE tubing (ID = 0.5 mm and OD = 1 mm). After that, connect the outlet ports to the media syringes using the same PTFE tubing and an orange tip precision adapter. Put them in a multi-syringe pump (like the Chemyx Fusion 200) and select the appropriate diameter of the syringe and desired flow rates. Finish the process by sealing the cell chamber ports with tape to avoid contamination.

Annex 7: Agilent 4294A Machine User Guide

The equipment has its own calibration that, in theory, is not lost. However, since it has been disconnected for quite some time, the reliability is not completely 100%. There is a load that is used for this calibration.

When the equipment is calibrated, the sensor needs to be calibrated as well, compensating for the impedance of the sensor part that is not intended to be measured (what we want to measure is the microfluidic device), because ultimately what we want to measure is a very small volume. Therefore, the ideal would be to "Have the system (the device) in short circuit and open circuit (without the cells)".

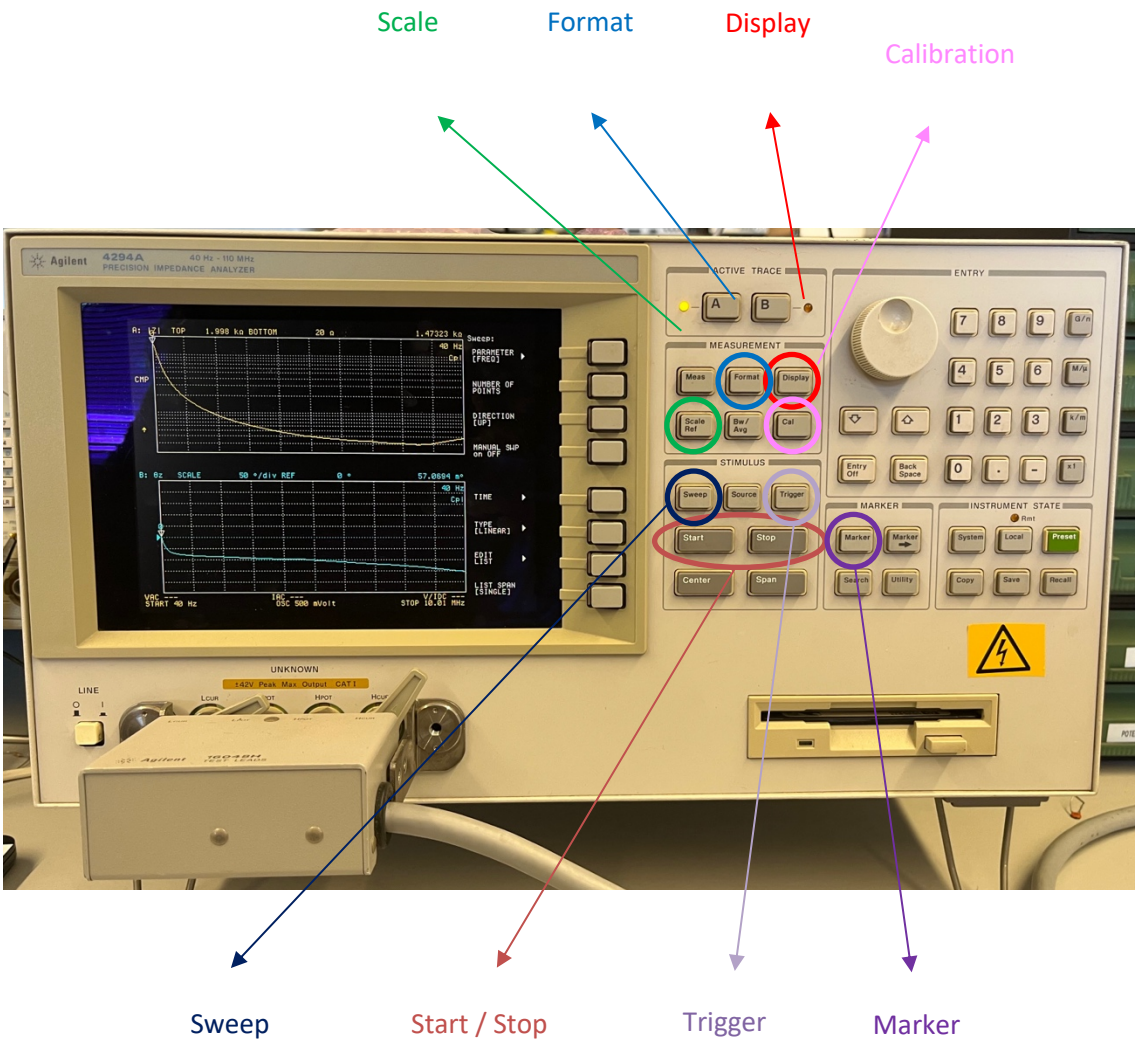

Steps to calibrate until the end of the equipment cable:

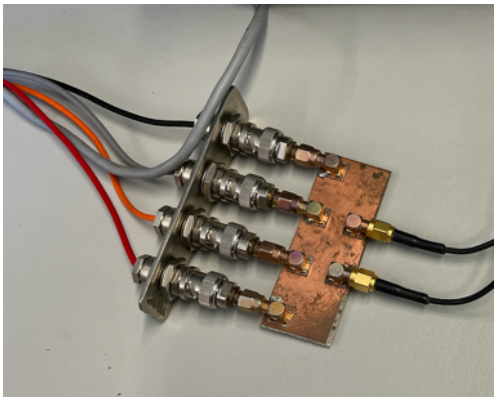

- Press the *Calibration* button.
- Press the *Fixture compensation* button (second button on the screen). There are three compensation measurements, which are used to compensate for all the impedances that are not intended to be measured: parasitic inductances, parasitic capacitances, and parasitic conductances.

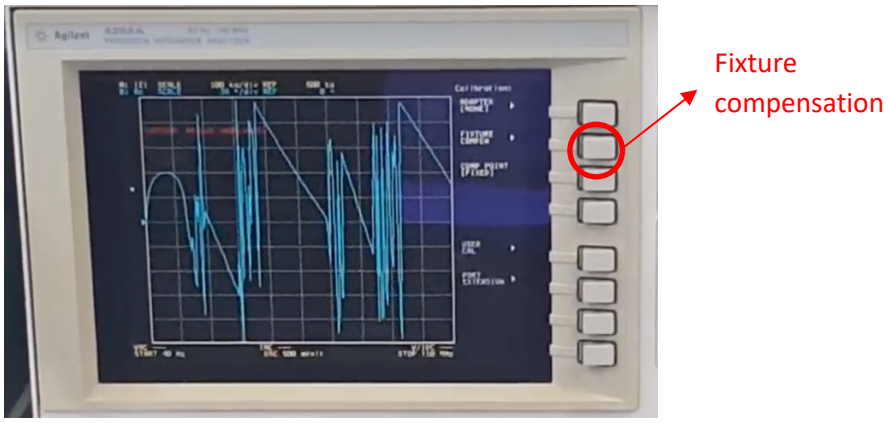

- Press the *Short* button (5th button on the screen): It performs a sweep at the full frequency of the equipment.
- Leave the sensor connected in open circuit.
- Press the *Open* button (4th button on the screen): This compensation measures the parasitic capacitance of the device. This way, the entire part that comes after the connection would be compensated.

Once we have this, we place the load (on the sensor, what we want to measure), and then it can be measured. But for now, the steps will be performed without placing any load.

Steps:

- Press the *Display* button.
- Press the *Split* button (1st button on the screen): It has two channels (A and B) to separate the two components. They can be separated using different formats, but the most commonly used format is as follows:

    - Top: Real/Module part.
    - Bottom: Imaginary/Phase part.

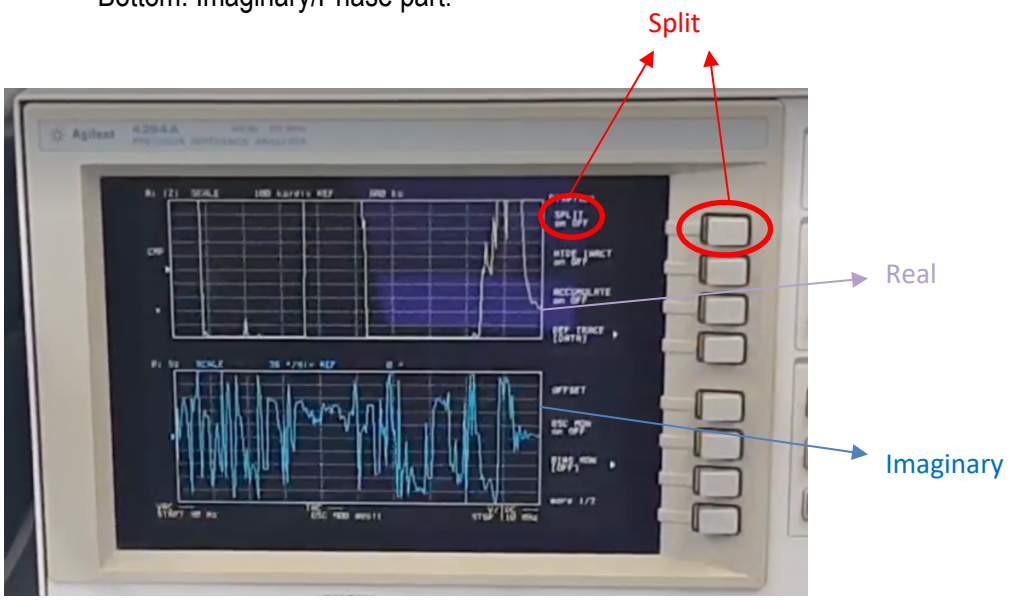

- Press the *Measurement* button to select the desired model, in case the format needs to be changed, always maintaining the Real and Imaginary parts:

    - Module/Phase.
    - Resistance (R: resistance/resistor) / Reactance (X: capacitance, i.e., capacitors / inductance, i.e., inductors).
    - Specific model of inductor + resistance in series.
    - Etc.

    Typically, measurements are taken using the first or second format, and the original signal (R + Im) is in phase or antiphase or in module and phase. Afterward, the necessary operations are performed.

If the format is Module/Phase: there is a sweep that can cover many different frequency scales. To choose one, in this case, a logarithmic scale, the following steps are taken:

- Press the *Sweep* button and select the logarithmic type. This changes the graph on the top (A).

In addition, it is expected that the impedance also has different scales in its value (module). To select one:

- Press the *Format* button and choose logarithmic. (Graph A also changes)

The graph on the bottom remains unchanged, as the phase goes from 0 to 90 (π).

To display the scale being used for measurement on the screen:

- Press the *Scale* button, then press the Autoscale button (1st button on the screen).

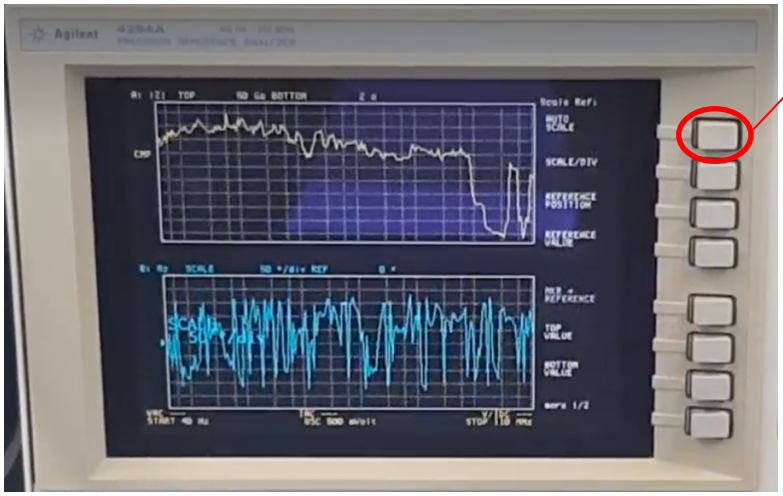

To choose which of the two graphs to modify at any given moment, there are two buttons, one for Channel A and another for Channel B.

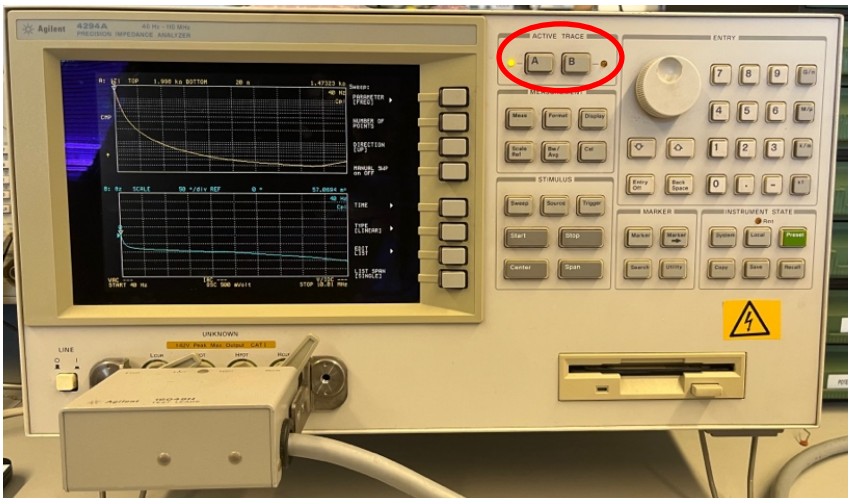

From here, a resistance is placed on the electrodes (since there is currently no device). It can be observed that it provides a constant response in the module (Channel A), which will be equal to the value of the resistance that has been applied.

- Press the Marker button.
- Move the dial to see the value through the function (in this case, constant). The function ranges from low frequencies to high frequencies (40Hz - 11MHz). At high frequencies, it can be observed that the function starts to decrease, approximately from 5MHz.
    - This equipment does not perform well due to the shielding of the sensor (electrodes), which functions like an antenna. From 5 MHz onwards, it starts to pick up anything (noise).
- Therefore, to determine the trend that the function follows, it stops at 5MHz. To do this, we will limit the maximum and minimum values (x-axis):
    - Press the *Start* button: 40Hz.
    - Press the *Stop* button: 5MHz.
    - Press the *Sweep* button: It is constantly sweeping unless a change is made
      → Press the *Trigger* button: The trigger is continuous, but the "Single" button needs to be pressed (2nd button on the screen) for it to perform a sweep, stop at the end, and not automatically start again until requested.

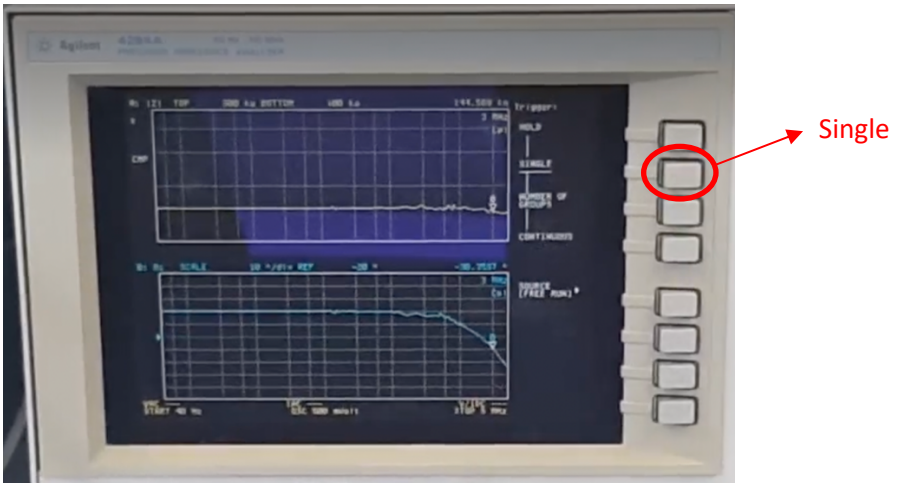

- Now, in Channel A, the function appears as a straight line (value R = ct), but with a slight drop at the end. → Problem: Several interferences are visible, which should not be happening.